INFLUENCE OF EXTERNAL PARAMETERS ON TRANSFORMER FRA SIGNATURE AND STATISTICAL INDICES

Auyez Khassenov, Bachelor of Electrical and Computer Engin eering

Submitted in fulfillment of the requirements

for the degree of Master of Science

in Electrical and Computer Engineering

School of Engineering

Department of Electrical and Computer Engineering

Nazarbayev University

53 Kabanbay Batyr Avenue,

Astana, Kazakhstan, 010000

Supervisors: Mehdi Bagheri, Prashant Jamwal

December 2018

DECLARATION

I hereby, declare that this manuscript, entitled “Influence of External Parameters on Transformer FRA Signature and Statistical Indices”, is the result of my own work except for quotations and citations which have been duly acknowledged. I also declare that, to the best of my knowledge and belief, it has not been previously or concurrently submitted, in whole or in part, for any other degree or diploma at Nazarbayev University or any other national or international institution.

Name: Auyez Khassenov

Date:12/12/2018

Acknowledgment

I would to thank my advisor Dr. Mehdi Bagheri for the guidance and support throughout the master program. I am also grateful to Dr. Prashant Jamwal for the support and sincere desire to help students.

Abstract

Frequency Response Analysis (FRA) is the common tool for transformer condition diagnosis. FRA allows to detect alterations in the transformer structure due to coverage of wide frequency range. Nevertheless, the frequency response is sensitive to external parameters. In this work, different connection schemes for external parameters are implemented and investigated. The theoretical justification is provided for each scenario. The measurement trend is visualized. The interpretation of frequency response signature requires expert knowledge. Statistical indices can be used for unbiased interpretation. Therefore, four statistical indices are employed to analyze the effect of external resistance, capacitance and inductance on the test objects.

Table of Contents

List of Figures

List of Tables

CHAPTER 1. INTRODUCTION AND LITERATURE REVIEW

Reliable power transmission and delivery are of great importance in the modern world. Among all the equipment used in power systems, transformers, which are subjected to weather conditions and mechanical and electrical faults, are considered the most significant transmission and distribution system equipment. Mechanical faults may occur during rough transportation, earthquakes or gas explosions in the transformer oil [1]The faults occurring at the power line induce unbalanced electromagnetic forces, which in turn lead to transformer winding deformation.

Because of the high maintenance cost of the transformer, economic losses are inevitable [2] Additionally, a danger for the staff and residents exists.

Although the design considerations of the transformer account for mechanical stability during fault conditions of power system operation, the damage incurred during transformer transportation or in the short circuit condition can result in deformation of the transformer active part. The faults can be of several types: axial or radial displacement of a winding, clamping structure failure, movement of the core, winding failure or loosened internal connections in a transformer. The slight changes in the structure of the equipment affect the RLC model of the winding and consequently the frequency response of the power transformer [3]

The widely used and well-researched method for off-line diagnosis of a transformer is frequency response analysis (FRA). The technique is well adapted to detecting faults at the core and windings. However, several disadvantages are associated with this method: the requirement to disconnect the transformer from the power line, the need for the reference normal condition of the winding frequency response or the “fingerprint” and the need for professional skills and trained manpower to perform frequency analysis.

The FRA methods can be grouped into two types, depending on the input signal: impulse frequency response analysis (IFRA) and sweep FRA (SFRA) [1], [4]. Through the injection of

the signal, the frequency response of the winding is obtained. In SFRA, the input is a sinusoidal signal with changing frequency, and the result is analyzed in the frequency domain. The first response is considered the “fingerprint”. The comparison between the first and subsequent responses gives the information on the presence and scale of the fault [5], [6]. SFRA is well adapted to and has been investigated for off-line mechanical fault diagnosis. Commercialized products and industrial standards associated with the off-line SFRA method exist for winding fault identification. The results of FRA give the winding impedance or transfer function against the frequency. The IFRA and SFRA techniques are usually performed off-line, and the performance is considered high, while on-line FRA is aimed at extracting as much information as possible. The on-line transformer FRA becomes more complicated with the response of the power grid (load, source) in addition to the transformer response. This additional parameters increase the degree of complexity associated with the FRA.

IFRA utilizes controlled low voltage pulses for excitation. Through the Fourier transform of the response and injected signals, the frequency response is obtained. Due to the low energy and short duration of the input signal, the normal operation of the transformer is not interrupted, which provides the potential for on-line IFRA application [7].

References [7], [8] studied the effect of a capacitive coupling circuit on the frequency response of the system based on a comparison of the windings frequency response with the on-line IFRA signature. This research determined that a constant distinction exists between the frequency responses of the transformer winding and

IFRA signature at medium and high frequency bands. Additionally, the resonance and antiresonance positions are the same for the two responses. These findings considerably contribute to the development of on-line transformer monitoring and diagnosis systems.

A recent study [9] addressed the bushing or external isolation capacitance that comes into play when frequency domain analysis measurements are performed on-line. The system requires off-

line calibration to extract the external capacitive reactance. The suggestion of this paper is to introduce inductive coupling probes and an ABCD two-port network to determine the impedance of the circuit. The key idea behind the experiment is to extract the in-circuit impedance without shutting down the equipment. The power transformer is not disconnected from the system; thus, the main drawback of off-line transformer diagnosis systems is addressed.

Another study [10] considered FRA to investigate the effect of transformer bushing failure on the FRA signature. This paper provides detailed simulation and analysis of the effect of external factors on the FRA signature of transformers. The bushing model and insulation oil condition noticeably affect the transformer linear model when subjected to FRA simulation analysis. The bushing introduces external capacitive components that significantly impact the FRA signature, especially at high frequencies. The paper also contributes to the investigation of the effect of moisture in the insulation material on the position of the resonance frequency and magnitude of the FRA signature.

A similar approach to study the circuit model of a transformer bushing in the frequency domain was demonstrated in [11] The finding of the research was that the failure level of the bushing is visible only starting from the 5% bushing failure level and affects the FRA signature of the transformer at a high frequency band.

A significant effort into on-line FRA was made in [12]. While off-line transformer analysis can perform well in detecting mechanical faults at all predefined frequencies, whole frequency spectrum analysis cannot be performed in on-line FRA. The response below 1 kHz was noisy and was not considered for on-line analysis. The authors investigated the effect of the bushing on on-line and off-line FRA, and the finding was that a larger capacitance of the transformer bushing causes less disturbance of the on-line FRA signature.

The various influences of the external environment on FRA were investigated and discussed in [13]-[15]. FRA is known to be sensitive to slight deformations in transformer winding; thus, the method is subjected to the impact of insulation characteristic changes, which vary over time due to material degradation. The main factors that affect insulation are the temperature and moisture content [13]. The study determined that depending on whether the moisture content is moving from paper to the insulation oil or from the oil to paper, the resonance points of the FRA spectrum will shift to higher or

lower frequencies, respectively. Also in [14], the effectiveness and capability of FRA in obtaining information on moisture migration in the insulation are discussed. FRA may be used as a tool to checking the drying process of a power transformer.

To date, much significant research has been performed in the area of on-line FRA. The focus is on the IFRA technique using controlled signal injection. The introduction of controlled signal injection brings several advantages for the IFRA method, one of the most significant being the reproducibility of on-line FRA. The tools associated with FRA are the fast Fourier transform and wavelet transform.

Other well-known diagnosis methods are the short circuit (SC) test and low voltage impulse (LVI) method. An SC test is simple and easy to reproduce, but at the same time, the technique is unable to distinguish weak, minor deformations. The LVI method is robust to external factors, such as grid and load, but lacks repeatability [16], [17].

The approach of short circuit impedance (SCI) measurement is commonly used for winding mechanical fault detection. The comparison is performed between the factory test value of the SC impedance and the measured value. A 3% difference in the SCI measurement is considered significant [18], [19]. For off-line SCI application, the measurement is performed as the transformer secondary side is shorted; however, for on-line application, this is physically

impossible due to the transformer being energized by the network. To account for transformer excitation, a two-port network is proposed for the transformer.

The importance of SCI measurement is discussed in [20]. In addition to the application of SCI measurements to transformer condition monitoring, standards exist that require specific conditions for transformer SCI measurements of the taps. The system protection calculations are based on the SC tap impedances of the transformer.

Another approach to on-line transformer condition monitoring is the vibration method. Transformer vibrations are considered as transformer inner part displacements around the reference point with definite periodicity. Studies [21]-[23] have discussed the contribution of vibration measurements to on-line transformer condition monitoring. The model of the transformer, which accounts for the on-line operating conditions of the transformer, shows the vibration behavior of different inner components. The findings presented in [22] indicate the dependency of the transformer tank vibration pattern on the current squared for winding vibrations and on the voltage squared for core vibrations.

Frequency Response Analysis

The technique commonly used in on-line transformer parameter estimation is FRA, and the stages of FRA can be defined as follows: 1) the measurement of an injected signal, 2) signal processing and 3) analysis of results [24], [25].

Significant efforts have been made to study and analyze the interturn SC fault of a transformer [26], [27]. Also, in [28] the digital image processing technique was proposed for short-circuit turn identification utilizing both magnitude and phase responses of a transformer, in [29] image processing is used on an actual power transformer winding. The significance of detecting interturn SCs is that their propagation can cause major losses in the power networks and lead to increased maintenance and operational costs. In [30], [31] the axial and radial faults of low voltage and high voltage windings of a power transformer were simulated and the

influence of the faults on the transformer equivalent circuit were analyzed. The proposed on-line FRA is a helpful tool for transformer condition monitoring and fault detection. Two FRA methods have been developed, namely, IFRA and SFRA. The idea behind IFRA is to inject a short controlled high voltage signal into a transformer winding. The duration of the signal is chosen to be short to avoid impacting the operation of the transformer, and the injection point is a capacitive coupling sensor due to the isolation requirements during the transformer operation. This paper illustrates results that contribute to the early stage on-line diagnosis of transformer interturn faults [26].

The transformer FRA is found to be very sensitive to the connectors used in the measurement procedure [32]-[34].

Works have been performed by other authors to locate the interdisc fault in a power transformer [35], [36], [37]. The challenge of the FRA method is to analyze the response in terms of locating the fault in the transformer winding. The methodology used in the papers allows locating the fault by comparing the results of normal and fault conditions of the winding. The measurements are performed by FRA equipment, and the correlation coefficient is introduced to evaluate the response under fault and normal conditions of the winding. The contribution of paper [35] to on-line transformer monitoring is that the fault can be located using a vector fitting algorithm and a Nyquist plot.

Another work [18] studied the mechanical deformation of a transformer winding, which may be caused by an external SC. The SC induces high values of the electromagnetic force, which may cause mechanical failure of the winding. The paper [18] discusses the SFRA and IFRA methods for transformer condition monitoring. The excitation signal for the transformer winding used in SFRA is sinusoidal with an varying frequency [38], [39], whereas IFRA makes use of short pulses of a controllable signal. The first measured frequency response under normal

operating conditions is considered the fingerprint, and the next measurements are compared with the fingerprint, revealing the fault, if any, and the scale of the fault.

Another paper [40] discusses the difference between the off-line and on-line FRA techniques. While off-line parameter estimation is widely used and is capable of providing essential information about the transformer, on-line measurements are aimed at obtaining as much data as the technology permits. More importantly, the paper provides an analysis of the transformer bushing test tap. The bushing introduces a capacitance to the test setup; thus, the results of the measurements have to take into account this additional capacitance. Additionally, the practical setup for on-line parameter estimation of delta and star connection types of windings was shown [40].

The work provided by Abeywickrama et al. [41] used the two winding transformer model to estimate basic parameters such as the winding impedance and transformation ratio. The authors claim that the advantage of the Transformer Explorer system is that no sensors have to be established for transformer condition estimation.

Although the frequency response signature provides the total impedance of the transformer and allows an expert to make decisions regarding the condition of the equipment, numerical indices are adapted for accurate interpretation of the transformer FRA signature and to allow nonexperts to interpret the results. Studies [42]-[48] have shown the effectiveness of numerical analysis for transformer FRA signature interpretation. A great effort has been made [49]-[51] to classify the transformer winding fault type, the location of the fault and the severity of the changes.

CHAPTER 2. PHYSICAL MODELING

This chapter is aimed at introducing the theoretical explanation behind the transformer frequency response signature. Models of the external resistance, capacitance and inductance are adapted and utilized for the simulation of transformer operation under different external parameters.

The frequency response analyzer is depicted in Figure 2.1

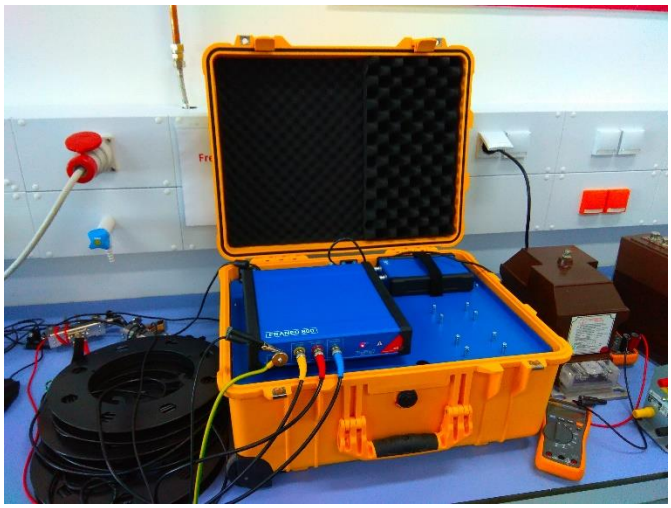

Figure 2.1.1 Frequency response analyzer

To model the external connections on the transformer winding, first, the impedance of coaxial cables was measured and found to be 50 Ω up to 2 MHz. The scheme of the measurement setup is presented in Figure 2.1.2. By adding different impedances to this measurement setup, we can analyze the impact of resistive, capacitive and inductive connections on the power transformer.

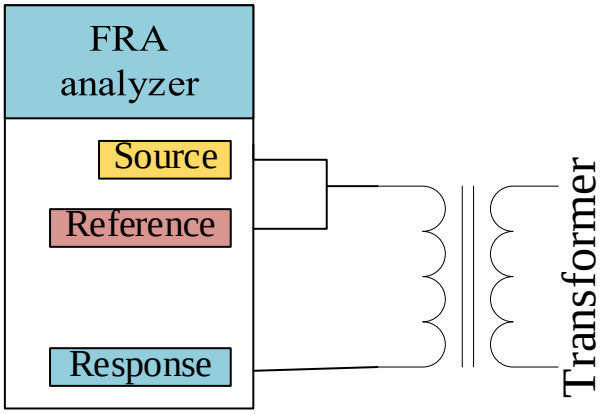

Figure 2.1.2 Measurement setup scheme

2.1. Resistance

Over the frequency range (2 Hz – 2 MHz) at which measurements are performed, the skin effect on the resistance of the conductor is expected. The models of the resistor in [52], [53]were checked; the impact of the skin effect was found to be insignificant, and a constant resistance throughout the measurement frequency range gives more accurate results. This result is due to the structure of the resistor used in the experiments, which is a variable resistor or rheostat.

2.1.1. Series Resistance

The series connection of a resistor is carried out by adding a resistance between the response terminal of the FRA analyzer and the transformer winding. The connection scheme is given in Figure 2.1.3.

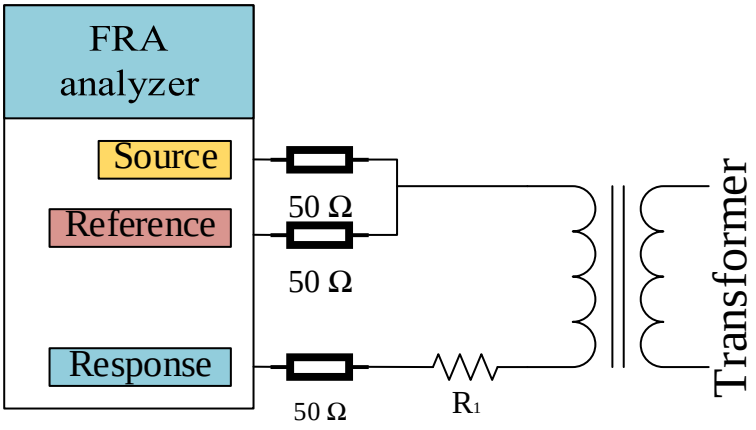

Figure 2.1.3. Series connection of external resistance

This case simulates the increase of the connection resistance due to the measurement setup. From circuit theory, the response of the system is:

$$Z_T = Z_W + R_1 + Z_{cable} \tag{1}$$

where Z_T is the total impedance of the setup, Z_W is the impedance of the transformer winding, Z_1 is the added series impedance and Z_{cable} is the total cable impedance, which is 75 Ω. Each cable impedance is 50 Ω; the source and reference terminals of the FRA analyzer are in parallel, giving a 25 Ω impedance in the connection, and the response terminal gives a 50 Ω impedance. Thus, in total, the cable impedance provides a 75 Ω resistance. According to (1), smaller values of R_1 result in the system responses being closer to the fingerprint response; i.e., the smaller the value of R_1 is, the closer the response is to the fingerprint.

The impedance of the winding is extracted from the equation of the transfer function [19], [54]:

$$k = 20\log_{10}\frac{50}{50 + Z_W} \tag{2}$$

meaning:

$$Z_W = 50\left(\frac{1}{10^{k/20}} - 1\right). \tag{3}$$

The resistance R_1 is modeled as a constant resistance. The comparison between the modeled circuit and the measured circuit for a 1 Ω series connected resistor is illustrated in Figure 2.1.4. A deviation between the theoretical and practical results is observed starting at 800 kHz from the plot. The two curves match in value below 800 kHz, importantly at approximately 200 kHz, where the impedance from the fingerprint is increased from 20 Ω to approximately 100 Ω. It is important to remember the influence of the connection setup on the transformer frequency response at high frequencies. Consequently, the behavior of the system becomes complex and unpredictable at high frequency, depending on the type of connectors, coaxial cable torsion, etc.

The next modeled resistance is 200 Ω. The behavior of this connection is shown in Figure 2.1.5. The modeled circuit behavior and the behavior of the measured circuit start to differ at approximately 60 kHz. By increasing the resistor connected in series to the winding to 200 Ω, the antiresonance points are shifted upwards. This phenomenon becomes even more noticeable as the additional resistor is increased further to 5 kΩ in Figure 2.1.6 and 1 MΩ in Figure 2.1.7.

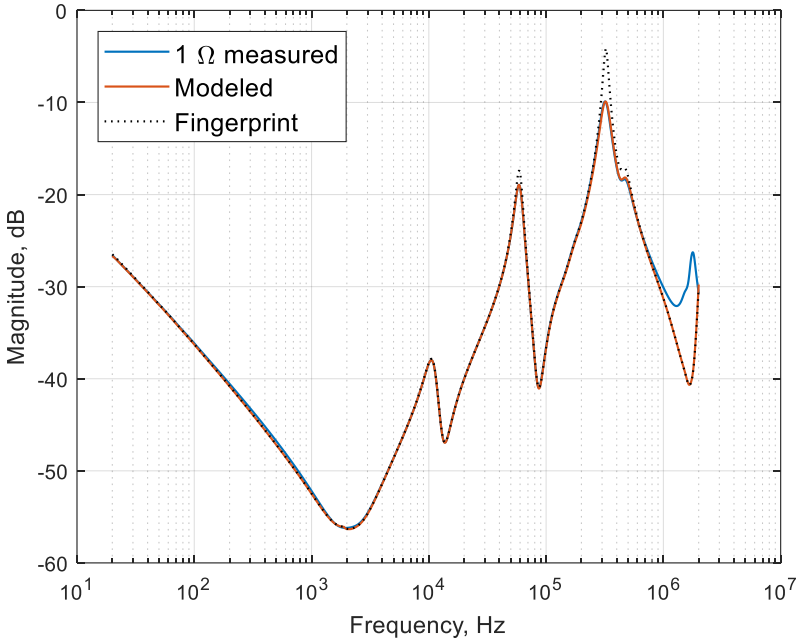

Figure 2.1.4 Comparison of measured and modeled 1 Ω series resistances for a 350 VA transformer

The deviation for the 1 MΩ resistor is due to the capacitance across the resistor, which comes into play above 5 kHz. In this case, the lower the series resistance is, the more accurate the predicted circuit behavior due to the fewer external components (capacitance and inductance) coming into series with the winding.

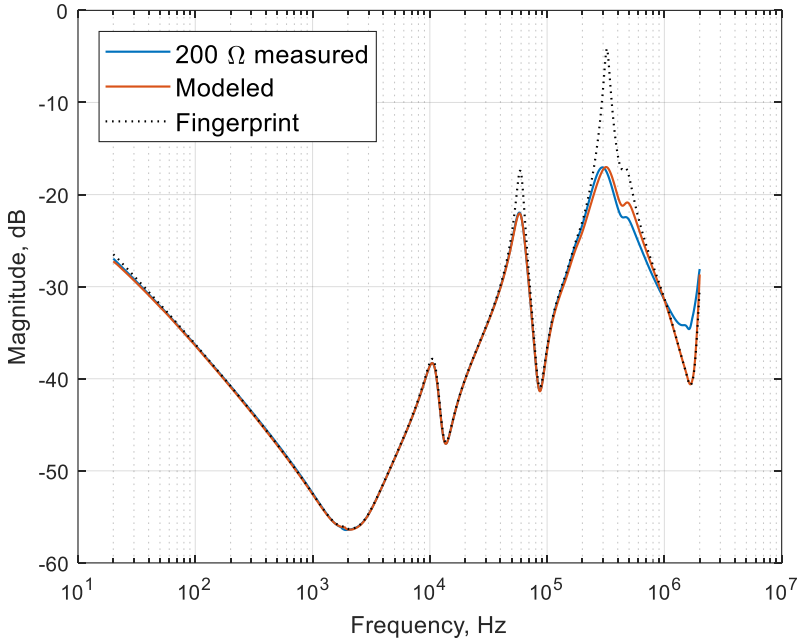

Figure 2.1.5 Comparison of measured and modeled 200 Ω series resistances for a 350 VA transformer

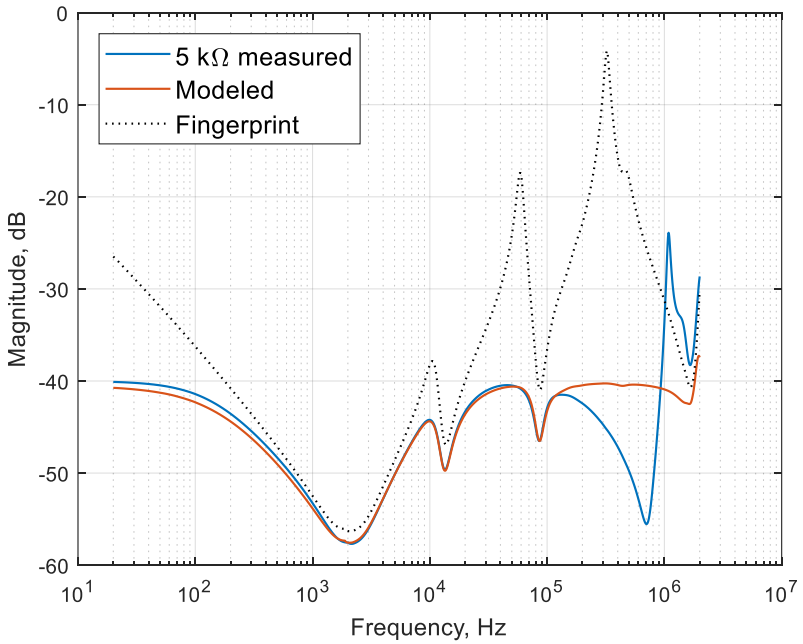

Figure 2.1.6 Comparison of measured and modeled 5 kΩ series resistances for a 350 VA transformer

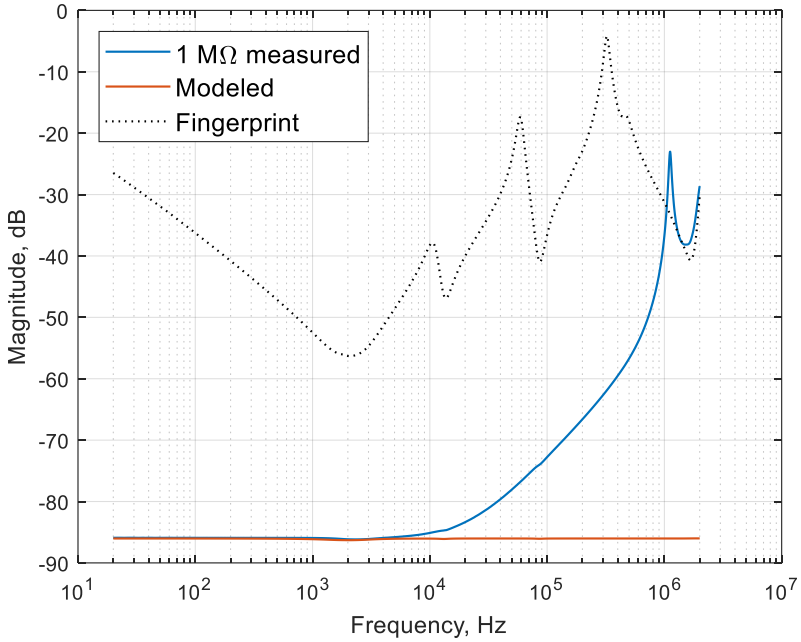

Figure 2.1.7 Comparison of measured and modeled 1 MΩ series resistances for a 350 VA transformer

2.1.2. Shunt Resistance

A shunt resistance is added between the end of the transformer winding and ground. The connection scheme is presented in Figure 2.1.8. From a practical point of view, this setup emulates the leakage from the measurement circuit. Additionally, authors [55] have referred to this connection as the measurement impedance.

The total impedance of this connection is found using (4):

$$Z_T = \frac{1250 + 75R_2 + Z_W(50 + R_2)}{R_2} \tag{4}$$

where Z_T is the total impedance of the system, Z_W is the winding impedance and R_2 is the connected external resistance. Using the same procedure for extracting the transformer winding impedance as in eqs. (2) and (3), we can obtain an accurate impedance value.

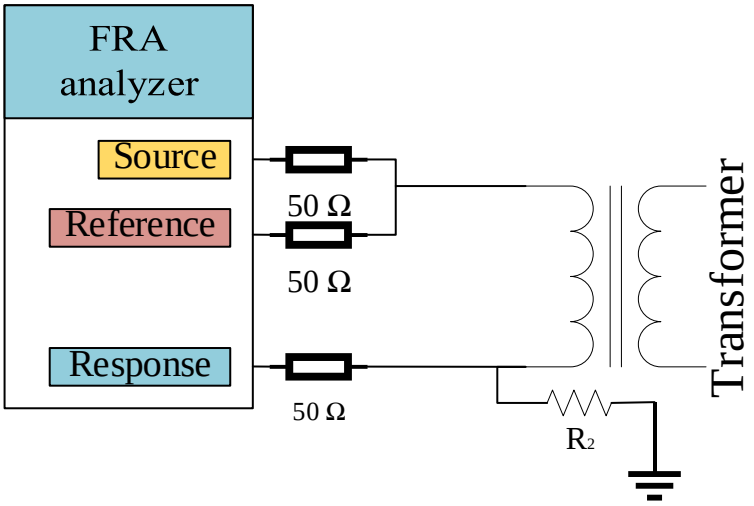

Figure 2.1.8 Shunt connection of an external resistance

In this scenario, according to eq. (4), when we increase the resistance, the total impedance will converge to the fingerprint value. This phenomenon can be seen more clearly if we simplify (4) to (5):

$$Z_T = Z_W + 75 + \frac{50Z_W + 1250}{R_2}. \tag{5}$$

If R_2 becomes infinitely large, then the total impedance becomes the fingerprint impedance, which is $75+Z_W$. This trend is shown in Figures 2.1.9 – 2.1.12. The illustration in Figure 2.1.9 demonstrates the behavior of a 1 Ω shunt resistance connected to the transformer winding. In fact, the behavior follows the predicted trend of increasing the total impedance of the system. Figure 2.1.10 presents the results obtained with the addition of a 200 Ω shunt resistor to the system. The response comes closer to the fingerprint, and the modeled circuit behavior fits the measured one better due to the larger resistance, which overlaps the influence of the connection inductance and capacitance. As we further increase the resistance, the modeled and measured impedances converge to the fingerprint.

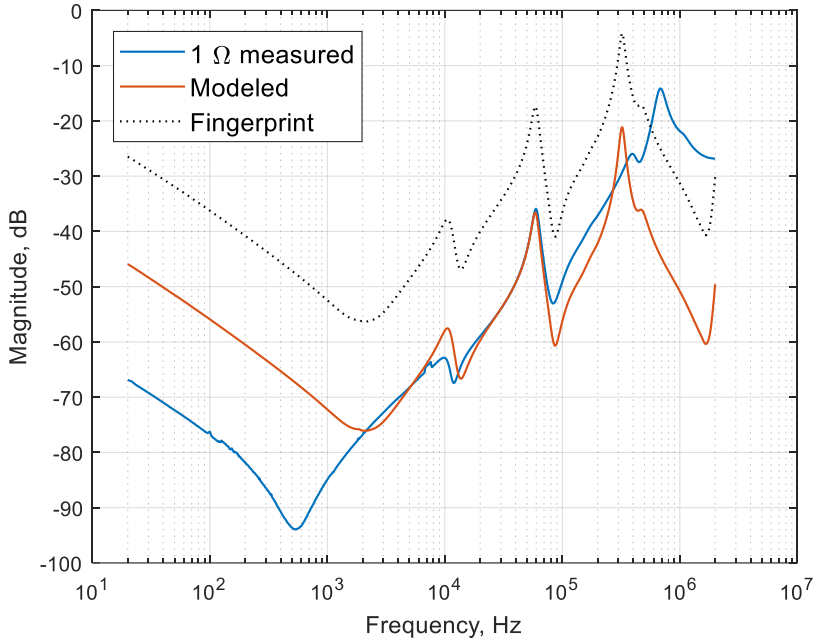

Figure 2.1.9 Comparison of measured and modeled 1 Ω shunt resistances for a 350 VA transformer

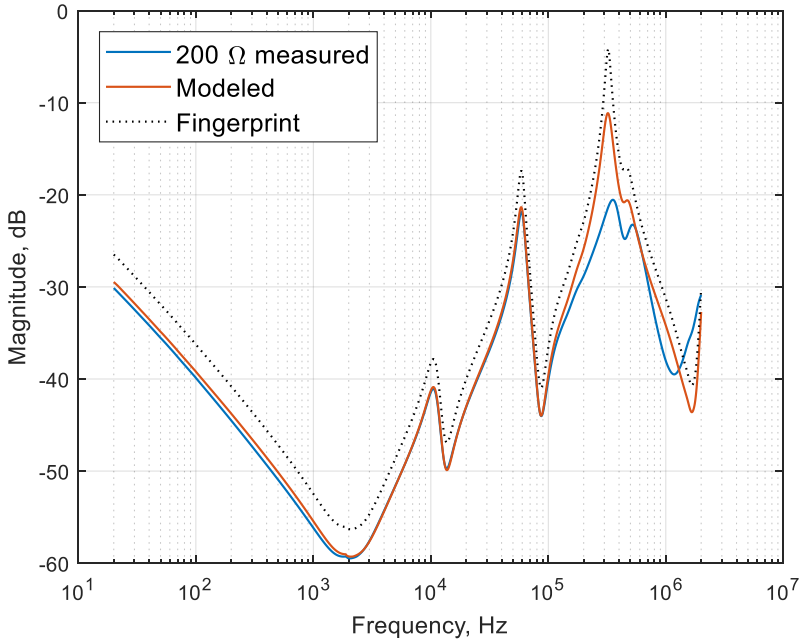

Figure 2.1.10 Comparison of measured and modeled 200 Ω shunt resistances for a 350 VA transformer

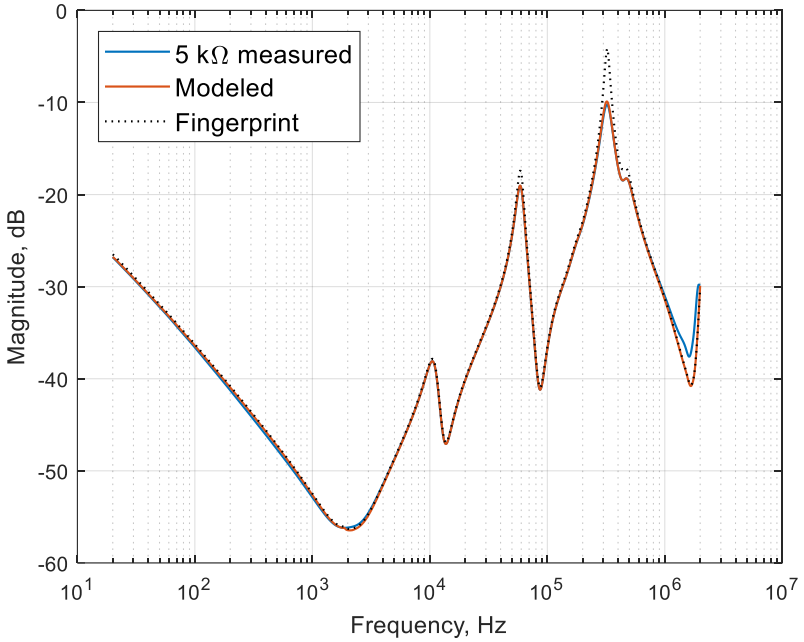

Figure 2.1.11 Comparison of measured and modeled 5 kΩ shunt resistances for a 350 VA transformer

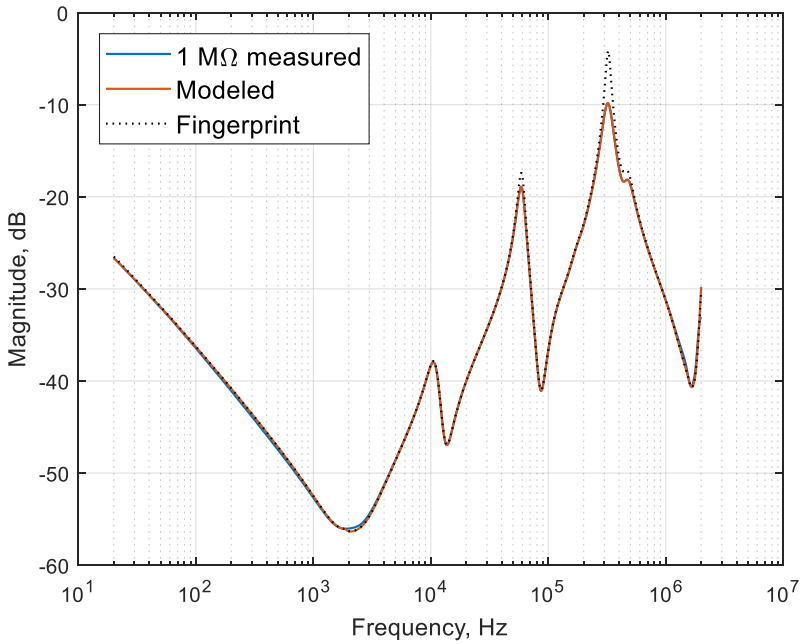

Figure 2.1.12 Comparison of measured and modeled 1 MΩ shunt resistances for a 350 VA transformer

2.1.3. Parallel Resistance

A parallel resistance is added in parallel to the transformer winding terminals. This connection setup simulates the SC of the winding. The scheme of SC condition is shown in Figure 2.1.13.

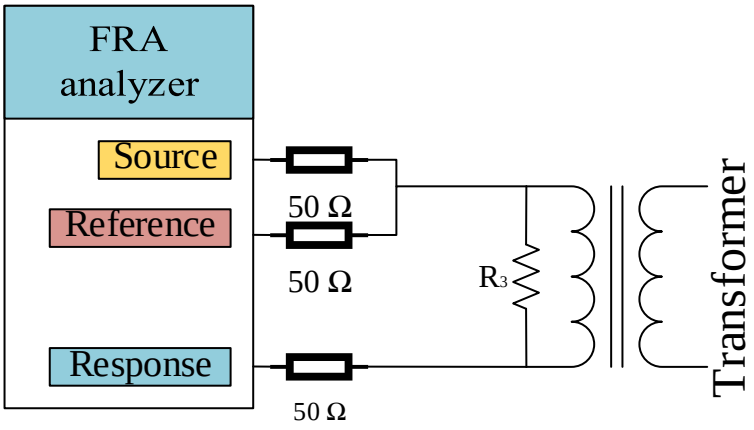

Figure 2.1.13 Parallel connection of an external resistance

The total impedance of this connection setup is given by (6):

$$Z_T = \frac{75(Z_W + R_3) + Z_W R_3}{Z_W + R_3}. \quad (6)$$

By rearranging the terms and simplifying, we obtain:

$$Z_T = 75 + \frac{Z_W R_3}{Z_W + R_3}. \quad (7)$$

If R_3 is small, then the total impedance will tend to 75 Ω. For the case when $Z_W << R_3$, the total impedance becomes $75+Z_W$, which is the fingerprint impedance. This trend can be observed from Figures 2.1.14 – 2.1.17.

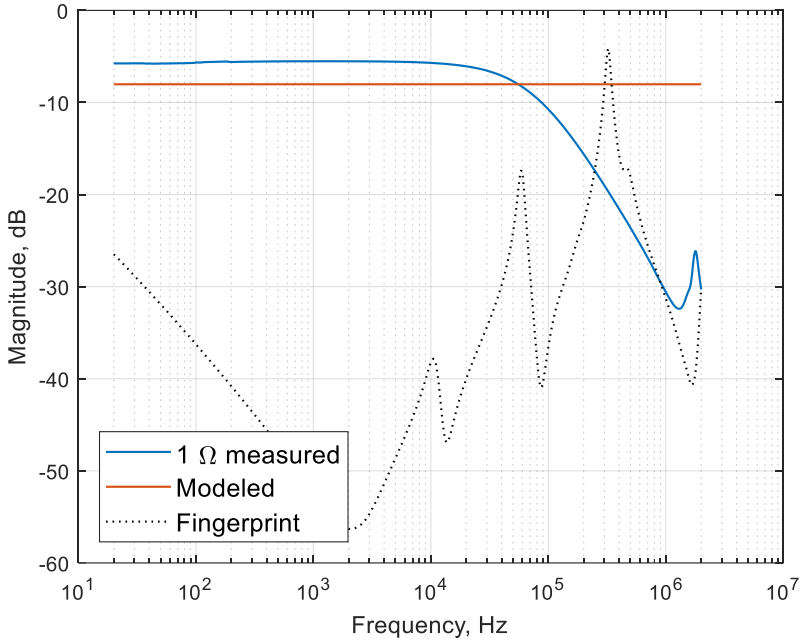

Figure 2.1.14 Comparison of measured and modeled 1 Ω parallel resistances for a 350 VA transformer

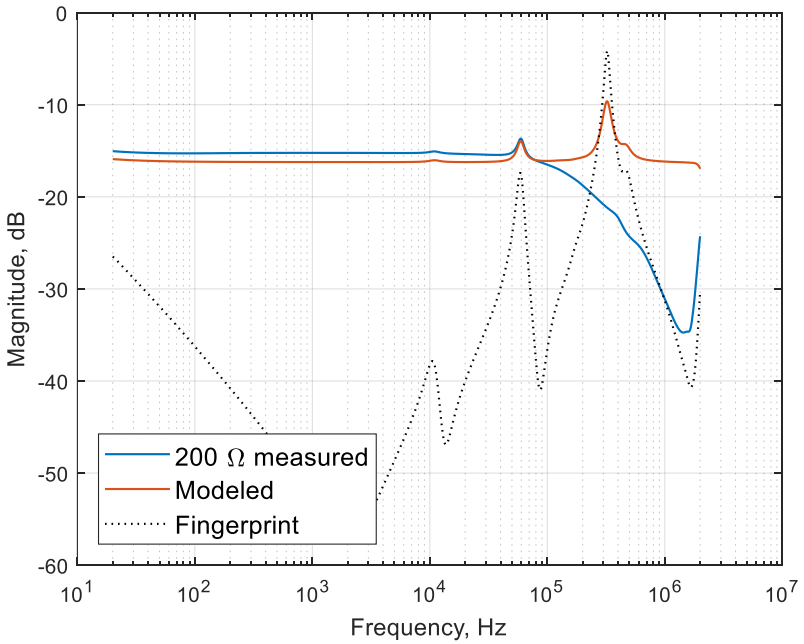

Figure 2.1.15 Comparison of measured and modeled 200 Ω parallel resistances for a 350 VA transformer

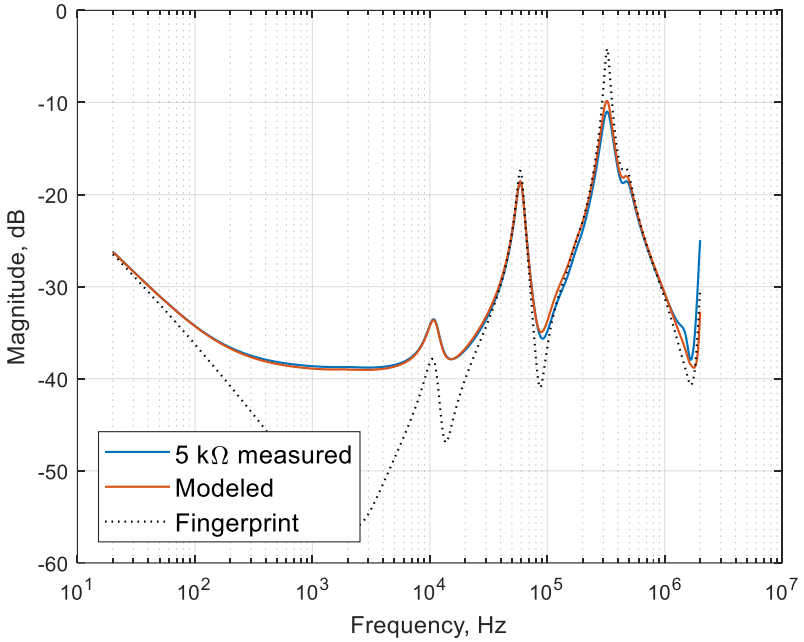

Figure 2.1.16 Comparison of measured and modeled 5 kΩ parallel resistances for a 350 VA transformer

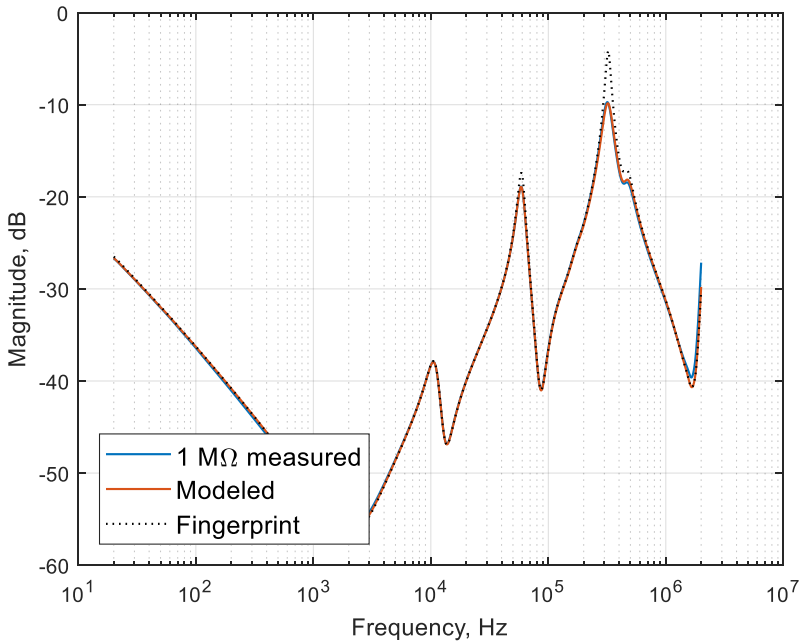

Figure 2.1.17 Comparison of measured and modeled 1 MΩ parallel resistances for a 350 VA transformer

2.2. Capacitance

The external capacitance is represented as a single capacitor. The impedance is calculated by using (8):

$$Z_C = \frac{1}{jwC}. \tag{8}$$

A capacitor is a reactive element with the impedance value being inversely proportional to the frequency of electric signal oscillations.

2.2.1. Series Capacitance

The scenario of a series capacitance emulates the series capacitance of the connection setup. The connection scheme is shown in Figure 2.2.1.

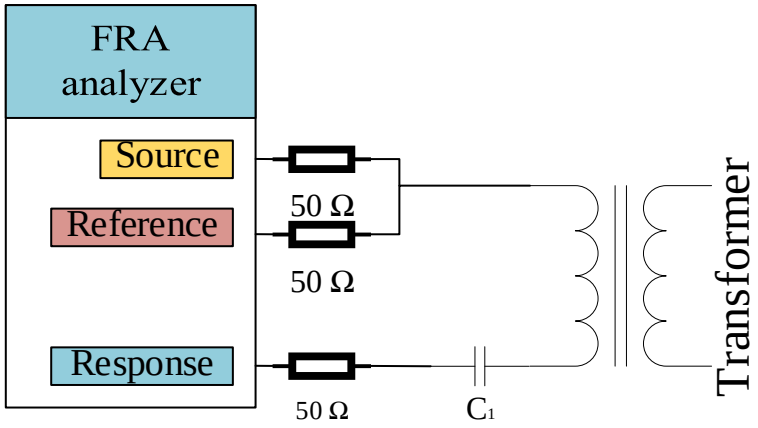

Figure 2.2.1 Series connection of an external capacitance

The total impedance of the system is calculated by (9):

$$Z_T = Z_W + Z_{C1} + Z_{cable} \tag{9}$$

where Z_{C1} is the impedance of the series capacitor. The phase of the capacitive impedance is -90°. Because the capacitive reactance inversely depends on the frequency, at low frequencies, the impedance of the capacitor will be high and will decrease as the frequency increases. In

addition, the impedance has an inverse dependence on the capacitance value. This trend is clearly observed in Figures 2.2.2 – 2.2.5. With a 100 pF series capacitor connected to the transformer, the total impedance of the system initially rises to 100 MΩ and then steadily decreases until it matches the fingerprint at the 1.5 MHz point. For a 1000 pF connected external capacitor, the starting total impedance of the system is 7 MΩ; for a 50 nF external capacitor, the impedance is 0.2 MΩ; and for a 2.2 µF external capacitor, the impedance is 3 kΩ.

As we increase the capacitance, the measured frequency response converges to the fingerprint. For a 2.2 µF connected capacitor, the deviation from the fingerprint remains up to 300 Hz, and above 300 Hz, the responses match. The modeled and measured frequency responses for the series capacitor scenario match well.

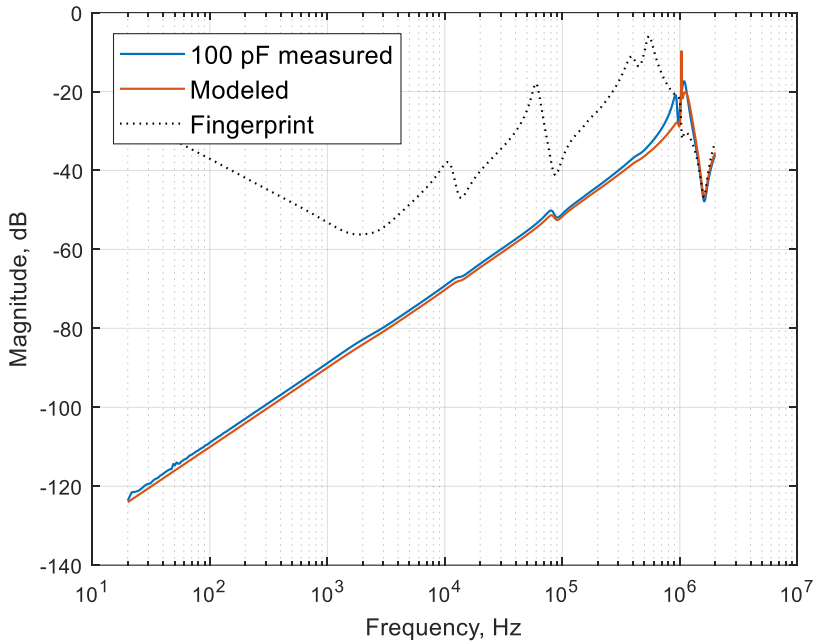

Figure 2.2.2 Comparison of measured and modeled 100 pF series capacitances for a 350 VA transformer

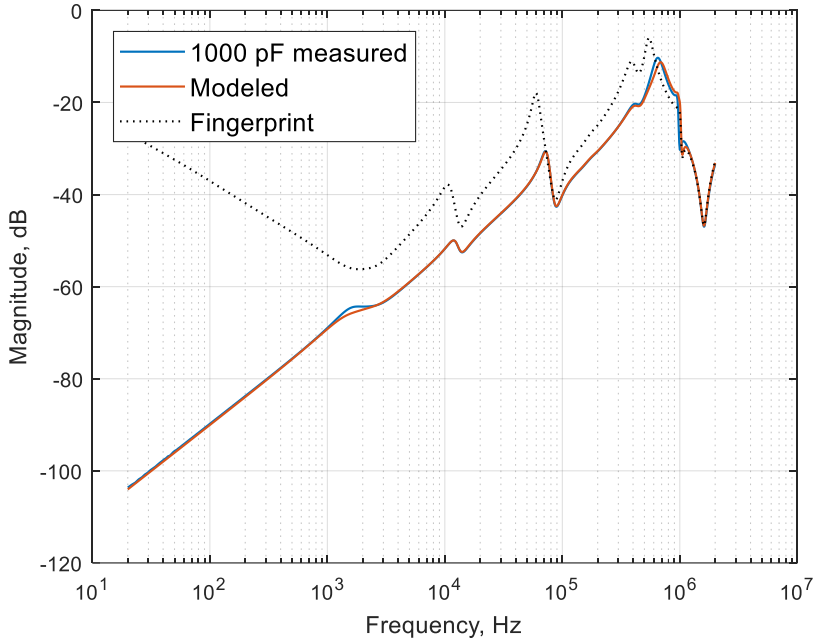

Figure 2.2.3 Comparison of measured and modeled 1000 pF series capacitances for a 350 VA transformer

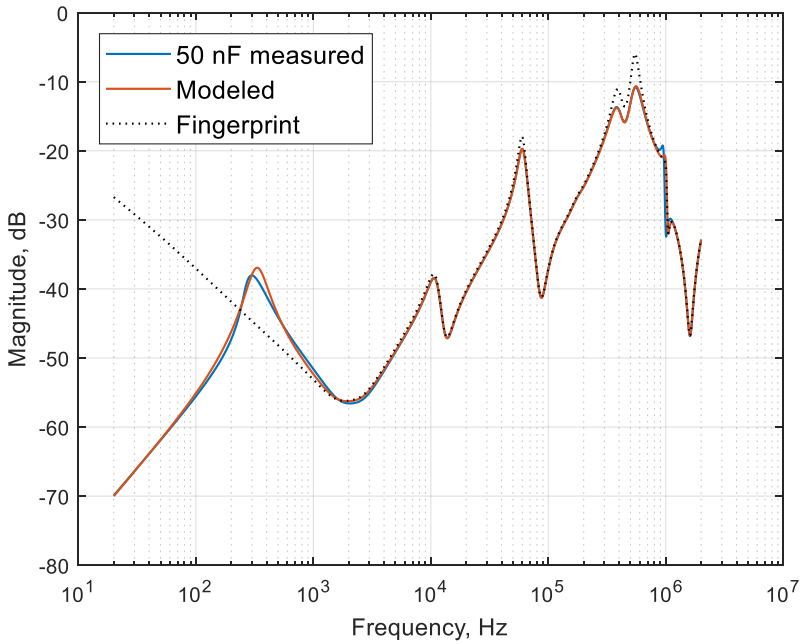

Figure 2.2.4 Comparison of measured and modeled 50 nF series capacitances for a 350 VA transformer

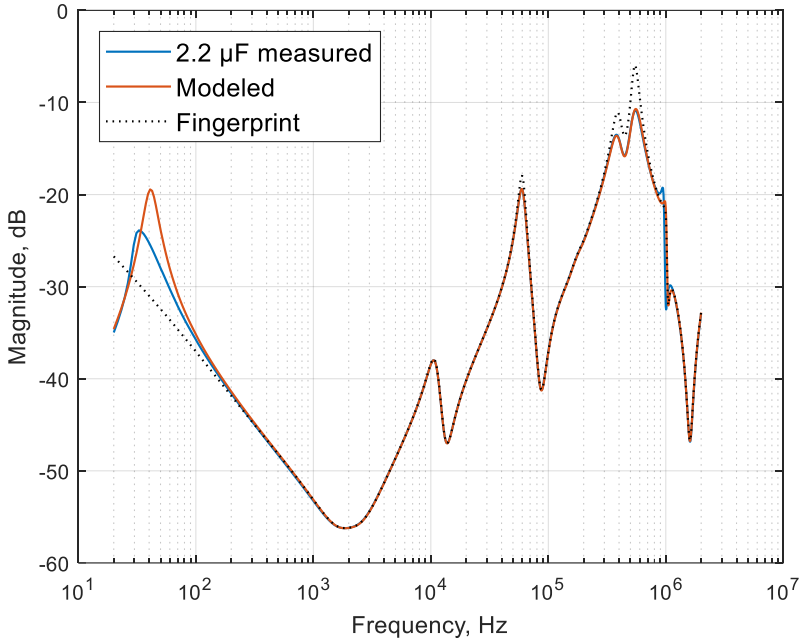

Figure 2.2.5 Comparison of measured and modeled 2200 nF series capacitances for a 350 VA transformer

2.2.2. Shunt Capacitance

A shunt capacitance emulates the capacitive leakage to ground at the measurement terminals on the transformer winding. Equal capacitors are connected at the beginning and end of the winding. The connection scheme is depicted in Figure 2.2.6.

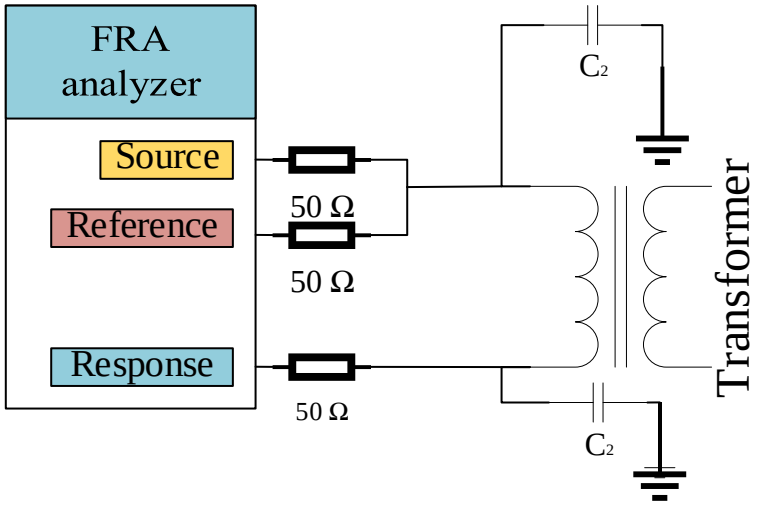

Figure 2.2.6 Shunt connection of an external capacitance

The total impedance of the system for this connection scheme is:

$$Z_T = \frac{2500Z_{C2} + 75Z_{C2}^2 + 1250Z_W + 75Z_W Z_{C2} + Z_W Z_{C2}^2}{Z_{C2}^2}. \quad (10)$$

By simplifying and rearranging, we obtain:

$$Z_T = 75 + Z_W + \frac{2500Z_{C2} + 1250Z_W + 75Z_W Z_{C2}}{Z_{C2}^2} \quad (11)$$

The above equations suggest that the total impedance increases as the impedance of the capacitor decreases. For small capacitor values, the total impedance indeed follows this trend. However, as the capacitance increases, the deviation between the theoretical behavior and actual behavior increases. When we address the shunt connection of reactive elements, the influence of internal connections on the frequency response analyzer is great because the capacitive reactance is small at high frequencies. In fact, we need to know the grounding impedance of the source, reference and response terminals. However, for manufacturing reasons, this information is unknown for a regular user. Thus, a difference is observed between the modeled and measured behaviors of the system at a higher frequency range for the capacitive impedance.

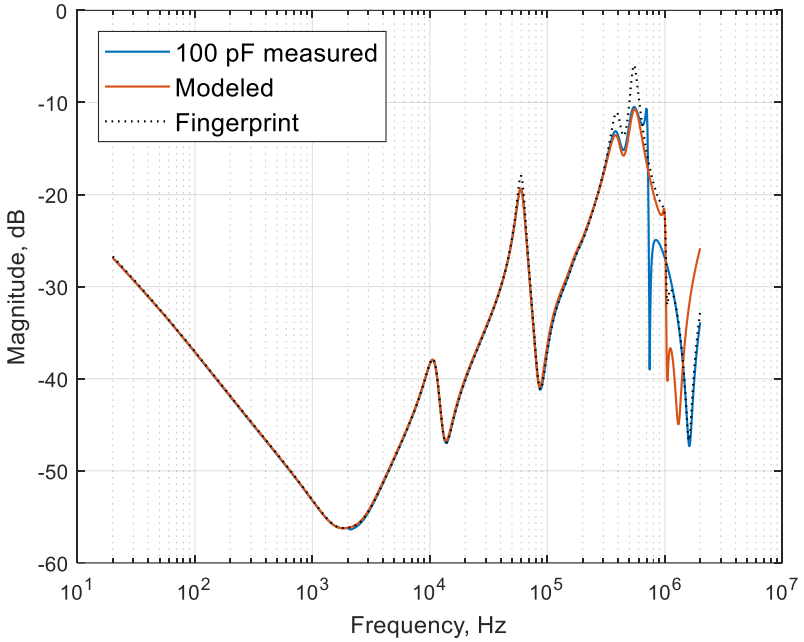

Figure 2.2.7 Comparison of measured and modeled 100 pF shunt capacitances for a 350 VA transformer

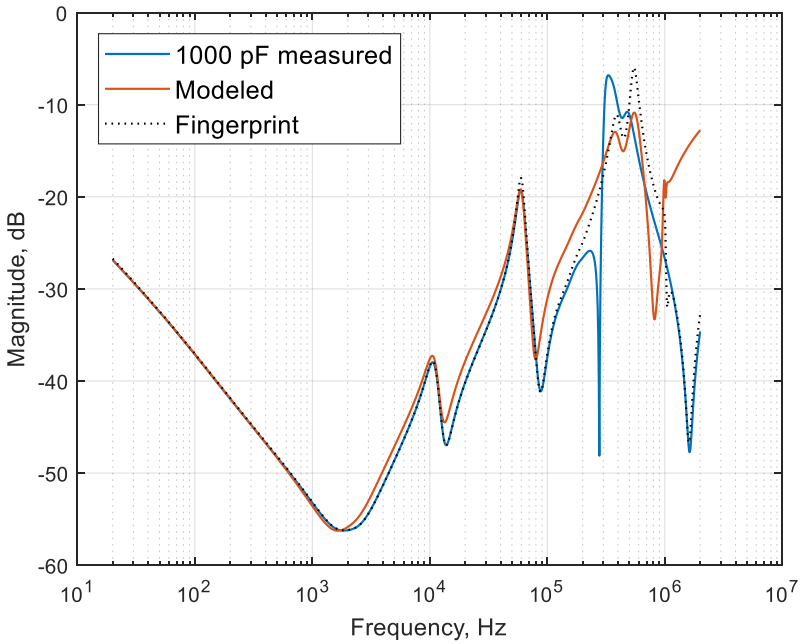

Figure 2.2.8 Comparison of measured and modeled 1000 pF shunt capacitances for a 350 VA transformer

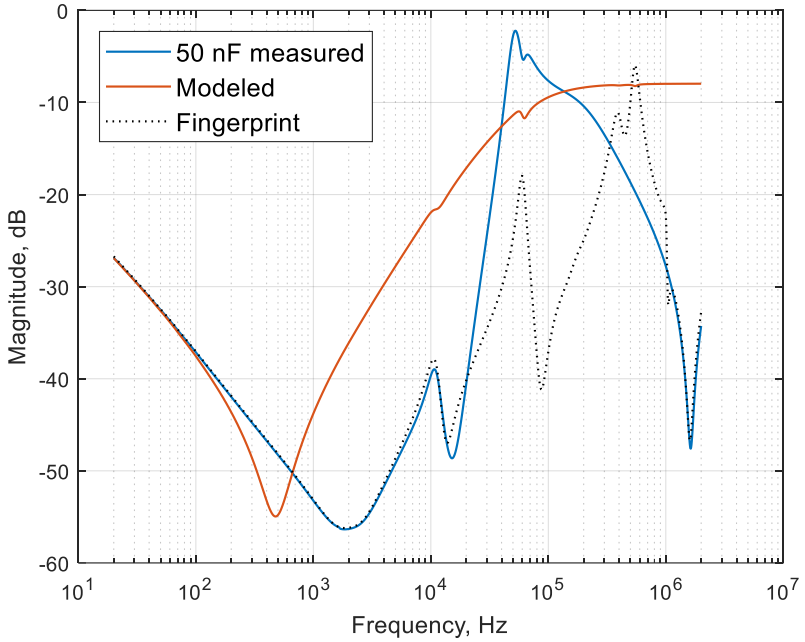

Figure 2.2.9 Comparison of measured and modeled 50 nF shunt capacitances for a 350 VA transformer

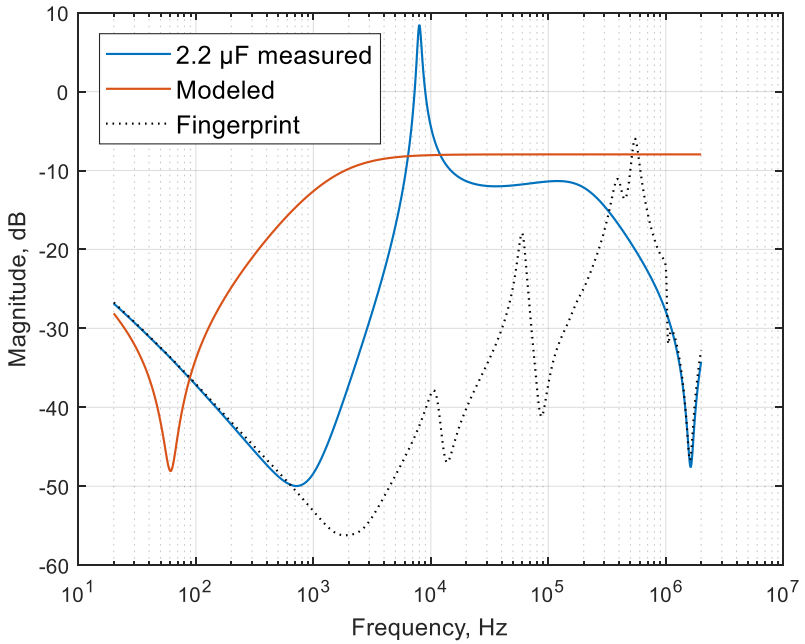

Figure 2.2.10 Comparison of measured and modeled 2200 nF shunt capacitances for a 350 VA transformer

2.2.3. Parallel Capacitance

The parallel connection of a capacitor to the transformer winding emulates the capacitive SC of the winding; i.e., the SC level increases as the frequency of the signal increase. At low frequencies, the capacitive impedance is high, and at high frequencies, the capacitive impedance is low. The connection scheme of the capacitor is shown in Figure 2.2.11.

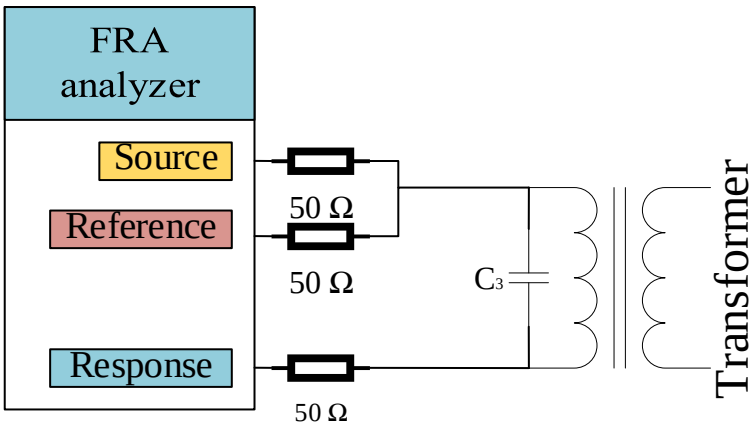

Figure 2.2.11 Parallel connection of an external capacitance

The total impedance of the system is given by (12):

$$Z_T = 75 + \frac{Z_W Z_{C3}}{Z_W + Z_{C3}} \tag{12}$$

According to the above equation, for $Z_W << Z_{C3}$, the total impedance of the system will be identical to the fingerprint. However, as the capacitive impedance changes with frequency, the response of the system highly depends on the frequency range. Z_{C3} decreases as the frequency increases, which is why at higher frequencies, the total impedance will deviate significantly from the fingerprint. This trend is clearly seen from Figures 2.2.12 –2.2.15.

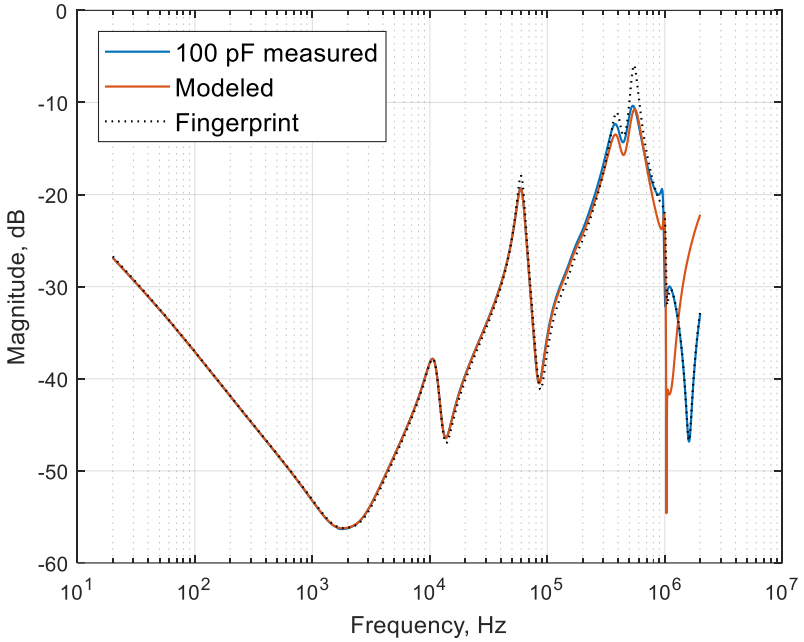

Figure 2.2.12 Comparison of measured and modeled 100 pF parallel capacitances for a 350 VA transformer

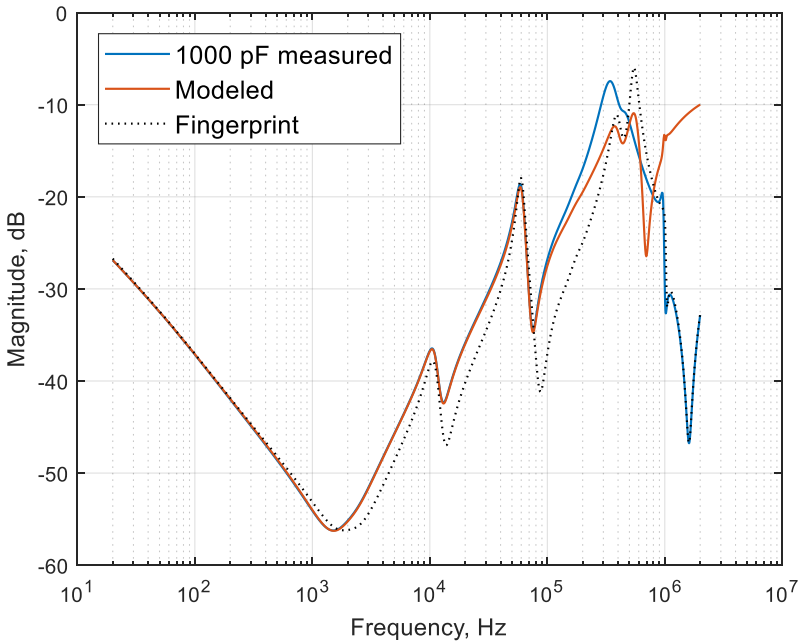

Figure 2.2.13 Comparison of measured and modeled 1000 pF parallel capacitances for a 350 VA transformer

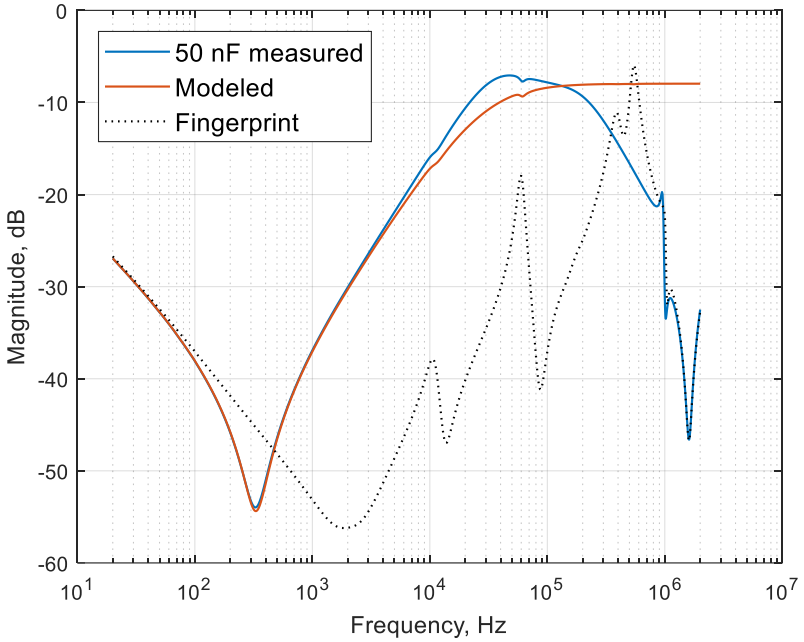

Figure 2.2.14 Comparison of measured and modeled 50 nF parallel capacitances for a 350 VA transformer

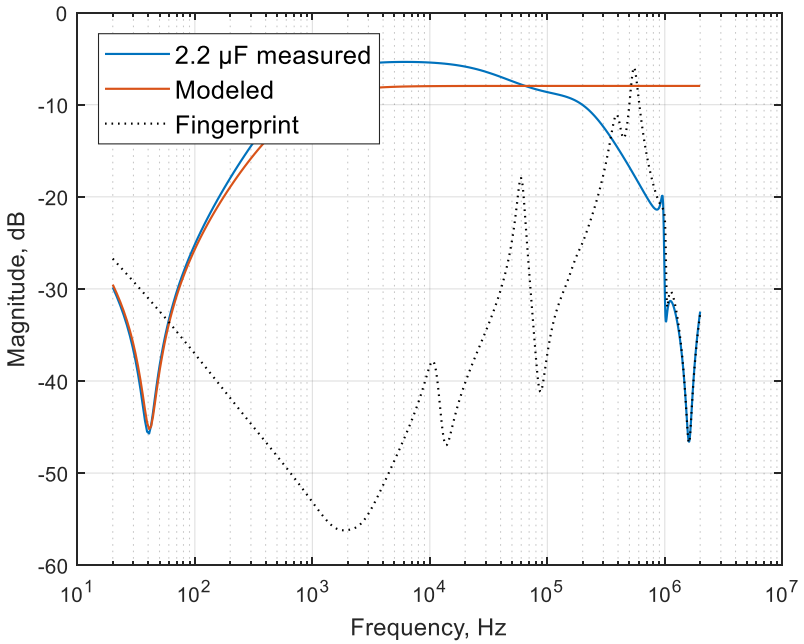

Figure 2.2.15 Comparison of measured and modeled 2200 nF parallel capacitances for a 350 VA transformer

2.3. Inductance

The external inductance is represented as a single inductor, and the impedance of this reactive element is calculated as in (13):

$$Z_L = jwL \tag{13}$$

This equation shows that the phase of this reactive impedance is 90°, and the value of the impedance is directly proportional to the electric signal oscillation frequency.

2.3.1. Series Inductance

A series inductance emulates the behavior of the inductive reactance of the frequency response analyzer connection cables. In case of cable torsion or twisting in circles, the inductive impedance from the connection setup comes into play. By varying the values of the series inductance, we can simulate different degrees of intervention in the system.

The connection scheme of the series inductor is presented in Figure 2.3.1:

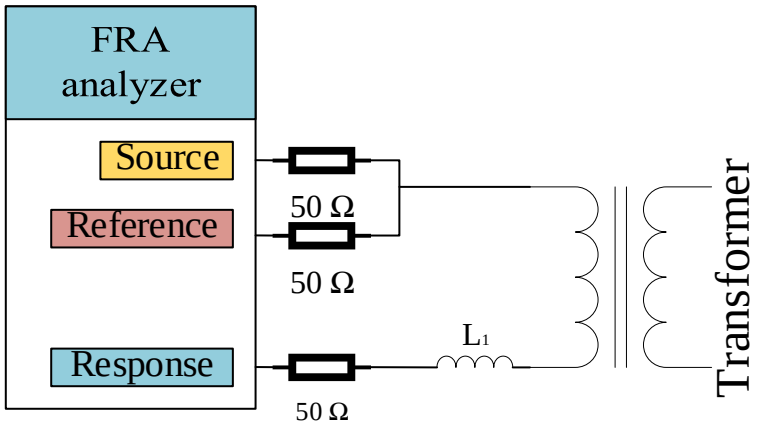

Figure 2.3.1 Series connection of an external inductance

The total impedance is calculated using (14):

$$Z_T = Z_W + Z_{L1} + Z_{cable} \tag{14}$$

where Z_T is the total impedance, Z_{L1} is the impedance of the inductor, and Z_{cable} is the cable impedance, which is 75 Ω. From the above equation, the total impedance will increase as the

frequency of the signal increases, which means that at higher frequencies, the fingerprint and the measured response will vary significantly. In addition, an increase in the external series inductance will lead to a greater deviation from the fingerprint. This trend is clearly visible in Figures 2.3.2 – 2.3.5. For the 22 µH external inductor in Figure 2.3.2, the fingerprint and measured response start diverging at 400 kHz. For the 110 µH external inductor in Figure 2.3.3, they start diverging at 120 kHz. As we increase the inductance further, the divergence of values starts at lower frequency.

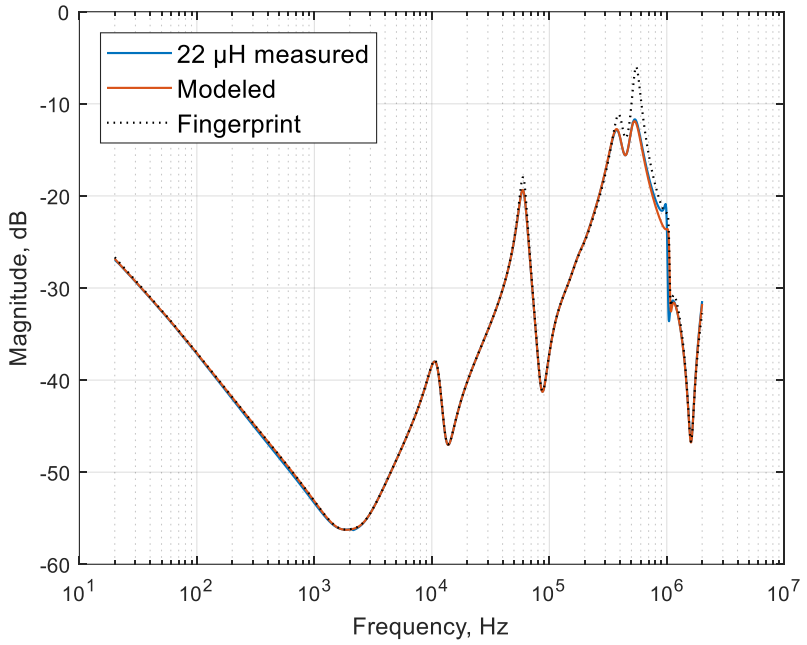

Figure 2.3.2 Comparison of measured and modeled 22 µH series inductances for a 350 VA transformer

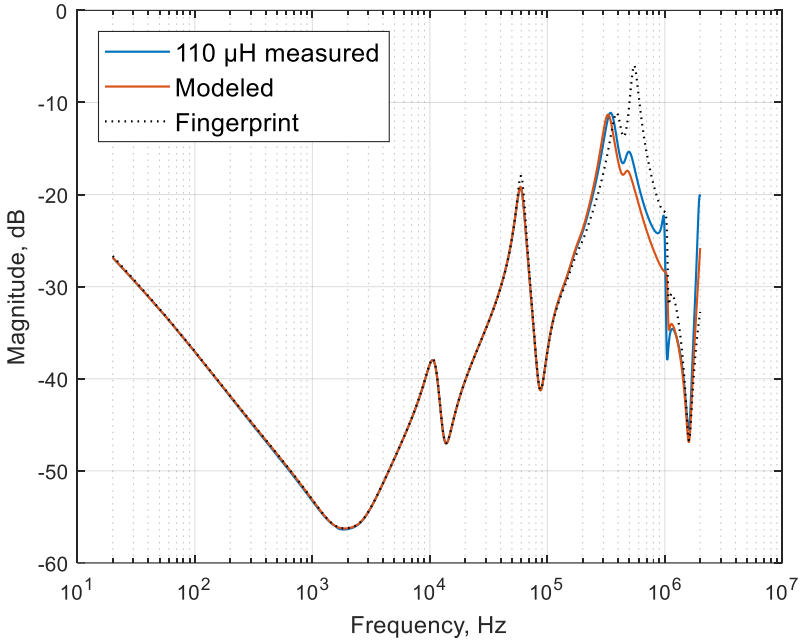

Figure 2.3.3 Comparison of measured and modeled 110 µH series inductances for a 350 VA transformer

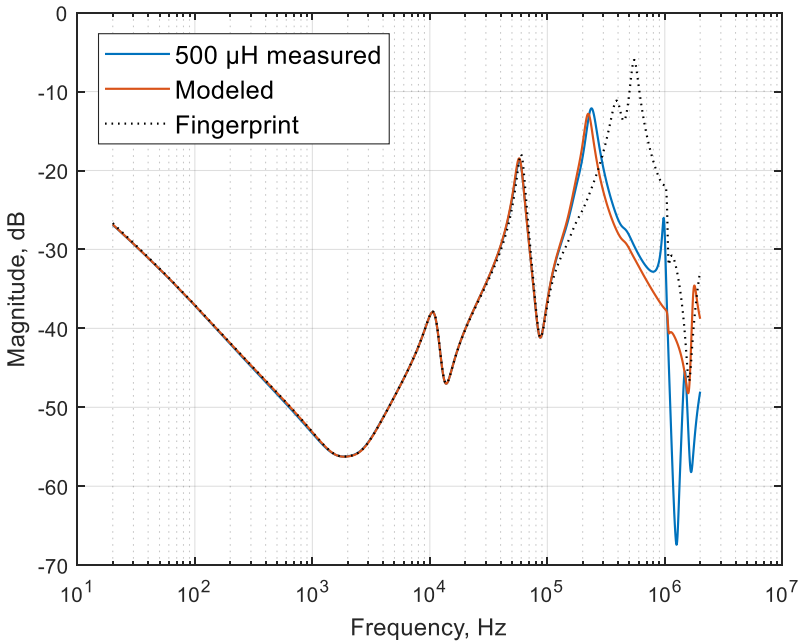

Figure 2.3.4 Comparison of measured and modeled 500 µH series inductances for a 350 VA transformer

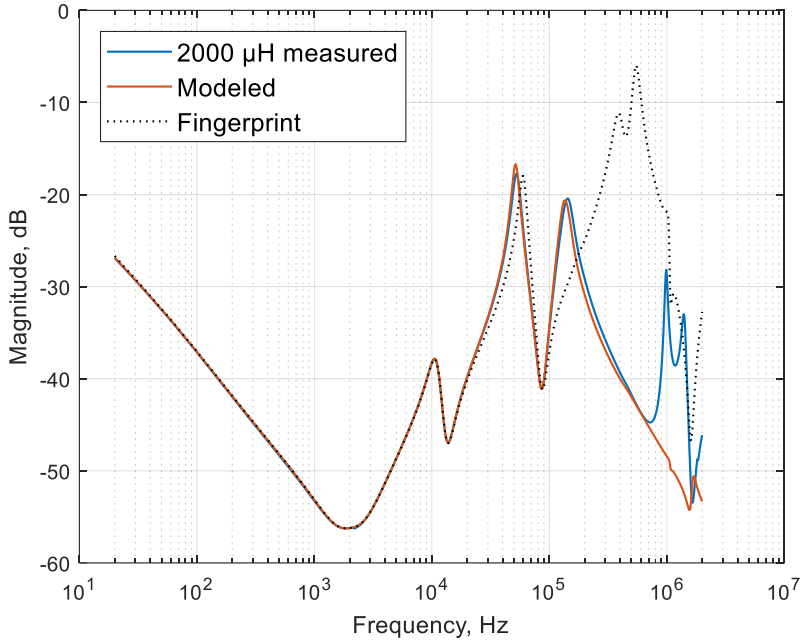

Figure 2.3.5 Comparison of measured and modeled 2000 µH series inductances for a 350 VA transformer

2.3.2. Shunt Inductance

A shunt inductance emulates the inductive leakage from the winding terminals. Unlike the capacitive leakage, the inductive leakage decreases as the frequency of the signal increases. The connection scheme is presented in Figure 2.3.6.

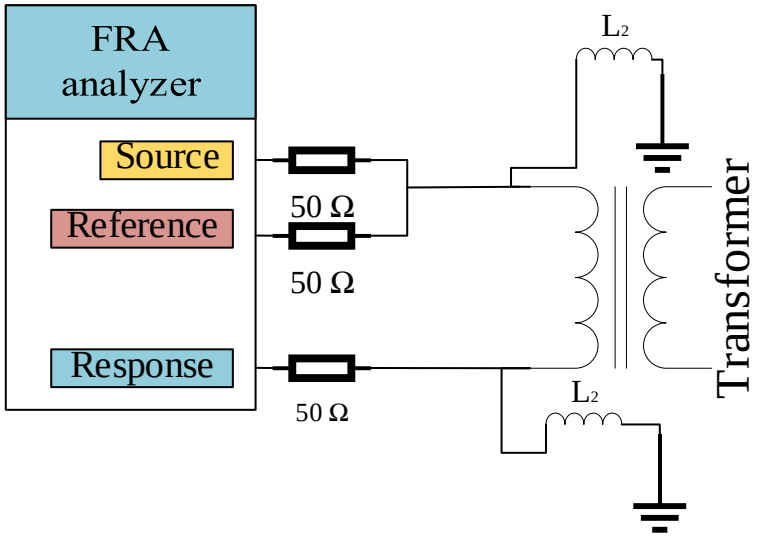

Figure 2.3.6 Shunt connection of an external inductance

The total impedance of the system in this scenario is calculated using (15):

$$Z_T = 75 + Z_W + \frac{2500Z_{L2} + 1250Z_W + 75Z_W Z_{L2}}{Z_{L2}^2}. \tag{15}$$

From the above equation, if the frequency of the signal or the value of the external inductor increases, then the total impedance will tend to $75+Z_W$, which is the fingerprint frequency response of the system. This tendency is seen from Figures 2.3.7 – 2.3.10.

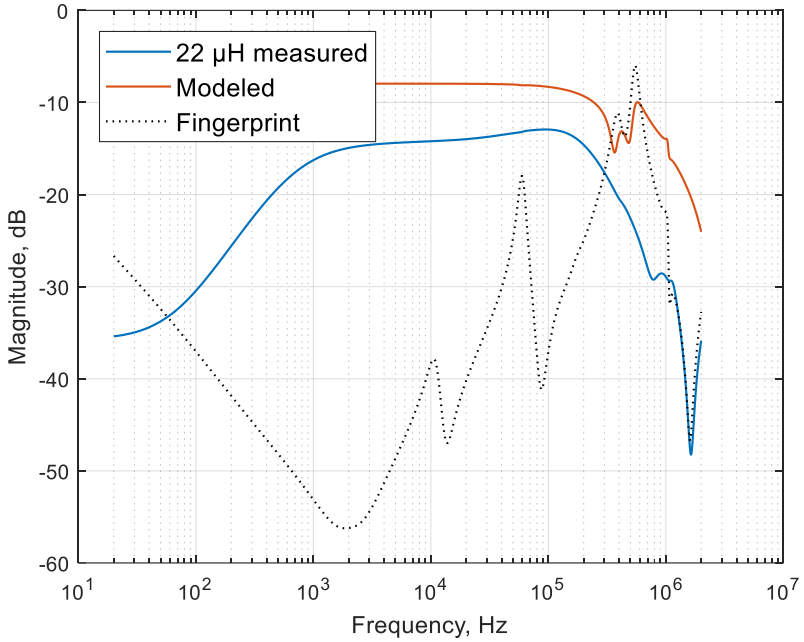

Figure 2.3.7 Comparison of measured and modeled 22 µH shunt inductances for a 350 VA transformer

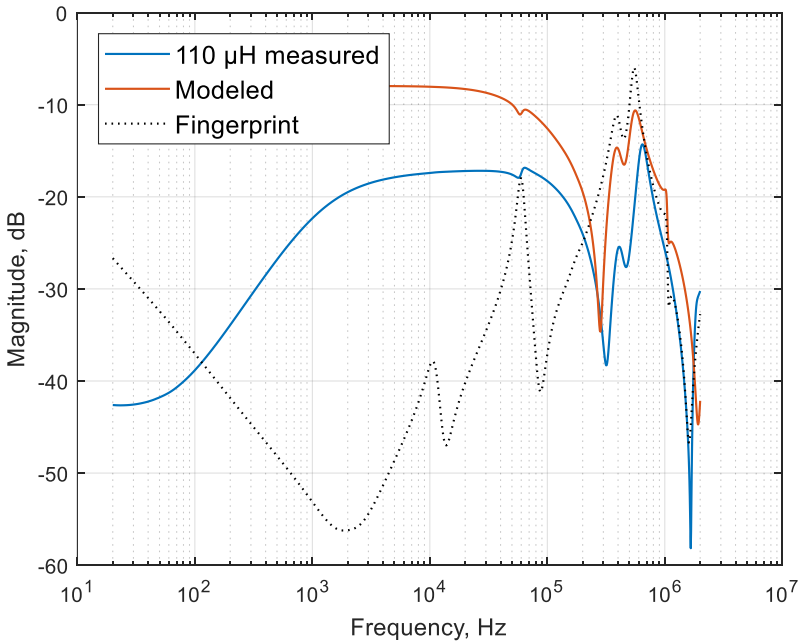

Figure 2.3.8 Comparison of measured and modeled 110 µH shunt inductances for a 350 VA transformer

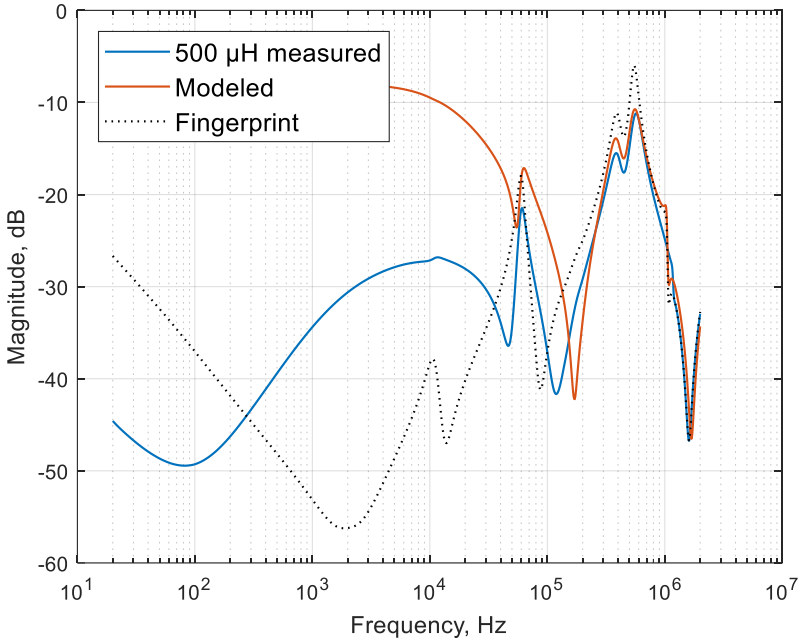

Figure 2.3.9 Comparison of measured and modeled 500 µH shunt inductances for a 350 VA transformer

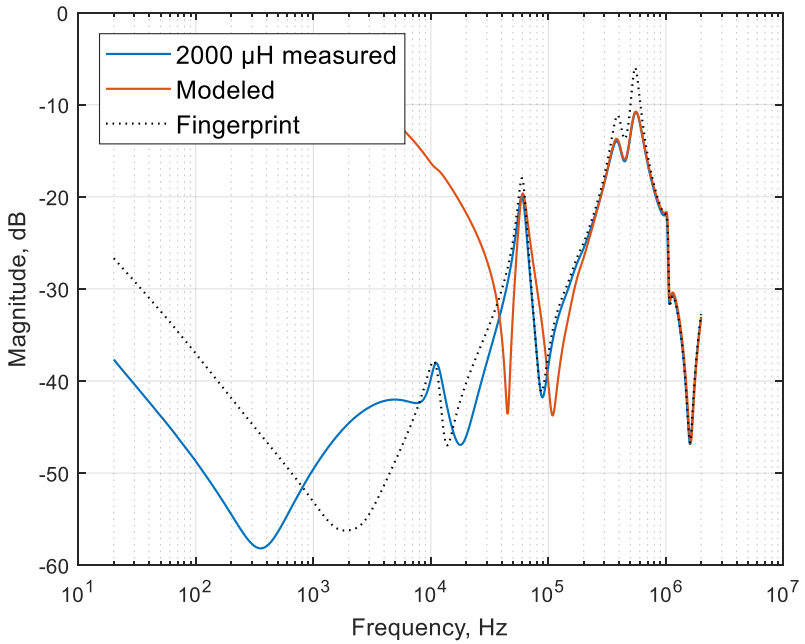

Figure 2.3.10 Comparison of measured and modeled 2000 µH shunt inductances for a 350 VA transformer

2.3.3. Parallel Inductance

A parallel inductance simulates the transformer winding variable degree of a SC. At low frequencies, the SC level is high, while at high frequencies, the SC level is low due to the direct relationship of the inductive reactance with the signal frequency. The connection scheme of this scenario is presented in Figure 2.3.11.

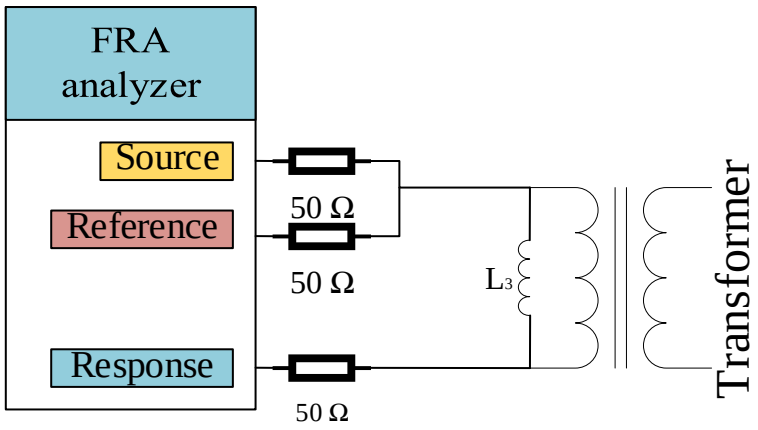

Figure 2.3.11 Parallel connection of an external inductance

The total impedance of the system is calculated as in (16):

$$Z_T = 75 + \frac{Z_W Z_{L3}}{Z_W + Z_{L3}} \tag{16}$$

From the above equation, if $Z_W << Z_{L3}$, then the total impedance will tend to $75 + Z_W$. The impedance of the external inductor increases with the frequency of the signal; hence, at higher frequencies, the fingerprint and the measured response will match. This behavior is visible in Figures 2.3.12 – 2.3.15

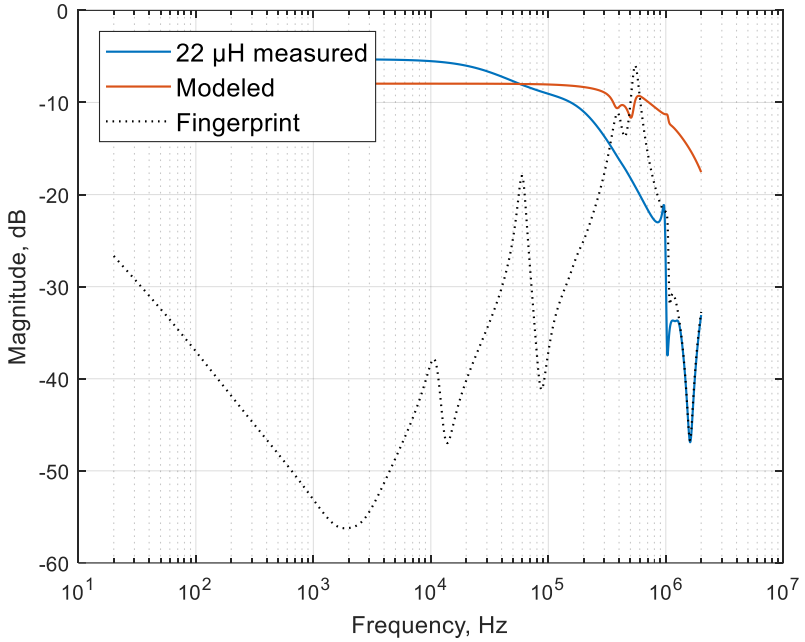

Figure 2.3.12 Comparison of measured and modeled 22 µH parallel inductances for a 350 VA transformer

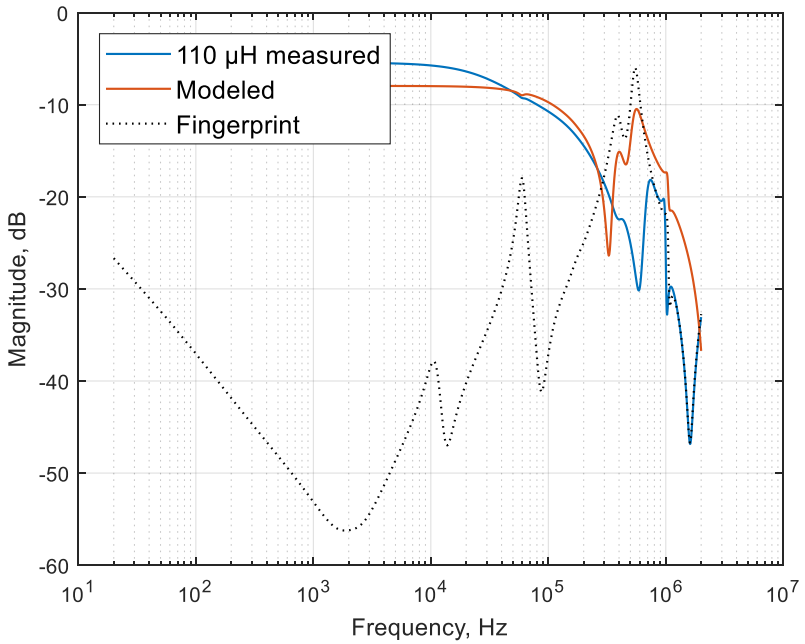

Figure 2.3.13 Comparison of measured and modeled 110 µH parallel inductances for a 350 VA transformer

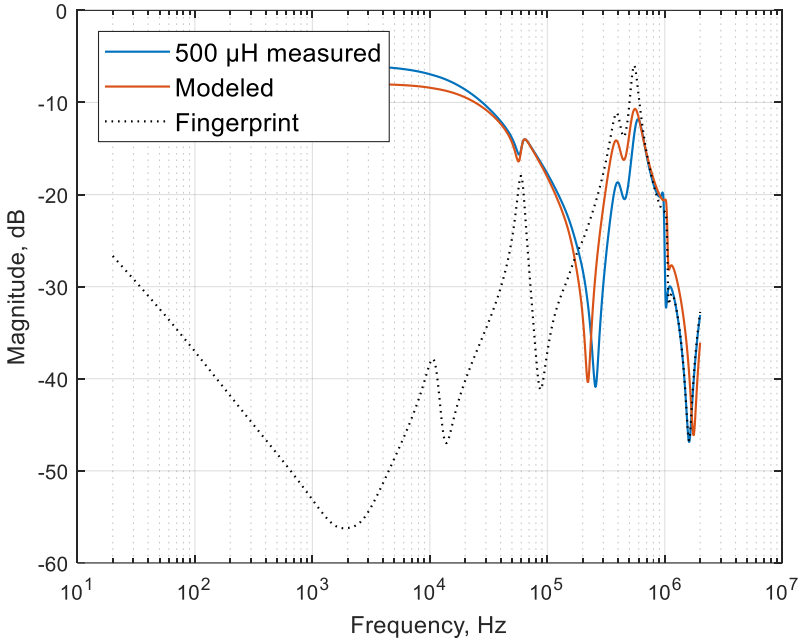

Figure 2.3.14 Comparison of measured and modeled 500 µH parallel inductances for a 350 VA transformer

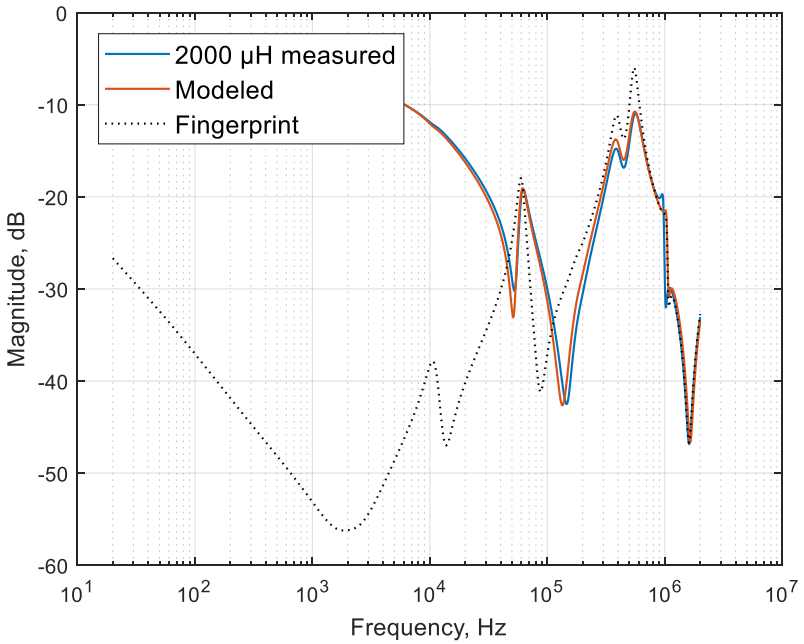

Figure 2.3.15 Comparison of measured and modeled 2000 µH parallel inductances for a 350 VA transformer

CHAPTER 3. TREND ANALYSIS

This chapter shows the behavior of a transformer winding with an external impedance connected. The trend of the changes is given for each test object for every connection configuration.

3.1 Resistance

This part of the chapter analyzes the influence of the resistor under different connection configurations on the following test objects: 40 kVA, 20 kVA, 760 VA and 350 VA power transformers.

3.1.1 40 kVA Power Transformer

The series resistance connection behavior for the 40 kVA transformer is shown in Figure 3.1.1. For small resistances, the frequency response differs from the fingerprint at very high frequencies above 1 MHz, while as the resistor value increases, the affected frequency region expands. For example, the addition of a 4 kΩ resistor causes a deviation from the original response starting at 20 kHz.

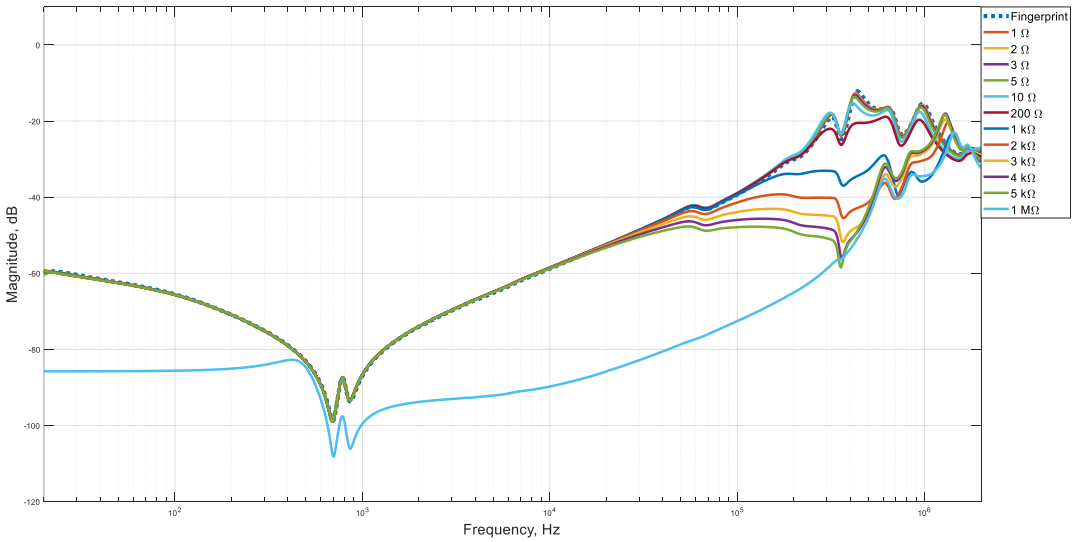

Figure 3.1.1 Response of the 40 kVA power transformer with a series resistance connection

The shunt connection of resistors affects the 40 kVA transformer frequency response, as demonstrated in Figure 3.1.2. The figure shows that low resistances affect the response to a larger extent compared to higher resistances. For instance, the response for the 200 Ω addition lies close to the fingerprint, whereas the response for the 2 Ω addition is significantly different from the original response.

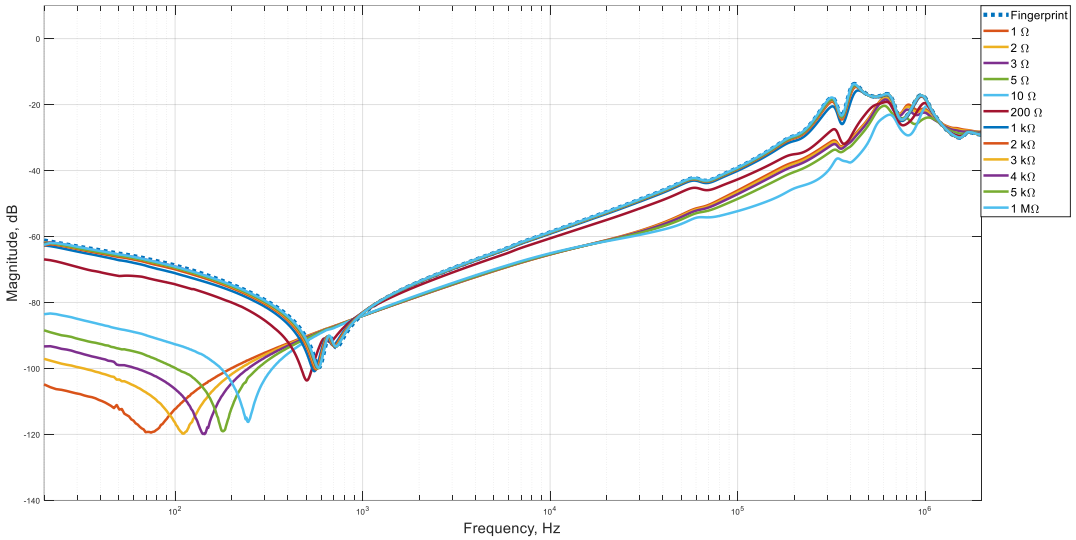

Figure 3.1.2 Response of the 40 kVA power transformer with a shunt resistance connection

The parallel resistance connection demonstrates the response of the test object under winding end-to-end SC conditions. The response of the transformer is depicted in Figure 3.1.3. The high frequency band for all measurements in this scenario is unaffected, and as the value of the resistance increases, the response approaches the fingerprint.

The behaviors of the remaining test objects are similar to the trend demonstrated for the 40 kVA transformer, but the frequency band over which the resistor affects the response changes with the test object.

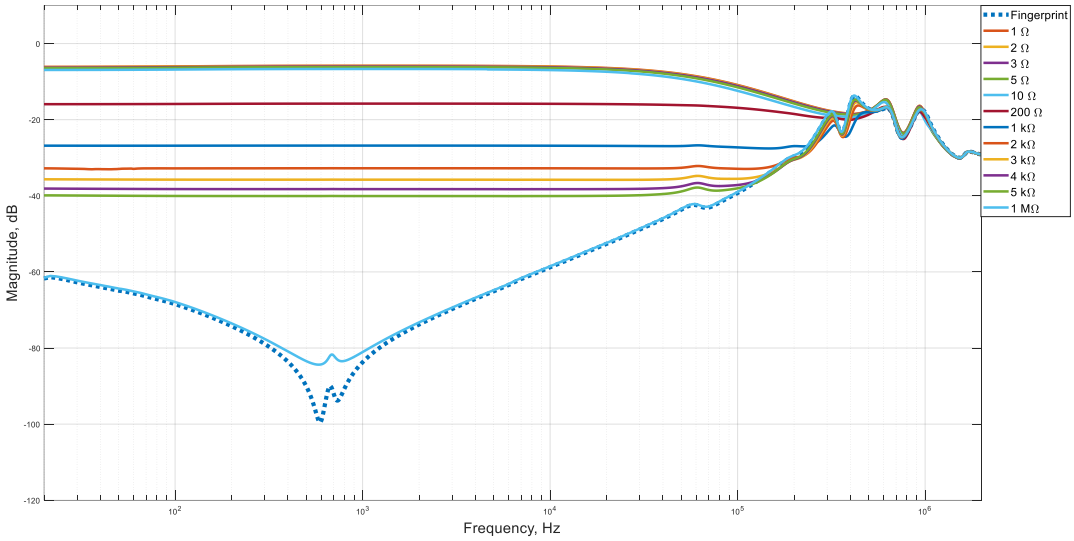

Figure 3.1.3 Response of the 40 kVA power transformer with a parallel resistance connection

3.1.2 20kVA Power Transformer

The series connection of a resistor for this test object affects the frequency response of the transformer as shown in Figure 3.1.4. Unlike the response of the 40 kVA transformer, the series resistance affects both the high and low frequency bands, as discussed in Chapter 2.1.1. This is also true for the remaining test objects due to the lower total impedance.

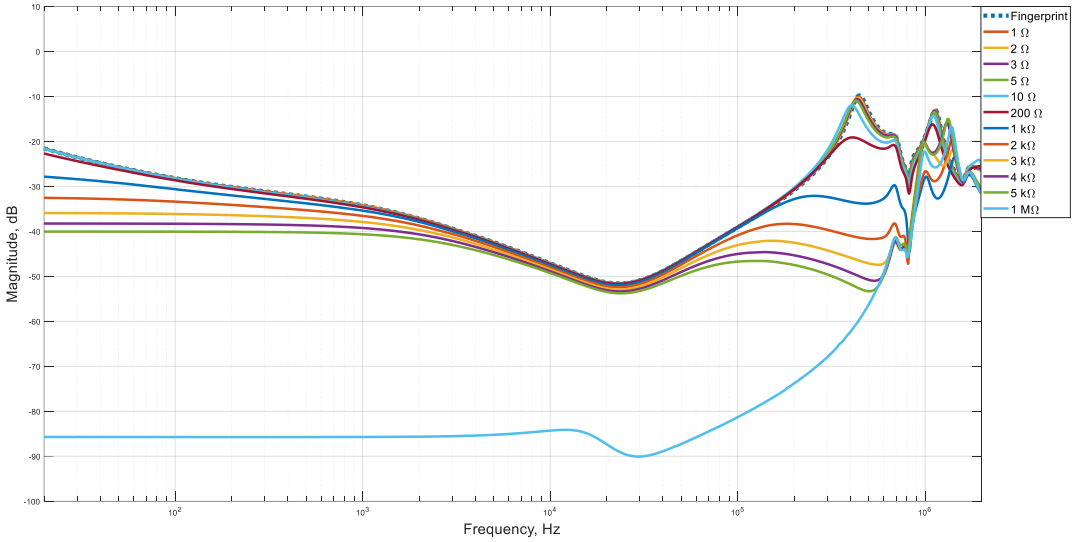

Figure 3.1.4 Response of the 20 kVA power transformer with a series resistance connection

The shunt resistance behavior of the 20 kVA transformer is demonstrated in Figure 3.1.5. The response for the 5 Ω resistance lies beyond the fingerprint, reaching the lowest point at -65 dB, while the 5 kΩ response is very close to the original one.

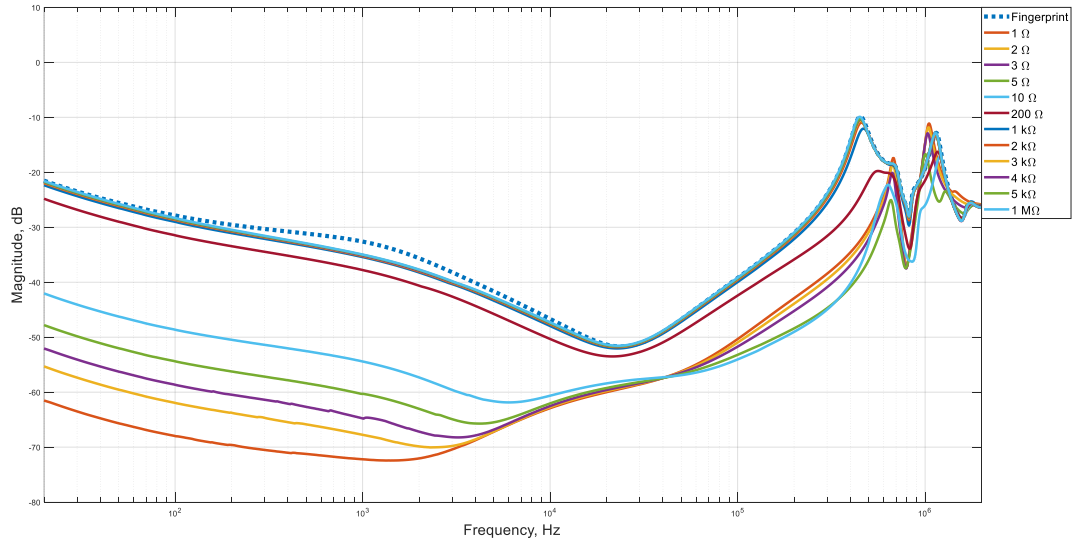

Figure 3.1.5 Response of the 20 kVA power transformer with a shunt resistance connection

The parallel resistance response for the 20 kVA transformer is shown in Figure 3.1.6. The region that is unaffected by the parallel resistance starts at 1.2 MHz.

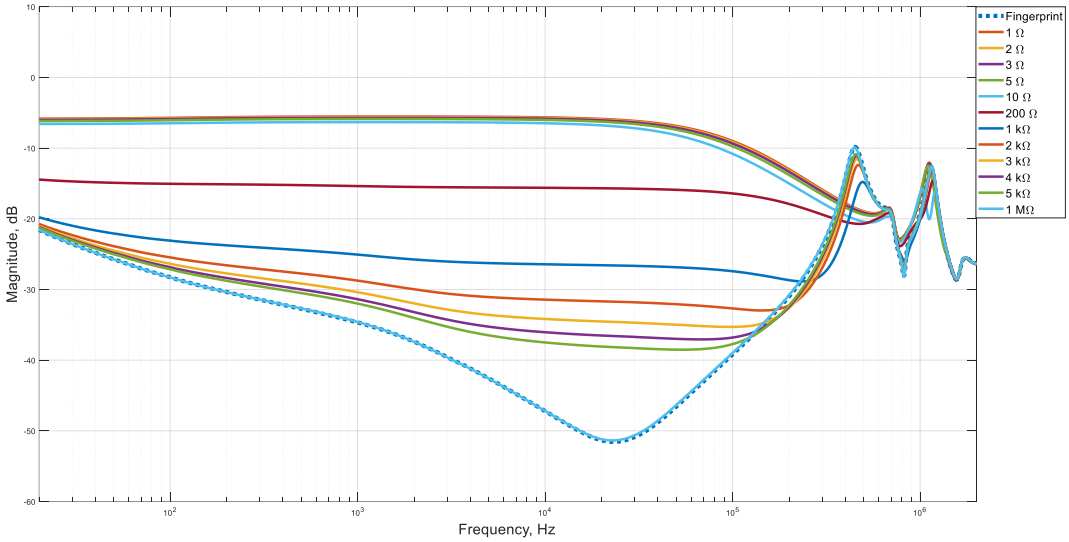

Figure 3.1.6 Response of the 20 kVA power transformer with a parallel resistance connection

3.1.3 760 VA Power Transformer

The series resistor response of the 760 VA transformer is depicted below in Figure 3.1.7. For this test object, the series resistor also affects the low and high frequency bands. The deviation from the fingerprint increases with increasing resistor value.

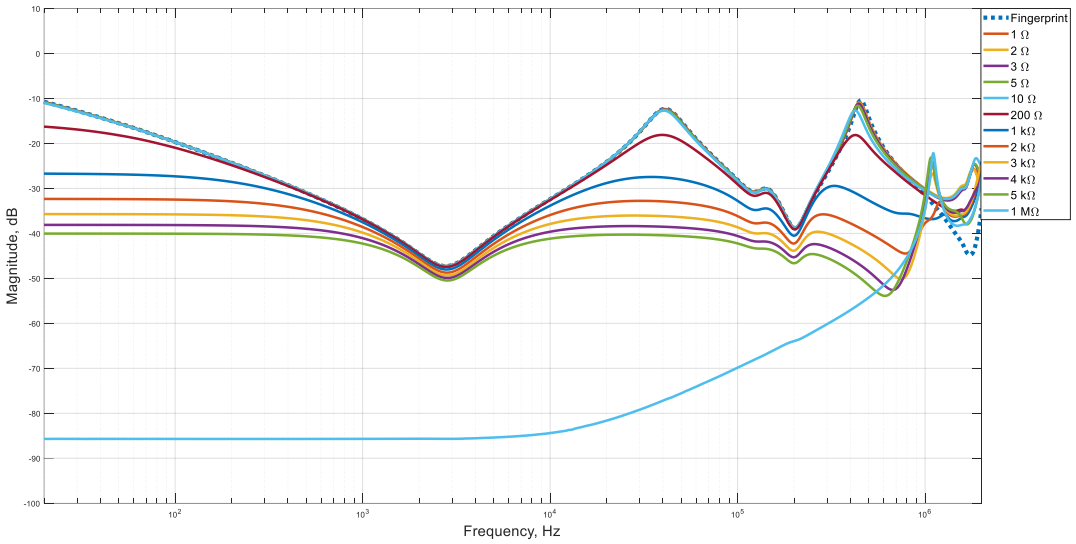

Figure 3.1.7 Response of the 760 VA power transformer with a series resistance connection

The addition of a shunt resistor affect the frequency response of the 760 VA transformer as shown in Figure 3.1.8. An increasing resistance value reduces the deviation of the response from the fingerprint.

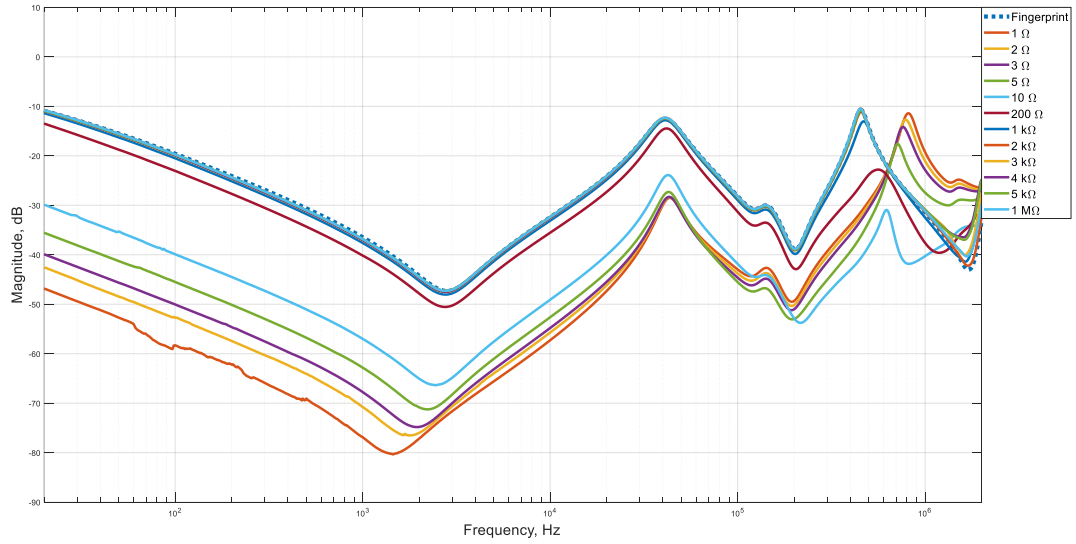

Figure 3.1.8 Response of the 760 VA power transformer with a shunt resistance connection

The behavior of this test object with an additional parallel resistance is demonstrated in Figure 3.1.9. Low resistance values more strongly affect the frequency response than higher resistance values.

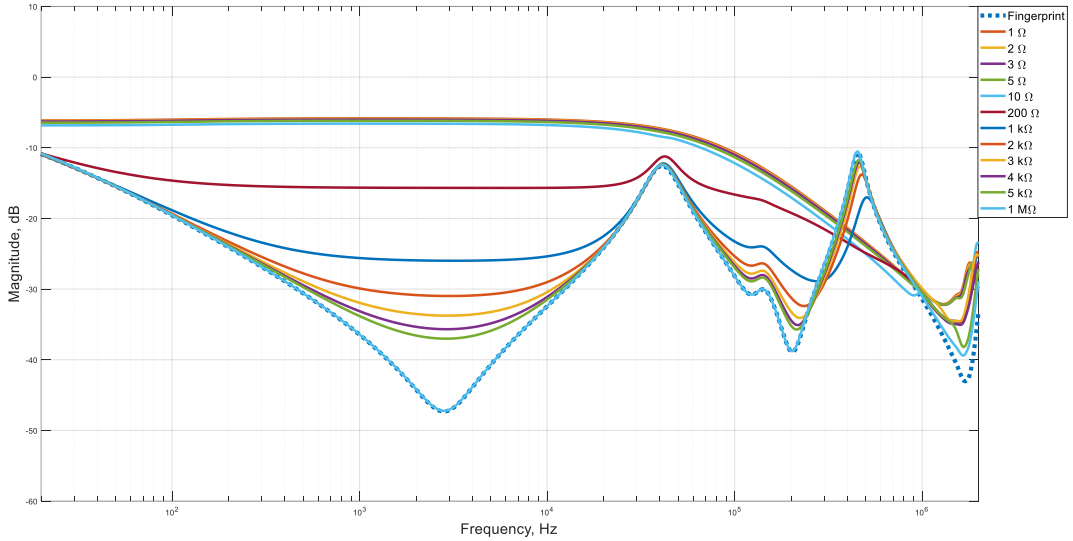

Figure 3.1.9 Response of the 760 VA power transformer with a parallel resistance connection

3.1.4 350 VA Power Transformer

The series resistor addition for this transformer also affects the low and high frequency bands of the frequency response. The response is shown in Figure 3.1.10.

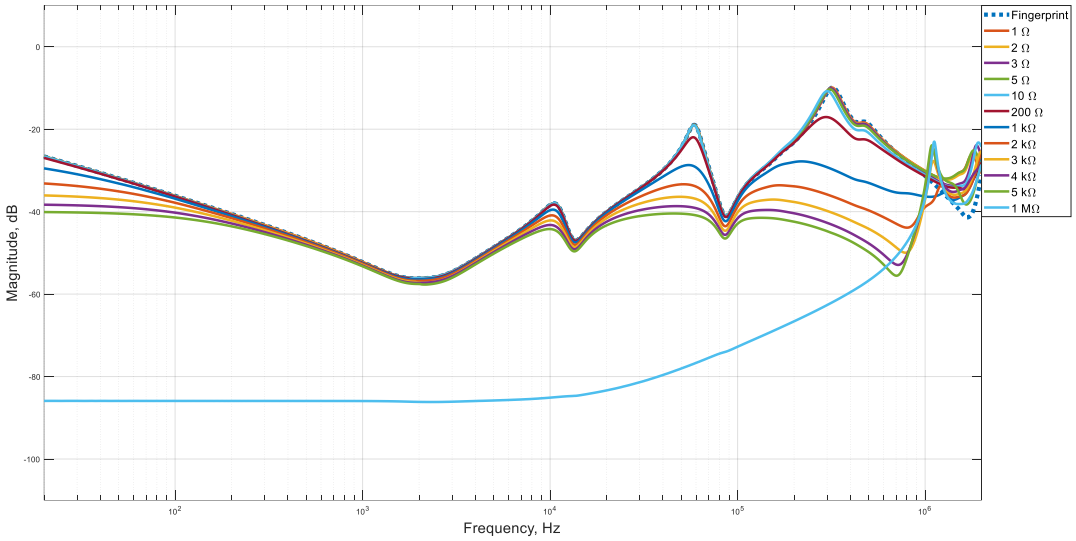

Figure 3.1.10 Response of the 350 VA power transformer with a series resistance connection

The additional shunt resistance response is shown in Figure 3.1.11. A lower resistance value shifts the curve downwards at low and mid-frequencies. As the resistor value increases, the response deviates less from the fingerprint.

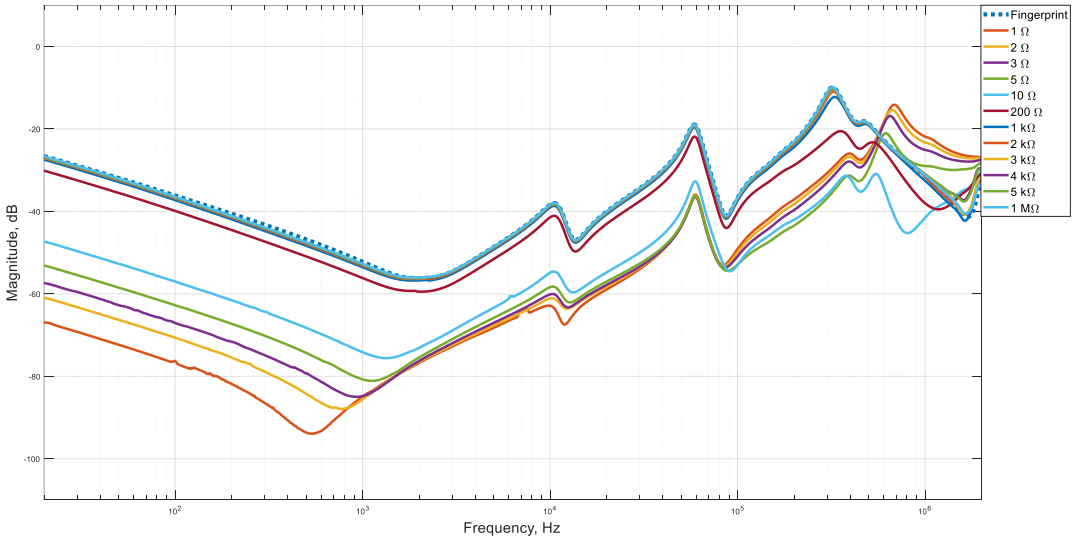

Figure 3.1.11 Response of the 350 VA power transformer with a shunt resistance connection

The SC behavior of the transformer winding is demonstrated in Figure 3.1.12. The influence of lower resistances on the frequency response is more significant than the influence of higher resistances.

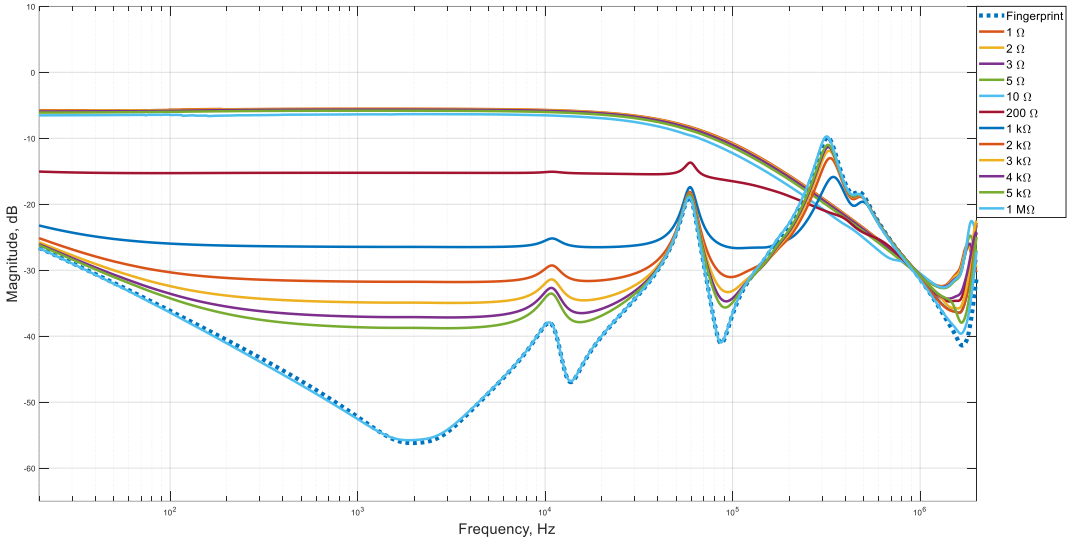

Figure 3.1.12 Response of the 350 VA power transformer with a parallel resistance connection

3.2 Capacitance

This part of the chapter analyzes the influence of an external capacitance on the frequency response signature of the test objects.

3.2.1 40 kVA Power Transformer

The series capacitance has the greatest influence on the lower frequency band of the response of the 40 kVA transformer, as shown in Figure 3.2.1. The first antiresonant point is shifted from -100 dB to -112 dB for the 100 pF series capacitance. As the value of the capacitor increases, the response signature moves towards the fingerprint.

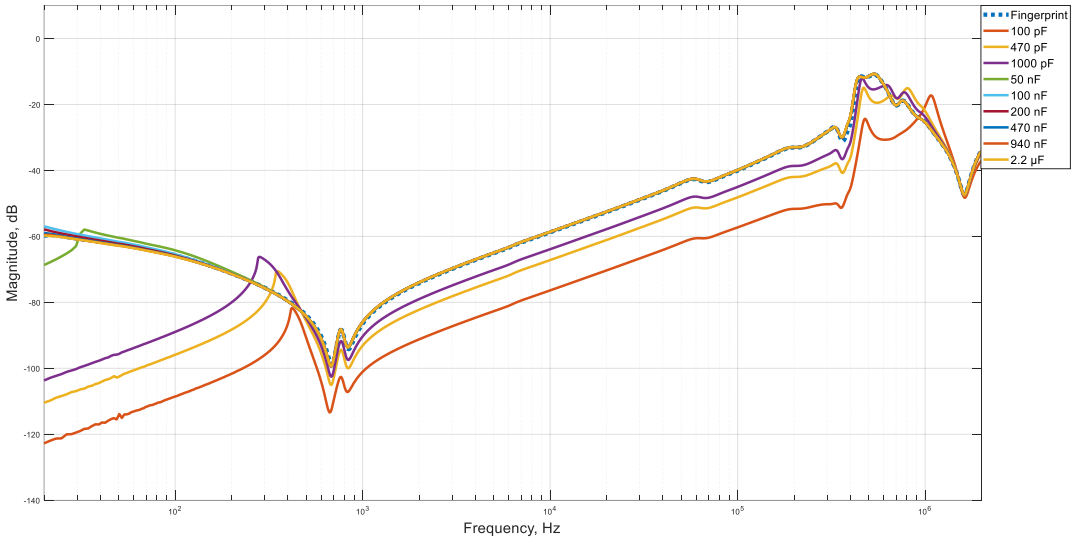

Figure 3.2.1 Response of the 40 kVA power transformer with a series capacitance connection

For the shunt capacitance responses in Figure 3.2.2, the larger the capacitance is, the greater the deviations of the response from the fingerprint. In addition, at some capacitor values, the value of the response crosses the 0 dB point, which means that the impedance of the system is negative. For instance, for the 2.2 µF shunt capacitance, the value of the response is greater than 0 dB within the 7 kHz to 9 kHz frequency range. This phenomenon can be due to the manufacturing techniques of an FRA analyzer. The analyzer may not be designed for measuring the response of test objects with shunt capacitances of this values, and the internal circuitry of the equipment cannot account for such an intervention in the system.

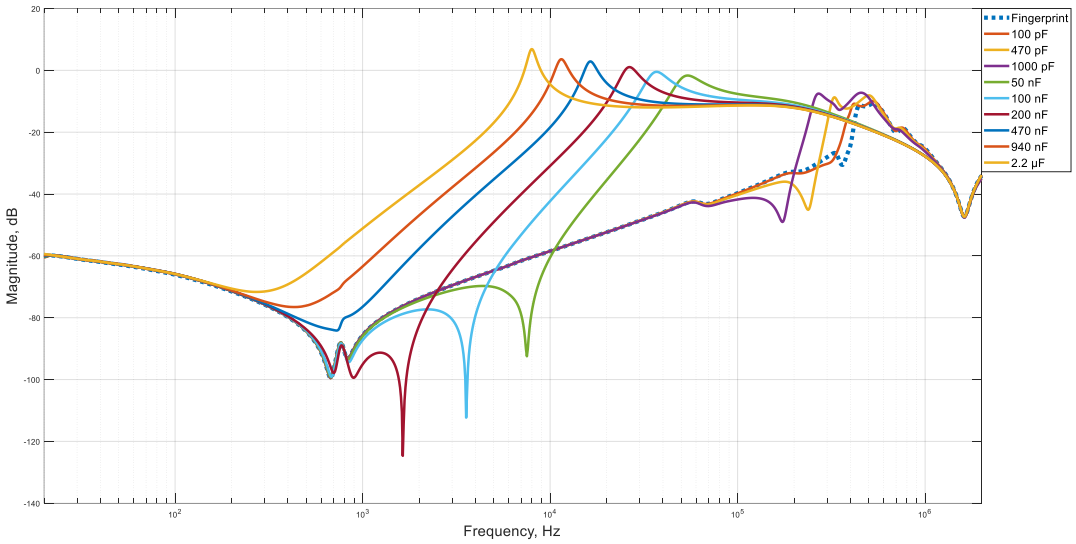

Figure 3.2.2 Response of the 40 kVA power transformer with a shunt capacitance connection

For the parallel capacitances in Figure 3.2.3, the very high frequency band above 1.2 MHz is unaffected by the parallel capacitance. As the value of the capacitive impedance decreases with increasing frequency, the SC degree of the winding terminals increases with increasing frequency of the signal. This result means that the high frequency band of the response is less subjected to the parallel capacitance.

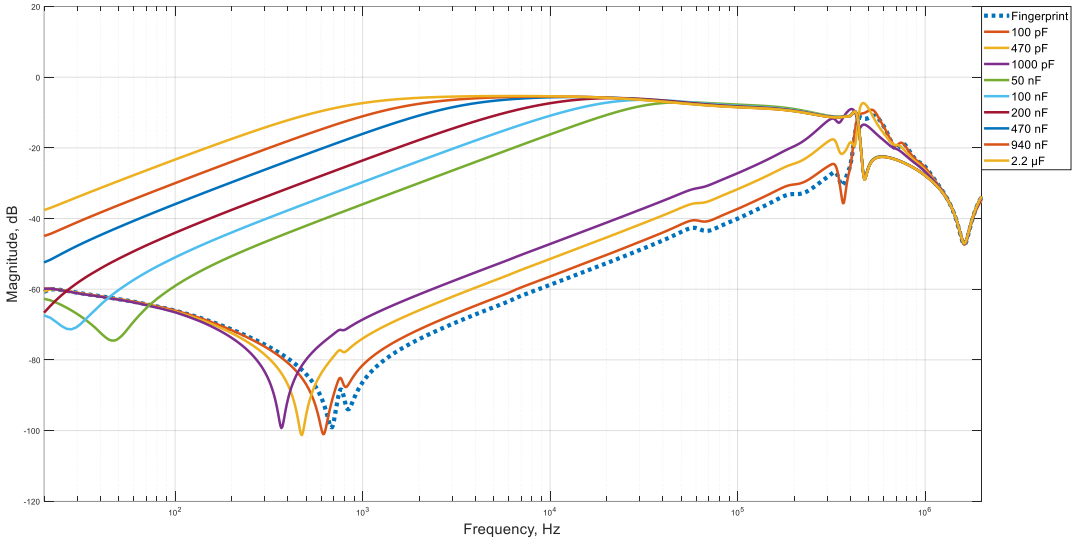

Figure 3.2.3 Response of the 40 kVA power transformer with a parallel capacitance connection

3.2.2 20 kVA Power Transformer

The response of the 20 kVA power transformer with a series capacitor is demonstrated in Figure 3.2.4, and the behavior is similar to that of the previous test object (40 kVA transformer). However, as the total impedance of the 20 kVA equipment is smaller than that of the 40 kVA equipment, the degree to which the capacitor affects the frequency response signature is greater.

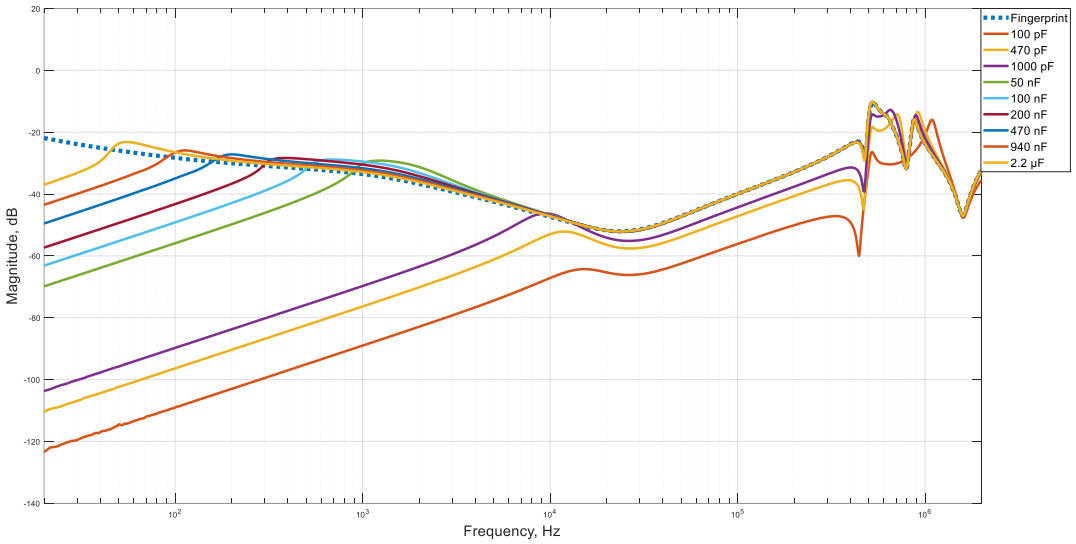

Figure 3.2.4 Response of the 20 kVA power transformer with a series capacitance connection

The shunt capacitance response is shown in Figure 3.2.5. We also observe a positive value on the graph at 200 nF, 470 nF, 940 nF and 2.2 µF.

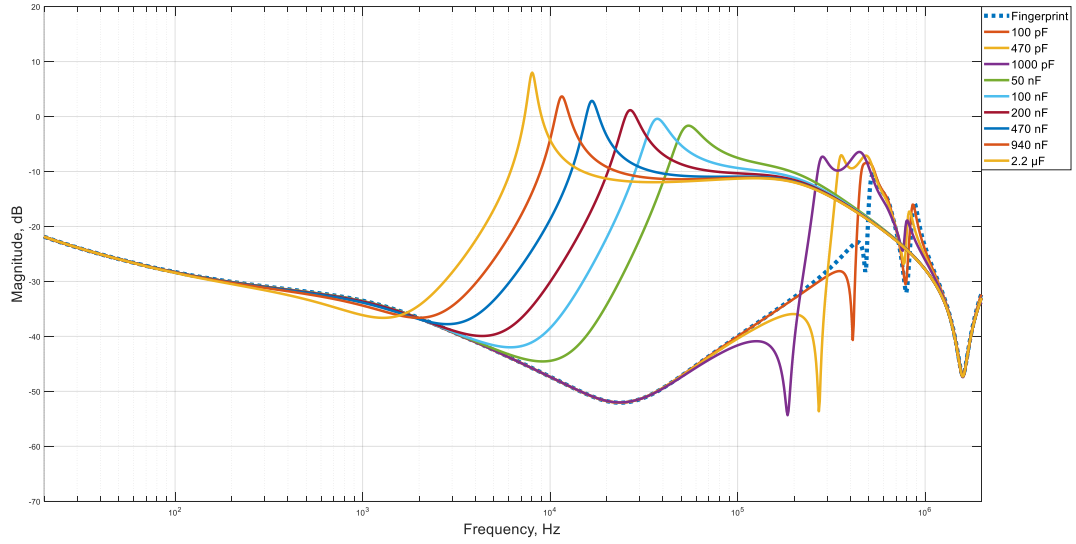

Figure 3.2.5 Response of the 20 kVA power transformer with a shunt capacitance connection

For the parallel capacitance response of the 20 kVA power transformer shown in Figure 3.2.6, the unaffected region of the response starts at 1.2-1.3 MHz.

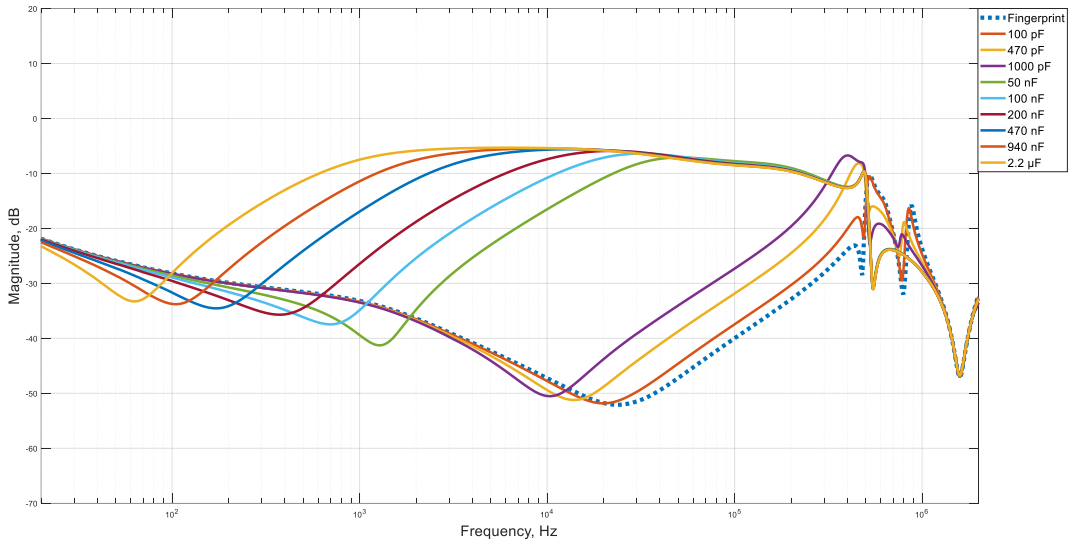

Figure 3.2.6 Response of the 20 kVA power transformer with a parallel capacitance connection

3.2.3 760 VA Power Transformer

The results of the addition of a series capacitor to the 760 VA transformer are shown in Figure 3.2.7. The same behavior as for the previous test objects is obtained: an increase in the capacitor value decrease the deviation of the response curve from the original one.

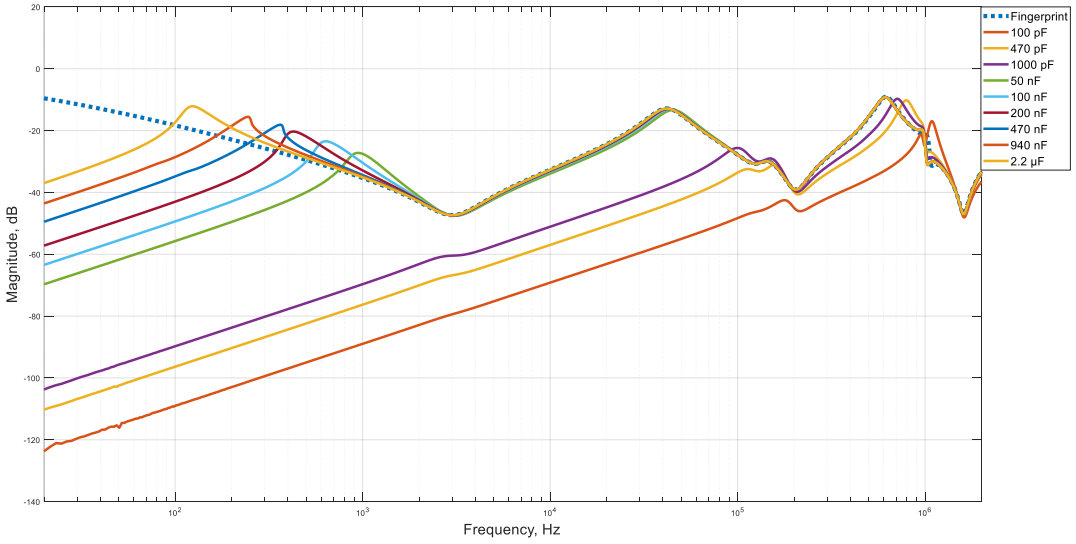

Figure 3.2.7 Response of the 760 VA power transformer with a series capacitance connection

The shunt capacitor scenario for the 760 VA test object also leads to a positive value of the response at 200 nF, 470 nF, 940 nF and 2.2 µF.

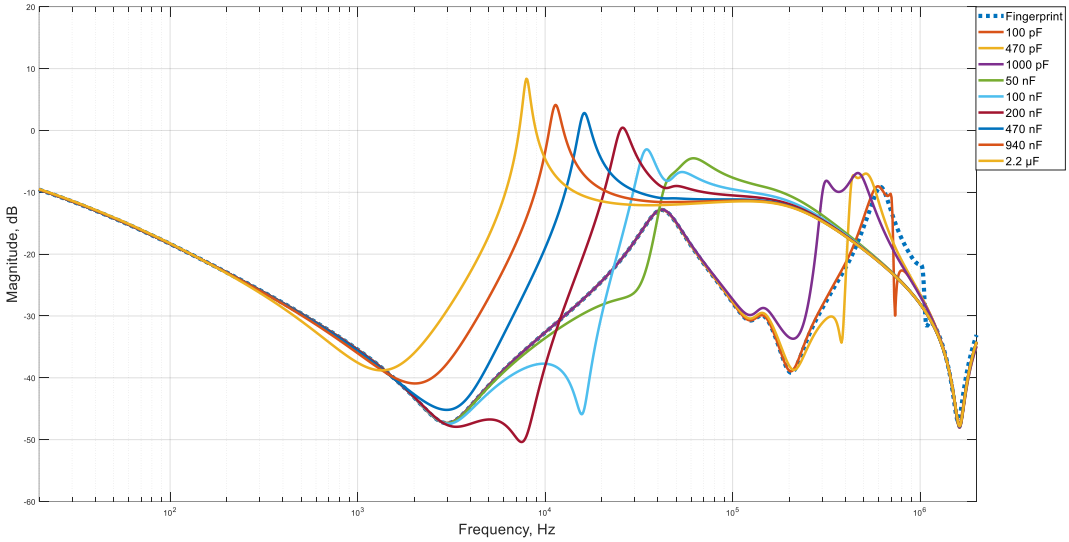

Figure 3.2.8 Response of the 760 VA power transformer with a shunt capacitance connection

For the case of the parallel capacitance effect on the 760 VA transformer, the region above 1 MHz is unaffected by the external capacitor, and the trend can be seen in Figure 3.2.9.

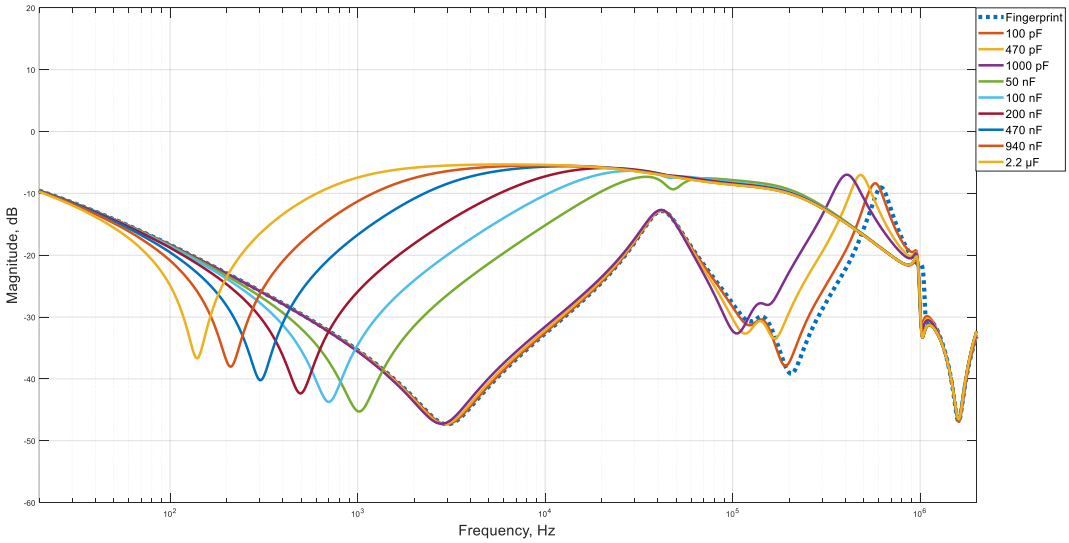

Figure 3.2.9 Response of the 760 VA power transformer with a parallel capacitance connection

3.2.4 350 VA Power Transformer

The same behavior for the 350 VA test object as for the previous test objects was observed: low capacitor values cause greater deviation of the curve than larger capacitor values. The trend can be seen in Figure 3.2.10.

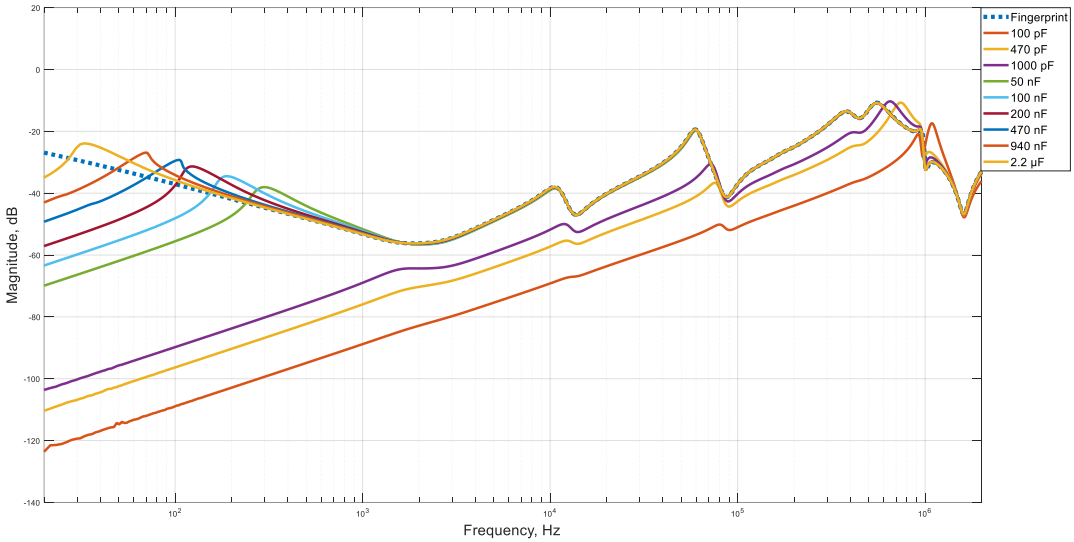

Figure 3.2.10 Response of the 350 VA power transformer with a series capacitance connection

The same capacitor values (200 nF, 470 nF, 940 nF and 2.2 µF) bring the frequency response signature to positive values.

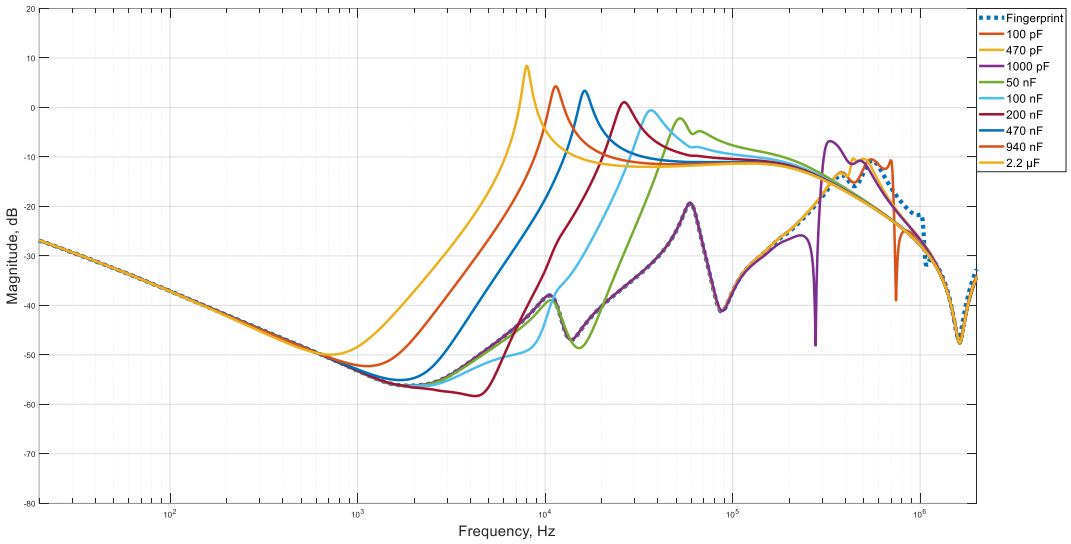

Figure 3.2.11 Response of the 350 VA power transformer with a shunt capacitance connection

For the parallel capacitance scenario, the region left unchanged from the fingerprint starts at approximately 1.2 MHz.

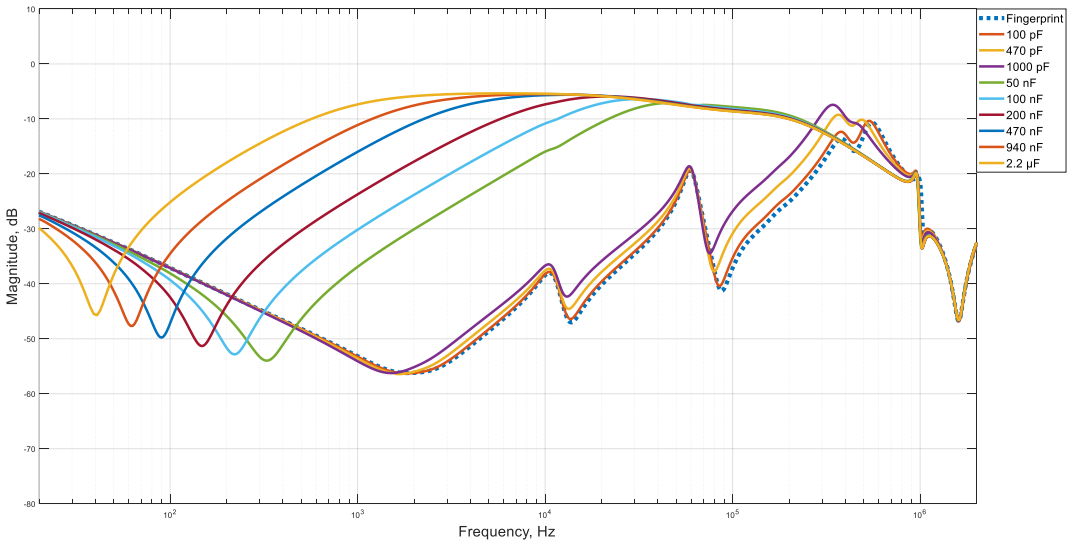

Figure 3.2.12 Response of the 350 VA power transformer with a parallel capacitance connection

3.3 Inductance

This part of the chapter demonstrates the impact of an external inductance connection on the transformer frequency response signature for the test objects.

3.3.1 40 kVA Power Transformer

The series inductance affects the higher frequency bands of the transformer frequency response. For the 40 kVA transformer, the FRA signature is as shown in Figure 3.3.1; as the inductance of the connection increases, the deviation of the response from the fingerprint increases. The 44 µH inductor addition affects the frequency band starting at 1.3 MHz, whereas the 2 mH inductor affects the curve above 40 kHz.

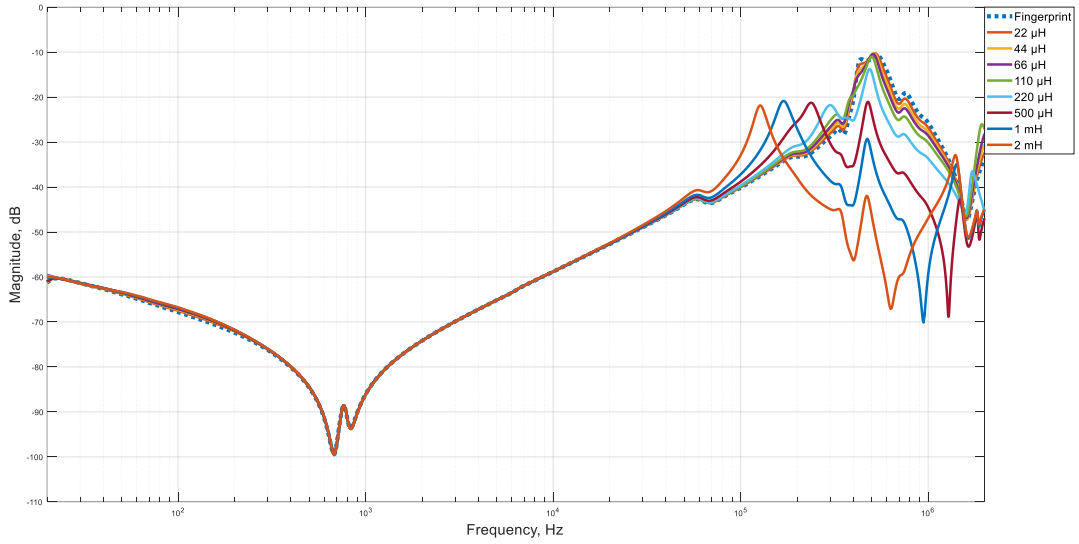

Figure 3.3.1 Response of the 40 kVA power transformer with a series inductance connection

The shunt inductance scenario does not affect the very high frequency region. The frequency region starting from 1.2 MHz is unchanged for all inductor values. This trend is visible in Figure 3.3.2.

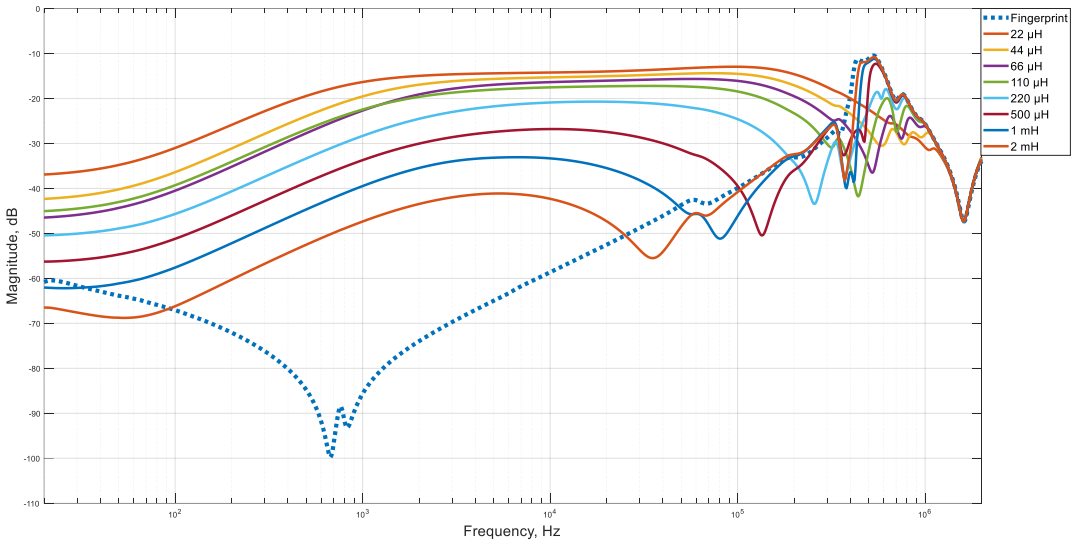

Figure 3.3.2 Response of the 40 kVA power transformer with a shunt inductance connection

The parallel inductance effect on the frequency response signature is similar to the resistive SC scenario, except that as the frequency increases, the SC level decreases, which is opposite to the capacitive impedance behavior. The behavior of the external inductance and trend are visible in Figure 3.3.3.

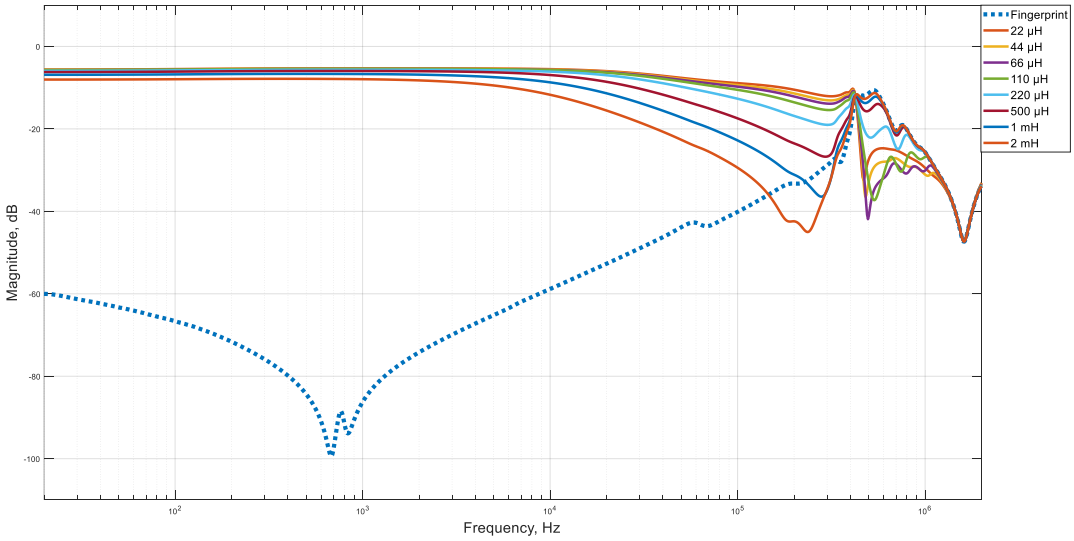

Figure 3.3.3 Response of the 40 kVA power transformer with a parallel inductance connection

3.3.2 20 kVA Power Transformer

The 20 kVA test object shows similar behaviors to the 40 kVA transformer. The changes in the signature appear starting at 40 kHz in Figure 3.3.4.

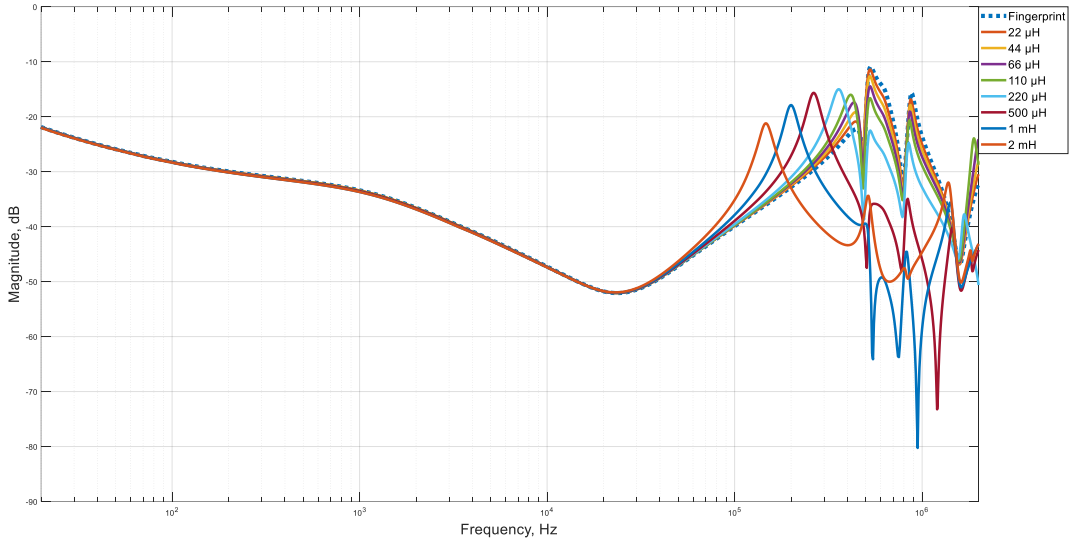

Figure 3.3.4 Response of the 20 kVA power transformer with a series inductance connection

The shunt inductance does not change the region beyond 1.3 MHz for the 20 kVA transformer. The trend is illustrated in Figure 3.3.5.

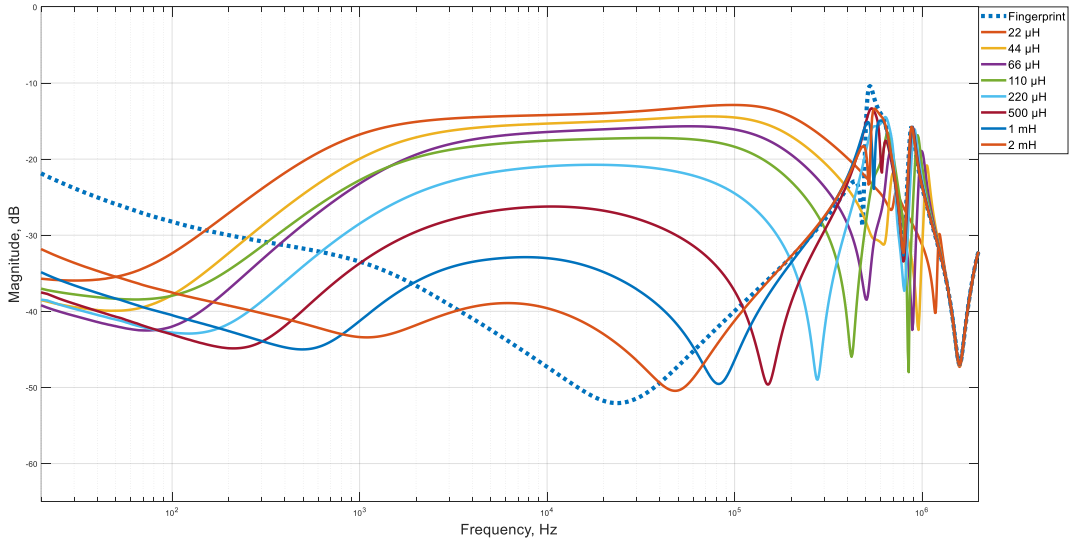

Figure 3.3.5 Response of the 20 kVA power transformer with a shunt inductance connection

The trend in the parallel inductance scenario for the 20 kVA test object is shown below in Figure 3.3.6.

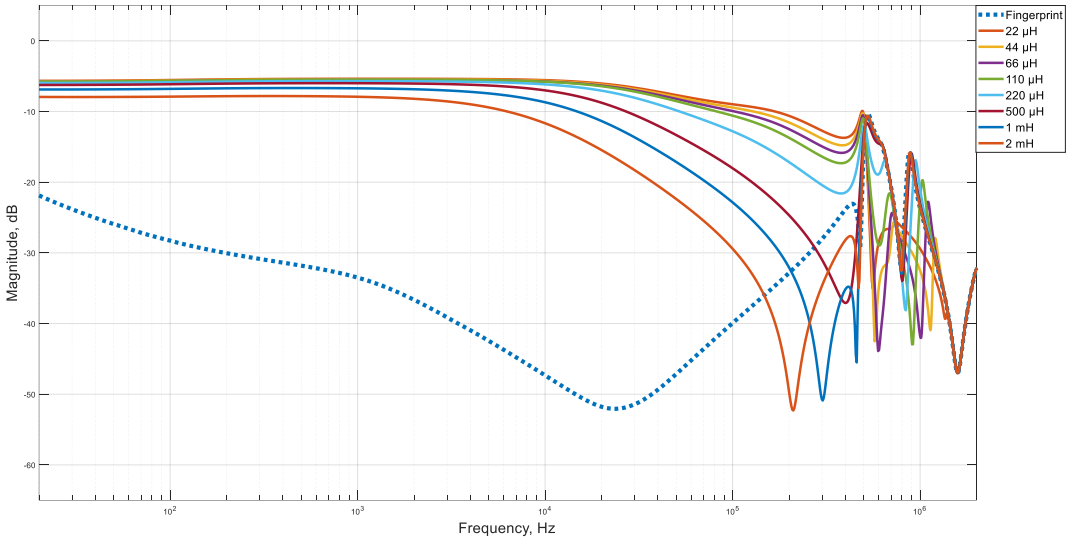

Figure 3.3.6 Response of the 20 kVA power transformer with a parallel inductance connection

3.3.3 760 VA Power Transformer

For smaller test objects, such as the 760 VA transformer, the series inductance more strongly affects the FRA signature. The frequency range starting at 10 kHz is altered by the external inductance. The trend is illustrated in Figure 3.3.7.

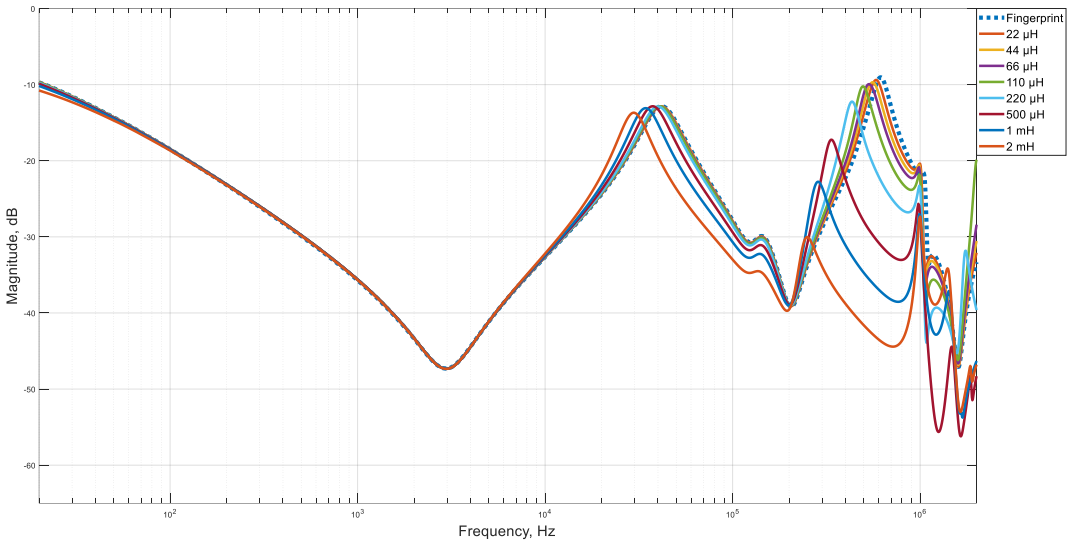

Figure 3.3.7 Response of the 760 VA power transformer with a series inductance connection

The frequency response signature for the 760 VA transformer in the shunt inductance scenario is shown in Figure 3.3.8.

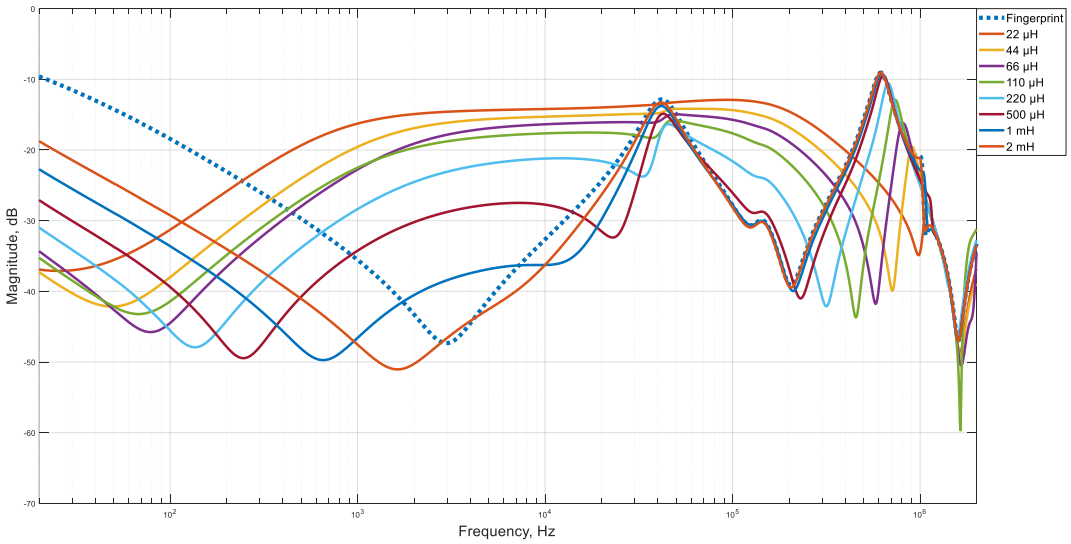

Figure 3.3.8 Response of the 760 VA power transformer with a shunt inductance connection

The inductive SC trend can be seen in Figure 3.3.9.

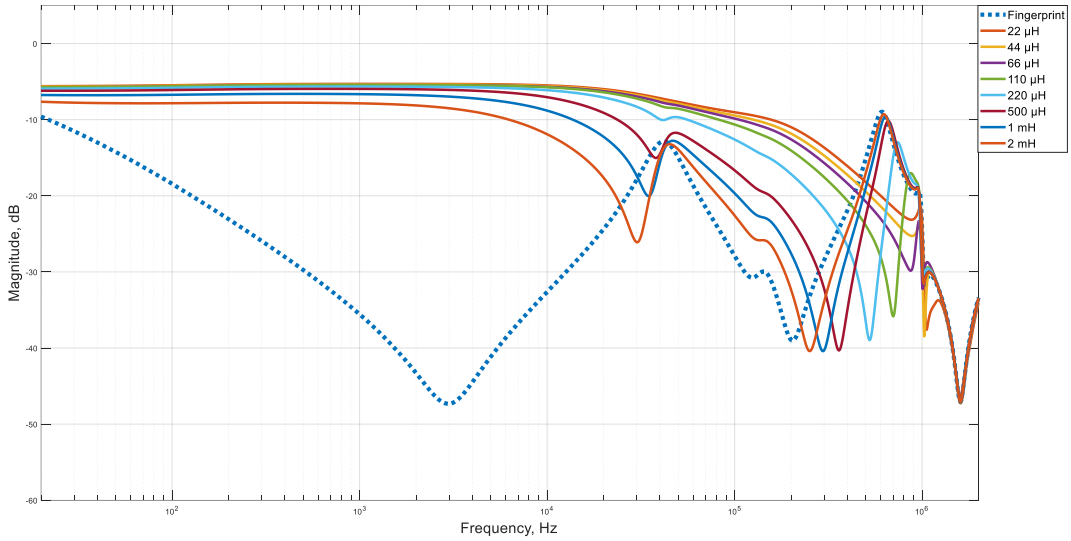

Figure 3.3.9 Response of the 760 VA power transformer with a parallel inductance connection

3.3.4 350 VA Power Transformer

The series inductance also affects the higher frequency range of the transformer frequency response signature. A larger inductor values increase the deviation from the fingerprint.

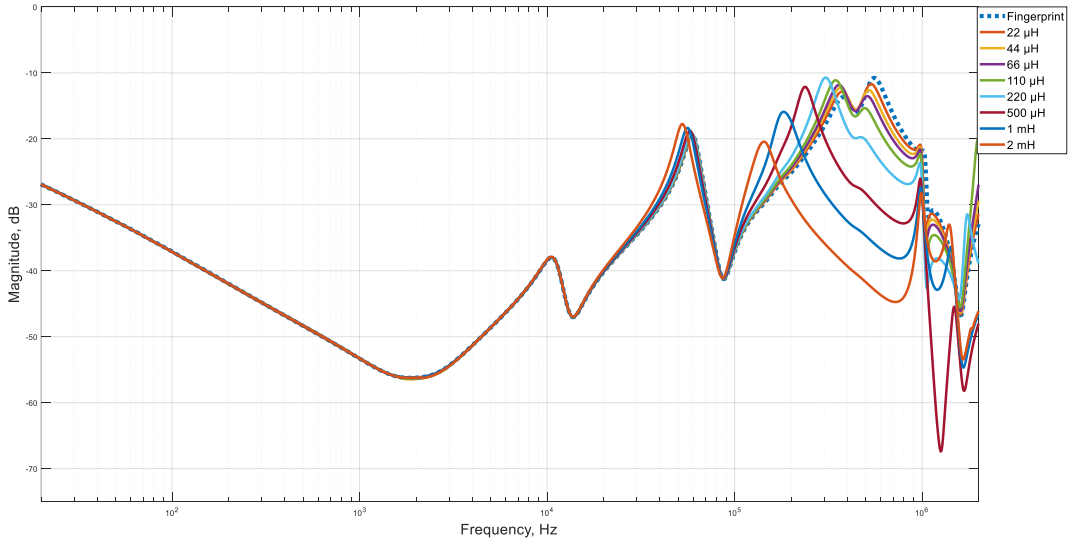

Figure 3.3.10 Response of the 350 VA power transformer with a series inductance connection

The trend of the frequency response signature with increasing shunt inductance is depicted in Figure 3.3.11.

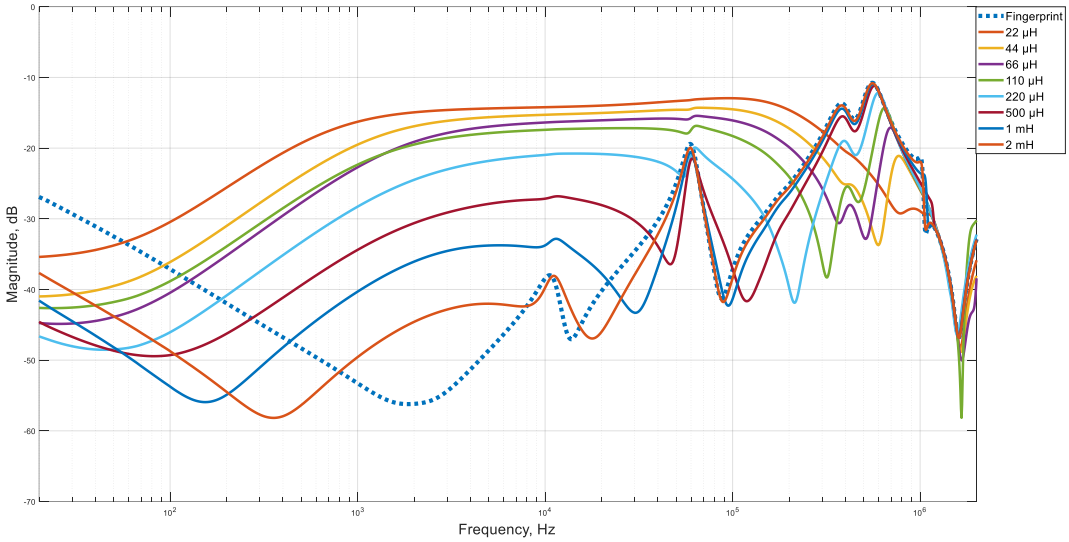

Figure 3.3.11 Response of the 350 VA power transformer with a shunt inductance connection

Figure 3.3.12 below shows the influence of an inductance parallel to the transformer winding on the transformer frequency response signature.

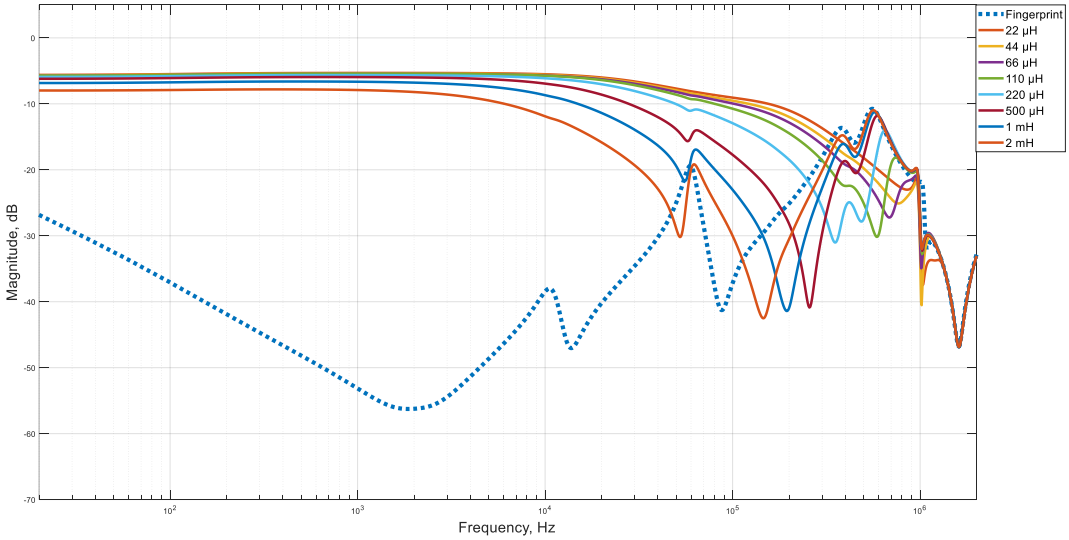

Figure 3.3.12 Response of the 350 VA power transformer with a parallel inductance connection

CHAPTER 4. STATISTICAL INDICES

This chapter provides the reader with a numerical analysis of the transformer frequency response signature. We adapted and used four statistical indicators for this study, namely, the correlation coefficient (CC), Euclidean distance (ED), absolute sum of logarithmic error (ASLE) and root mean square error (RMSE). The chapter is divided into three parts. The first part of the chapter addresses the resistance, the second shows the impact of the capacitance on the numerical indices, and the last part addresses the inductance. Each part of the chapter contains the results for all test objects and all connection configurations for the circuit element each part is allocated for.

Correlation Coefficient

The first index is the widely used CC, which shows how much measured and fingerprint traces coincide. The estimation of the CC is done according to (17) [55]-[57]:

$$CC = \frac{\sum_{i=1}^{N} X(i)Y(i)}{\sqrt{\sum_{i=1}^{N}[X(i)]^2 \sum_{i=1}^{N}[Y(i)]^2}} \tag{17}$$

where X and Y are the data sets of the transformer FRA signature and N is the number of data points. In this paper, Y is the fingerprint, and X is the trace under analysis.

Euclidean Distance

The numerical coefficient that represents the distance between the fingerprint and measured trace is known as the ED and is obtained using (18) [55],[57]:

$$ED = \sqrt{\sum_{i=1}^{N}[Y(i) - X(i)]^2} \ . \tag{18}$$

Root Mean Square Error

The RMSE represents the difference between corresponding data points. It is basically an evaluation of the coincidence of measurement values of the reference and test traces. The RMSE can be estimated by (19) [42], [56], [57]:

$$RMSE = \sqrt{\frac{1}{N}\sum_{i=1}^{N}\left(\frac{|Y(i)|-|X(i)|}{\frac{1}{N}\sqrt{\sum_{i=1}^{N}|X(i)|}}\right)^2} \quad . \tag{19}$$

Absolute Sum of Logarithmic Error

The ASLE provides a comparison of two data sets on the logarithmic scale and is calculated using (20) [42], [56], [57]:

$$ASLE = \frac{\sum_{i=1}^{N}|20\log_{10}Y(i) - 20\log_{10}X(i)|}{N} \quad . \tag{20}$$

4.1 Numerical Analysis

This part of the chapter analyzes the impact of a resistor in series, shunt and parallel connection schemes by utilizing the four statistical indices.

In the series resistance configuration, the resistor is placed between the end of the winding and the response terminal of the SFRA equipment. This scenario illustrates the behavior of numerical indices when a series impedance is introduced to the transformer circuit. In the case of a resistive impedance, the CC demonstrates less sensitivity to varying resistor values compared to the ED, ASLE and RMSE (Table 1). In particular, the CC remains the same when the resistance changes from 1 Ω to 3 Ω for the 40 kVA transformer, whereas the other three indices are sensitive to this slight alteration. Moreover, the CC does not detect the vertical shift of the trace, yet it changes as the shape of the curve deviates from that of the fingerprint [55]. For the 40 kVA transformer data in Table 1, the influence of a series connection is insignificant due to the high impedance at the transformer coming from the core and winding inductance. For instance, the CC remains 1.000 for series resistances below 5 Ω, although the ASLE is observed to vary in this region. Studies [20], [59]have discussed the critical values of numerical indices for fault detection.

Table 1. Comparison of Statistical Methods for FRA Interpretation of 40 kVA Transformer

Test Config.	Statistical Method	1 Ω	2 Ω	3 Ω	5 Ω	10 Ω	200 Ω
Series resistance	*CC*	1.0000	1.0000	1.0000	0.9999	0.9998	0.9996
	ED	9.7976	11.4594	13.0796	18.3448	33.1389	51.9324
	ASLE	0.0652	0.0783	0.0896	0.1253	0.2176	0.3092
	RMSE	0.0059	0.0069	0.0079	0.0111	0.0200	0.0313
Shunt resistance	*CC*	0.9837	0.9844	0.9857	0.9875	0.9888	0.9983
	ED	497.2168	494.5923	479.9023	458.5238	437.8658	142.5473
	ASLE	1.5521	1.5794	1.6027	1.6675	1.8086	0.7074
	RMSE	0.2949	0.2933	0.2846	0.2720	0.2597	0.0845
Parallel resistance	*CC*	0.5898	0.5933	0.5979	0.6041	0.6220	0.8501
	ED	1626.6434	1624.3235	1621.1757	1616.4661	1602.2602	1379.8086
	ASLE	14.5446	14.4542	14.3347	14.1542	13.6264	8.8386
	RMSE	0.9651	0.9637	0.9618	0.9590	0.9506	0.8186
		1 kΩ	**2 kΩ**	**3 kΩ**	**4 kΩ**	**5 kΩ**	**1 MΩ**
Series resistance	*CC*	0.9945	0.9910	0.9887	0.9871	0.9860	0.9780
	ED	194.0076	251.0738	284.6894	306.6968	322.6438	788.8126
	ASLE	0.9182	1.1428	1.2520	1.3401	1.3973	3.5813
	RMSE	0.1170	0.1515	0.1717	0.1850	0.1946	0.4759
Shunt resistance	*CC*	0.9998	0.9999	1.0000	1.0000	1.0000	1.0000
	ED	45.0470	24.8615	16.2163	10.5518	10.4606	5.4185
	ASLE	0.1946	0.0972	0.0601	0.0431	0.0403	0.0190
	RMSE	0.0267	0.0147	0.0096	0.0063	0.0062	0.0032
Parallel resistance	*CC*	0.9316	0.9511	0.9582	0.9633	0.9667	0.9994
	ED	1102.1417	956.7063	885.6524	827.8843	786.2477	77.3077
	ASLE	5.4363	4.1375	3.5865	3.1789	2.9058	0.1219
	RMSE	0.6539	0.5676	0.5254	0.4912	0.4665	0.0459

A CC below 0.9998 or an ASLE above 0.4 was found to indicate the fault condition of a power transformer, and the healthy condition of a power transformer can be referred to as the "green area". According to this analysis, for the 40 kVA transformer, the critical values of the series resistance that cause the fault condition are between 10 Ω and 200 Ω. For the 20 kVA, 760 VA and 350 VA transformers, according to the data in Table 2, Table 3 and Table 4, respectively, the impact of an introduced external series resistance is more noticeable from the

variation of the numerical indices. For all the data in tables in this chapter, the green area of transformer operation is marked in green font.

Table 2. Comparison of Statistical Methods for FRA Interpretation of 20 kVA Transformer

Test Config.	Statistical Method	1 Ω	2 Ω	3 Ω	5 Ω	10 Ω	200 Ω
Series resistance	*CC*	1.0000	1.0000	1.0000	0.9999	0.9996	0.9989
	ED	3.6017	5.7636	9.0953	14.4185	31.2625	54.1522
	ASLE	0.0273	0.0410	0.0698	0.1084	0.2211	0.3449
	RMSE	0.0034	0.0054	0.0085	0.0134	0.0291	0.0504
Shunt resistance	*CC*	0.9572	0.9664	0.9719	0.9776	0.9844	0.9973
	ED	825.0181	744.9195	696.1649	640.9752	538.3162	141.5936
	ASLE	4.2329	4.0391	3.9391	3.8683	3.4149	1.0965
	RMSE	0.7769	0.7015	0.6556	0.6036	0.5069	0.1333
Parallel resistance	*CC*	0.7010	0.7049	0.7088	0.7155	0.7300	0.9179
	ED	908.2576	905.3936	902.4521	896.7299	881.8866	661.5828
	ASLE	12.1204	12.0113	11.9036	11.7053	11.2155	6.0703
	RMSE	0.8417	0.8390	0.8363	0.8310	0.8173	0.6131
		1 kΩ	**2 kΩ**	**3 kΩ**	**4 kΩ**	**5 kΩ**	**1 MΩ**
Series resistance	*CC*	0.9876	0.9802	0.9750	0.9710	0.9687	0.9717
	ED	199.3582	270.4837	325.1635	368.1127	402.2416	1375.1167
	ASLE	1.1570	1.5949	1.8719	2.1410	2.3754	6.8151
	RMSE	0.1855	0.2516	0.3025	0.3425	0.3742	1.2794
Shunt resistance	*CC*	0.9996	0.9997	0.9997	0.9997	0.9997	0.9998
	ED	49.0192	40.5877	37.6597	36.6782	34.7185	32.7955
	ASLE	0.3613	0.2697	0.2408	0.2252	0.2082	0.1909
	RMSE	0.0462	0.0382	0.0355	0.0345	0.0327	0.0309
Parallel resistance	*CC*	0.9743	0.9861	0.9906	0.9930	0.9947	1.0000
	ED	398.4837	288.6358	233.4369	197.4675	170.9705	6.2148
	ASLE	2.7173	1.7077	1.2628	1.0104	0.8354	0.0456
	RMSE	0.3693	0.2675	0.2163	0.1830	0.1584	0.0058

The shunt impedance, also referred to as the measurement impedance in [55], acts as a voltage divider for the response terminal of the FRA analyzer and emulates the leakage from the transformer circuit. The higher the value of the shunt impedance is, the less the deviation from the fingerprint of the 40 kVA transformer for a resistive impedance (Table 1), a capacitive

impedance (Table 5) and an inductive impedance (Table 9). A resistive impedance above 1 kΩ gives the green area of the transformer condition.

Table 3. Comparison of Statistical Methods for FRA Interpretation of 760 VA Transformer

Test Config.	Statistical Method	1 Ω	2 Ω	3 Ω	5 Ω	10 Ω	200 Ω
Series resistance	*CC*	0.9898	0.9894	0.9892	0.9889	0.9879	0.9849
	ED	176.2397	177.8020	178.9318	182.9991	188.6277	201.5141
	ASLE	0.5657	0.5713	0.5768	0.6203	0.6818	0.8911
	RMSE	0.1634	0.1667	0.1680	0.1697	0.1749	0.1856
Shunt resistance	*CC*	0.9348	0.9449	0.9510	0.9622	0.9789	0.9947
	ED	852.8452	768.0760	724.8208	648.9933	544.8178	142.4622
	ASLE	5.6090	5.3013	5.1164	4.7083	4.1305	1.2288
	RMSE	0.9124	0.8217	0.7754	0.6943	0.5828	0.6524
Parallel resistance	*CC*	0.7754	0.7775	0.7793	0.7840	0.7871	0.9285
	ED	685.0916	682.7471	680.1398	675.2208	661.9312	467.5211
	ASLE	9.8102	9.7213	9.6268	9.4403	8.9893	4.3761
	RMSE	0.7329	0.7304	0.7276	0.7224	0.7081	0.5002
		1 kΩ	**2 kΩ**	**3 kΩ**	**4 kΩ**	**5 kΩ**	**1 MΩ**
Series resistance	*CC*	0.9805	0.9647	0.9515	0.9432	0.9412	0.8832
	ED	238.9808	349.3364	427.7219	482.7485	520.0726	1512.2691
	ASLE	1.6818	2.4033	2.8864	3.2184	3.3948	7.0397
	RMSE	0.2216	0.3240	0.3967	0.4477	0.4823	1.4025
Shunt resistance	*CC*	0.9995	0.9998	0.9998	0.9999	1.0000	1.0000
	ED	77.0722	70.2552	60.6232	55.5093	50.6588	21.7701
	ASLE	0.3106	0.2676	0.2160	0.1833	0.1490	0.0899
	RMSE	0.4073	0.2883	0.1949	0.0694	0.0542	0.0233
Parallel resistance	*CC*	0.9807	0.9906	0.9938	0.9957	0.9972	0.9998
	ED	266.6180	188.1881	153.7528	126.2909	103.7969	28.1790
	ASLE	1.7806	1.0782	0.8135	0.6194	0.4973	0.0735
	RMSE	0.2852	0.2013	0.1645	0.1351	0.1110	0.0301

A comparison of FRA results is provided for the 20 kVA, 760 VA and 350 VA transformers with an external shunt resistance in Tables 2-4, an external shunt capacitance in Tables 6-8 and an external shunt inductance in Tables 10-12.

Table 4. Comparison of Statistical Methods for FRA Interpretation of 350 VA Transformer

Test Config.	Statistical Method	1 Ω	2 Ω	3 Ω	5 Ω	10 Ω	200 Ω
Series resistance	*CC*	0.9998	0.9998	0.9997	0.9997	0.9996	0.9990
	ED	58.9691	62.2123	67.4223	69.0878	72.0493	95.8907
	ASLE	0.2086	0.2101	0.2119	0.2693	0.2814	0.3570
	RMSE	0.0418	0.0464	0.0615	0.0717	0.0804	0.1152
Shunt resistance	*CC*	0.9665	0.9733	0.9776	0.9822	0.9901	0.9977
	ED	820.4574	737.0370	687.8597	631.3460	535.8905	133.6338
	ASLE	4.2497	4.0239	3.8594	3.6141	3.3216	1.0386
	RMSE	0.6869	0.6170	0.5759	0.5285	0.4486	0.1119
Parallel resistance	*CC*	0.6694	0.6702	0.6731	0.6784	0.6950	0.8844
	ED	1000.3041	999.0812	996.4502	991.8106	977.9401	762.1284
	ASLE	12.3298	12.2820	12.1803	12.0018	11.5053	6.5946
	RMSE	0.8346	0.8336	0.8314	0.8275	0.8159	0.6359
		1 kΩ	**2 kΩ**	**3 kΩ**	**4 kΩ**	**5 kΩ**	**1 MΩ**
Series resistance	*CC*	0.9920	0.9834	0.9760	0.9706	0.9677	0.9634
	ED	168.3883	255.6812	318.1068	362.1094	393.0481	1242.6328
	ASLE	0.9614	1.4261	1.7591	1.9945	2.1555	6.1161
	RMSE	0.1411	0.2142	0.2665	0.3034	0.3293	1.0412
Shunt resistance	*CC*	0.9997	0.9998	0.9999	1.0000	1.0000	1.0000
	ED	32.0411	17.1665	14.9298	12.2314	10.2548	5.7733
	ASLE	0.2572	0.1276	0.0985	0.0711	0.0601	0.0302
	RMSE	0.0268	0.0144	0.0125	0.0161	0.0097	0.0065
Parallel resistance	*CC*	0.9669	0.9820	0.9880	0.9909	0.9928	0.9999
	ED	490.3520	373.8029	311.0185	271.1328	236.9636	19.1665
	ASLE	3.1541	2.1025	1.6326	1.3604	1.1220	0.0541
	RMSE	0.4091	0.3119	0.2595	0.2262	0.1977	0.0160

When an impedance is connected in parallel to the winding, it can emulate a winding SC, the severity of which depends on the value of the parallel impedance. In the case of a resistive impedance, the magnetic effect of the winding is canceled out, as discussed in [60]. The inductive effects of the core and winding are the significant contributors to the transformer maximum impedance, which occurs at the first resonant point.

Table 5. Comparison of Statistical Methods for Interpretation of Capacitive Impedance of 40 kVA Transformer

Test Config.	Statistical Method	100 pF	470 pF	1000 pF	50 nF	100 nF
Series capacitance	*CC*	0.9875	0.9908	0.9928	0.9999	1.0000
	ED	673.7770	405.6357	299.3604	24.7608	12.9116
	ASLE	2.7341	1.4865	0.9826	0.0532	0.0417
	RMSE	0.3930	0.2366	0.1746	0.0144	0.0075
Shunt capacitance	*CC*	0.9997	0.9985	0.9967	0.9628	0.9506
	ED	42.6986	102.0794	148.4196	495.5996	570.1387
	ASLE	0.1188	0.3964	0.7024	3.6937	4.3903
	RMSE	0.0250	0.0597	0.0868	0.2898	0.3334
Parallel capacitance	*CC*	0.9993	0.9946	0.9873	0.8863	0.8582
	ED	78.0708	224.9653	344.0060	1040.1591	1155.1064
	ASLE	0.3408	1.0953	1.8697	7.5680	8.7263
	RMSE	0.0455	0.1312	0.2006	0.6065	0.6736
		200 nF	**470 nF**	**940 nF**	**2.2 µF**	
Series capacitance	*CC*	1.0000	1.0000	1.0000	1.0000	
	ED	11.7266	11.5476	11.9456	12.4334	
	ASLE	0.0416	0.0436	0.0458	0.0481	
	RMSE	0.0068	0.0067	0.0070	0.0073	
Shunt capacitance	*CC*	0.9365	0.9251	0.9081	0.8862	
	ED	645.0046	733.3525	827.2672	929.4865	
	ASLE	5.1304	5.7170	6.3390	6.9294	
	RMSE	0.3765	0.4267	0.4810	0.5382	
Parallel capacitance	*CC*	0.8262	0.7737	0.7286	0.6736	
	ED	1259.6024	1377.3031	1450.5329	1518.5481	
	ASLE	9.8773	11.3277	12.3205	13.3789	
	RMSE	0.7345	0.8031	0.8458	0.8855	

When we connect a smaller impedance in parallel to the winding, the current mostly flows through the smaller impedance until, as the frequency of the signal increases, the transformer impedance reaches a value comparable to the parallel impedance. For the 40 kVA transformer, the “green area” starts at parallel impedance values above 1 MΩ.

Table 6. Comparison of Statistical Methods for Interpretation of Capacitive Impedance of 20 kVA Transformer

Test Config.	Statistical Method	100 pF	470 pF	1000 pF	50 nF	100 nF
Series capacitance	*CC*	0.9097	0.9064	0.9088	0.9663	0.9789
	ED	1353.8780	1063.5696	927.2276	350.2568	261.0355
	ASLE	5.5319	4.1028	3.4186	1.2413	0.9197
	RMSE	1.1899	0.9348	0.8149	0.3078	0.2294
Shunt capacitance	*CC*	0.9986	0.9946	0.9905	0.9066	0.8816
	ED	63.0500	122.6197	162.0184	506.7546	567.1308
	ASLE	0.1945	0.5521	0.8576	3.6882	4.2971
	RMSE	0.0554	0.1078	0.1424	0.4454	0.4985
Parallel capacitance	*CC*	0.9992	0.9918	0.9810	0.8292	0.7968
	ED	50.3743	158.9497	239.7081	671.5725	726.1694
	ASLE	0.2592	0.9569	1.5563	5.5929	6.4697
	RMSE	0.0444	0.1401	0.2113	0.5919	0.6400
		200 nF	**470 nF**	**940 nF**	**2.2 μF**	
Series capacitance	*CC*	0.9875	0.9950	0.9979	0.9993	
	ED	193.0879	118.6811	76.7163	42.9599	
	ASLE	0.6739	0.4073	0.2630	0.1555	
	RMSE	0.1697	0.1043	0.0674	0.0378	
Shunt capacitance	*CC*	0.8621	0.8441	0.8315	0.8199	
	ED	609.7141	647.1395	671.7903	692.0169	
	ASLE	4.8488	5.1742	5.5534	5.8511	
	RMSE	0.5347	0.5653	0.5860	0.5987	
Parallel capacitance	*CC*	0.7714	0.7411	0.7254	0.7117	
	ED	765.9582	811.8061	837.9714	863.5188	
	ASLE	7.2739	8.4545	9.2706	10.1782	
	RMSE	0.6751	0.7155	0.7385	0.7611	

Table 7. Comparison of Statistical Methods for Interpretation of Capacitive Impedance of 760 VA Transformer

Test Config.	Statistical Method	100 pF	470 pF	1000 pF	50 nF	100 nF
Series capacitance	*CC*	0.8820	0.8781	0.8783	0.9241	0.9417
	ED	1515.0415	1204.5334	1056.8954	460.9594	376.6791
	ASLE	7.4412	5.8056	5.0000	1.8784	1.5515
	RMSE	1.6704	1.3281	1.1653	0.5082	0.4153
Shunt capacitance	*CC*	0.9991	0.9976	0.9921	0.9554	0.9552
	ED	40.0055	67.0950	120.6225	283.4673	284.4031
	ASLE	0.1528	0.3928	0.7245	2.4688	2.5563
	RMSE	0.0440	0.0738	0.1327	0.3120	0.3130
Parallel capacitance	*CC*	0.9991	0.9942	0.9872	0.9166	0.8844
	ED	41.2838	103.9900	154.0452	400.8059	466.5723
	ASLE	0.2171	0.6163	0.9452	4.0556	4.9513
	RMSE	0.0455	0.1146	0.1698	0.4419	0.5144
		200 nF	**470 nF**	**940 nF**	**2.2 μF**	
Series capacitance	*CC*	0.9588	0.9769	0.9864	0.9929	
	ED	299.9723	215.5232	161.4766	114.4852	
	ASLE	1.2594	0.9092	0.6985	0.5491	
	RMSE	0.3307	0.2376	0.1780	0.1262	
Shunt capacitance	*CC*	0.9516	0.9438	0.9265	0.9016	
	ED	295.0848	323.4745	373.7485	428.0743	
	ASLE	3.1674	3.4697	3.9260	4.3237	
	RMSE	0.3245	0.3516	0.4040	0.4558	
Parallel capacitance	*CC*	0.8498	0.7997	0.7705	0.7443	
	ED	523.6611	592.1938	627.8227	657.8377	
	ASLE	5.7660	6.8951	7.6490	8.4514	
	RMSE	0.5773	0.6528	0.6921	0.7252	

Table 8. Comparison of Statistical Methods for Interpretation of Capacitive Impedance of 350 VA Transformer

Test Config.	Statistical Method	100 pF	470 pF	1000 pF	50 nF	100 nF
Series capacitance	*CC*	0.9555	0.9551	0.9557	0.9846	0.9909
	ED	1156.6293	855.0113	720.0293	235.0796	172.9933
	ASLE	5.0965	3.4904	2.7176	0.5861	0.4267
	RMSE	0.9710	0.7178	0.6045	0.1973	0.1452
Shunt capacitance	*CC*	0.9993	0.9996	0.9983	0.9695	0.9574
	ED	46.9650	35.1366	73.1102	306.9846	361.7903
	ASLE	0.1655	0.1960	0.4289	2.5878	3.3024
	RMSE	0.0394	0.0295	0.0614	0.2578	0.3038
Parallel capacitance	*CC*	0.9998	0.9984	0.9958	0.9048	0.8691
	ED	28.0244	74.0279	122.7358	571.5540	660.3712
	ASLE	0.1624	0.5374	0.9189	5.0272	6.0401
	RMSE	0.0235	0.0622	0.1031	0.4800	0.5546
		200 nF	**470 nF**	**940 nF**	**2.2 µF**	
Series capacitance	*CC*	0.9950	0.9980	0.9992	0.9997	
	ED	125.5001	78.7090	50.3167	28.9789	
	ASLE	0.3115	0.1925	0.1266	0.0774	
	RMSE	0.1054	0.0661	0.0422	0.0243	
Shunt capacitance	*CC*	0.9451	0.9298	0.9153	0.8962	
	ED	409.1664	469.5078	521.3276	578.5107	
	ASLE	3.8534	4.2677	4.7898	5.2622	
	RMSE	0.3425	0.3894	0.4323	0.4754	
Parallel capacitance	*CC*	0.8300	0.7799	0.7493	0.7143	
	ED	741.5047	831.8286	883.6388	933.9527	
	ASLE	7.0655	8.3757	9.2545	10.2706	
	RMSE	0.6227	0.6986	0.7421	0.7844	

Table 9. Comparison of Statistical Methods for Interpretation of Inductive Impedance of 40 kVA Transformer

Test Config.	Statistical Method	22 µH	44 µH	66 µH	110 µH
Series inductance	*CC*	1.0000	0.9999	0.9998	0.9994
	ED	14.2287	27.5564	40.0573	65.1342
	ASLE	0.0815	0.1528	0.2164	0.3371
	RMSE	0.0083	0.0160	0.0233	0.0378
Shunt inductance	*CC*	0.8406	0.8623	0.8785	0.8799
	ED	1306.8023	1236.1209	1174.5621	1165.2397
	ASLE	8.8845	8.0252	7.2968	6.9427
	RMSE	0.7614	0.7202	0.6843	0.6789
Parallel inductance	*CC*	0.5314	0.5291	0.5273	0.5366
	ED	1633.6377	1631.0467	1629.2137	1625.5017
	ASLE	15.8345	15.6930	15.5569	15.3517
	RMSE	0.9511	0.9496	0.9485	0.9464
		220 µH	**0.5 mH**	**1 mH**	**2 mH**
Series inductance	*CC*	0.9984	0.9915	0.9857	0.9790
	ED	104.7220	248.5483	322.5986	393.2972
	ASLE	0.5507	1.0710	1.3068	1.5059
	RMSE	0.0608	0.1443	0.1873	0.2284
Shunt inductance	*CC*	0.9122	0.9346	0.9507	0.9681
	ED	1031.4934	885.6018	744.4027	571.2819
	ASLE	5.4860	4.0001	2.8805	1.8611
	RMSE	0.6010	0.5160	0.4337	0.3329
Parallel inductance	*CC*	0.5730	0.5969	0.6194	0.6454
	ED	1608.1298	1582.3893	1546.2356	1497.2507
	ASLE	14.5614	13.4104	12.1400	10.7957
	RMSE	0.9363	0.9213	0.9002	0.8717

Table 10. Comparison of Statistical Methods for Interpretation of Inductive Impedance of 20 kVA Transformer

Test Config.	Statistical Method	22 µH	44 µH	66 µH	110 µH
Series inductance	*CC*	0.9999	0.9996	0.9990	0.9980
	ED	17.5929	31.7415	51.1077	74.7034
	ASLE	0.0908	0.1699	0.2668	0.3781
	RMSE	0.0155	0.0279	0.0450	0.0658
Shunt inductance	*CC*	0.8507	0.8537	0.8586	0.8815
	ED	678.7964	648.7374	622.4029	585.8881
	ASLE	5.9176	5.3091	4.8543	4.3803
	RMSE	0.5972	0.5707	0.5476	0.5154
Parallel inductance	*CC*	0.6698	0.6664	0.6717	0.6928
	ED	919.0601	916.4644	912.2240	903.4116
	ASLE	12.6195	12.4698	12.2664	12.0434
	RMSE	0.8084	0.8061	0.8024	0.7946
		220 µH	**0.5 mH**	**1 mH**	**2 mH**
Series inductance	*CC*	0.9947	0.9771	0.9641	0.9747
	ED	124.3064	272.7370	344.4399	284.2607
	ASLE	0.6102	1.0725	1.2572	1.2026
	RMSE	0.1094	0.2401	0.3033	0.2503
Shunt inductance	*CC*	0.9041	0.9383	0.9683	0.9871
	ED	510.5473	406.1944	296.0550	198.9343
	ASLE	3.4501	2.4886	1.7385	1.1574
	RMSE	0.4492	0.3574	0.2605	0.1750
Parallel inductance	*CC*	0.7258	0.7473	0.7646	0.8153
	ED	879.1933	838.9471	797.9969	728.4828
	ASLE	11.2654	10.1845	9.1579	7.7488
	RMSE	0.7733	0.7379	0.7019	0.6408

Table 11. Comparison of Statistical Methods for Interpretation of Inductive Impedance of 760 VA Transformer

Test Config.	Statistical Method	22 µH	44 µH	66 µH	110 µH
Series inductance	*CC*	0.9995	0.9990	0.9985	0.9965
	ED	31.2449	42.0226	52.8293	80.4458
	ASLE	0.1209	0.2035	0.2729	0.4236
	RMSE	0.0343	0.0461	0.0580	0.0883
Shunt inductance	*CC*	0.8558	0.8533	0.8580	0.8784
	ED	508.9080	501.7397	494.4676	459.1874
	ASLE	4.9352	4.5481	4.2382	3.8361
	RMSE	0.5594	0.5515	0.5435	0.5047
Parallel inductance	*CC*	0.7226	0.7268	0.7275	0.7254
	ED	696.7659	692.6335	689.8603	688.1508
	ASLE	10.4735	10.3072	10.1799	10.0200
	RMSE	0.7656	0.7611	0.7580	0.7561
		220 µH	**0.5 mH**	**1 mH**	**2 mH**
Series inductance	*CC*	0.9936	0.9820	0.9795	0.9695
	ED	111.2716	207.2306	217.1596	272.9592
	ASLE	0.6066	1.0203	1.1515	1.4538
	RMSE	0.1222	0.2275	0.2384	0.2997
Shunt inductance	*CC*	0.9041	0.9379	0.9724	0.9889
	ED	419.0495	358.3388	276.9743	203.0671
	ASLE	3.1188	2.3372	1.6823	1.2253
	RMSE	0.4606	0.3939	0.3045	0.2232
Parallel inductance	*CC*	0.7379	0.7672	0.7947	0.8275
	ED	673.1091	640.3019	608.1451	565.5205
	ASLE	9.4217	8.3295	7.2985	6.0876
	RMSE	0.7396	0.7036	0.6682	0.6214

Table 12. Comparison of Statistical Methods for Interpretation of Inductive Impedance of 350 VA Transformer

Test Config.	Statistical Method	22 µH	44 µH	66 µH	110 µH
Series inductance	*CC*	0.9998	0.9996	0.9993	0.9981
	ED	26.6604	37.4328	47.7725	76.9447
	ASLE	0.1104	0.1830	0.2449	0.3978
	RMSE	0.0224	0.0314	0.0401	0.0646
Shunt inductance	*CC*	0.8616	0.8728	0.8833	0.8944
	ED	738.3311	687.7414	642.9026	627.4025
	ASLE	6.2706	5.5393	4.9536	4.6405
	RMSE	0.6198	0.5773	0.5397	0.5266
Parallel inductance	*CC*	0.6291	0.6311	0.6340	0.6322
	ED	1017.8801	1014.9689	1011.9992	1010.6430
	ASLE	12.7648	12.6371	12.5105	12.4055
	RMSE	0.8552	0.8528	0.8503	0.8492
		220 µH	**0.5 mH**	**1 mH**	**2 mH**
Series inductance	*CC*	0.9963	0.9833	0.9849	0.9761
	ED	108.3058	249.1436	230.1789	292.3999
	ASLE	0.6172	1.1464	1.2083	1.4305
	RMSE	0.0909	0.2092	0.1932	0.2455
Shunt inductance	*CC*	0.9217	0.9528	0.9670	0.9865
	ED	523.8576	397.1639	318.9268	213.1096
	ASLE	3.4319	2.2310	1.5640	0.9120
	RMSE	0.4397	0.3334	0.2677	0.1789
Parallel inductance	*CC*	0.6432	0.6630	0.6956	0.7391
	ED	997.9126	974.3995	939.6735	889.1275
	ASLE	11.8640	10.9084	9.7369	8.3516
	RMSE	0.8385	0.8187	0.7895	0.7471

CHAPTER 5. CONCLUSION AND FUTURE WORK

Different connection schemes were tested using Frequency Response Analysis (FRA) on 40 kVA, 20 kVA, 760 VA, 350 VA power transformers. The frequency range used in the study was up to 2 MHz. The total impedance equations for series, shunt and parallel connection of external impedance were derived and practically validated. The derivation of the equations was based on the circuit analysis and impedance expressions for RLC network elements. The trend for each test object followed the theoretical pattern. The series impedance connection simulated the resistance and reactance coming directly from the connection terminals of the testing equipment. The shunt impedance simulated the leakage from the transformer winding terminals due to FRA analyzer connection. At certain frequency values, the frequency response signature of test objects obtained positive values, meaning that the total impedance of the test object becomes negative. Mainly, this phenomenon might be due to uncertainties and approximations algorithms used in FRA analyzer. The parallel impedance scenario demonstrated the behavior of transformer FRA signature under winding short circuit condition. Depending on the size of a test object, the influence of the same external parameter was different. For series impedance connection, the impact of external impedance was more significant for smaller test objects.

On the contrary, the frequency response signatures of larger test objects are more affected by shunt and parallel external impedance. Also, the green zone for each transformer was identified. The critical value of numerical indices for identification of transformer faulty condition was presented. The critical value of the numerical index gives the borderline for the healthy condition of transformer operation. It was found out that the largest test object in this study, namely 40 kVA distribution transformer, was less subjected to frequency response signature change due to an addition of external impedance for all connection

schemes according to statistical indices.

This gives the theoretical justification and practical validation of how the change in the parameters of external connections affect the frequency response signature of a transformer. The change in connection impedance can be erroneously interpreted as a fault.

For the future work the external impedances consisting of a combination of R, L, C such as RL, RC, LC can be utilized for analysis of their impact on transformer FRA signature. Also, machine learning algorithms can be implemented to automate the process of green zone determination for different test objects

REFERENCES

[1] G. U. Nnachi and D. V. Nicolae, "Diagnostic methods of frequency response analysis for power transformer winding a review," *2016 IEEE International Power Electronics and Motion Control Conference (PEMC)*, Varna, 2016, pp. 563-568.

[2] Y. Han and Y. H. Song, "Condition monitoring techniques for electrical equipment-a literature survey," in *IEEE Transactions on Power Delivery*, vol. 18, no. 1, pp. 4-13, Jan. 2003.

[3] H. Rahimpour, S. Mitchell and S. Rahimpour, "Online monitoring of power transformers using impulse frequency response analysis," *2017 Iranian Conference on Electrical Engineering (ICEE)*, Tehran, 2017, pp. 1390-1394.

[4] E. Gomez-Luna, G. Aponte Mayor, C. Gonzalez-Garcia and J. Pleite Guerra, "Current Status and Future Trends in Frequency-Response Analysis With a Transformer in Service," in *IEEE Transactions on Power Delivery*, vol. 28, no. 2, pp. 1024-1031, April 2013.

[5] A. Abu-Siada and O. Aljohani, "Detecting incipient radial deformations of power transformer windings using polar plot and digital image processing," in *IET Science, Measurement & Technology*, vol. 12, no. 4, pp. 492-499, 7 2018.

[6] A. S. Masoum, N. Hashemnia, A. Abu-Siada, M. A. S. Masoum and S. M. Islam, "Online Transformer Internal Fault Detection Based on Instantaneous Voltage and Current Measurements Considering Impact of Harmonics," in IEEE Transactions on Power Delivery, vol. 32, no. 2, pp. 587-598, April 2017.

[7] Z. Zhao, C. Yao, X. Zhao, N. Hashemnia and S. Islam, "Impact of capacitive coupling circuit on online impulse frequency response of a power transformer," in *IEEE Transactions on Dielectrics and Electrical Insulation*, vol. 23, no. 3, pp. 1285-1293, June 2016.

[8] C. Yao et al., "Transformer winding deformation diagnostic system using online high frequency signal injection by capacitive coupling," in IEEE Transactions on Dielectrics and Electrical Insulation, vol. 21, no. 4, pp. 1486-1492, August 2014.

[9] S. B. Rathnayaka, K. Y. See, M. Prajapati, K. Li, N. B. Narampanawe and F. Fan, "Inductive coupling method for on-line frequency response analysis (FRA) for transformer winding diagnostic," *TENCON 2017 - 2017 IEEE Region 10 Conference*, Penang, 2017, pp. 88-92.

[10] N. Hashemnia, A. Abu-Siada and S. Islam, "Detection of power transformer bushing faults and oil degradation using frequency response analysis," in *IEEE Transactions on Dielectrics and Electrical Insulation*, vol. 23, no. 1, pp. 222-229, February 2016.

[11] O. Aljohani and A. Abu-siada, "Identification of the minimum detection of transformer bushing failure based on Frequency Response Analysis (FRA)," *2016 IEEE 2nd Annual Southern Power Electronics Conference (SPEC)*, Auckland, 2016, pp. 1-5.

[12] M. Bagheri, S. Nezhivenko and B. T. Phung, "Loss of low-frequency data in on-line frequency response analysis of transformers," in *IEEE Electrical Insulation Magazine*, vol. 33, no. 5, pp. 32-39, September-October 2017.

[13] M. Bagheri, B. T. Phung and T. Blackburn, "Influence of moisture content variation on Frequency Response Analysis of transformer winding," *2014 IEEE Electrical Insulation Conference (EIC)*, Philadelphia, PA, 2014, pp. 333-337.

[14] M. Bagheri, B. T. Phung and T. Blackburn, "Influence of temperature and moisture content on frequency response analysis of transformer winding," in *IEEE Transactions on Dielectrics and Electrical Insulation*, vol. 21, no. 3, pp. 1393-1404, June 2014.

[15] M. Bagheri, B. T. Phung, T. Blackburn and A. Naderian, "Influence of temperature on frequency response analysis of transformer winding," *2013 IEEE Electrical Insulation Conference (EIC)*, Ottawa, ON, 2013, pp. 40-44.

[16] G. Chen, H. Song, Y. Zhang, X. Zhang and Z. Hao, "Transformer impedence circle character based winding deformation online monitoring," *2015 5th International Conference on Electric Utility Deregulation and Restructuring and Power Technologies (DRPT)*, Changsha, 2015, pp. 2304-2309.

[17] Y. Cheng, X. Pan, W. Chang and J. Bi, "Analysis of the influence of outside equipments on the online deformation detection of transformers," *2016 IEEE International Conference on High Voltage Engineering and Application (ICHVE)*, Chengdu, 2016, pp. 1-4.

[18] M. Bagheri, M. S. Naderi and T. Blackburn, "Advanced transformer winding deformation diagnosis: moving from off-line to on-line," in *IEEE Transactions on Dielectrics and Electrical Insulation*, vol. 19, no. 6, pp. 1860-1870, December 2012.

[19] IEEE Guide for Diagnostic Field Testing of Electric Power Apparatus - Part 1: Oil Filled Power Transformers, Regulators, and Reactors," in IEEE Std 62-1995, vol., no., pp. 1-64, 1 December 1995

[20] T. Chiulan and B. Pantelimon, "A practical example of power transformer unit winding condition assessment by means of short-circuit impedance measurement," *2009 IEEE Bucharest PowerTech*, Bucharest, 2009, pp. 1-4.

[21] J. Seo, H. Ma and T. K. Saha, "A Joint Vibration and Arcing Measurement System for Online Condition Monitoring of Onload Tap Changer of the Power Transformer," in *IEEE Transactions on Power Delivery*, vol. 32, no. 2, pp. 1031-1038, April 2017.

[22] B. Garcia, J. C. Burgos and A. M. Alonso, "Transformer tank vibration modeling as a method of detecting winding deformations-part I: theoretical foundation," in *IEEE Transactions on Power Delivery*, vol. 21, no. 1, pp. 157-163, Jan. 2006.

[23] M. Bagheri, S. Nezhivenko, M.S. Naderi, and A. Zollanvari, “A new vibration analysis approach for transformer fault prognosis over cloud environment”, Int J Electr power Energy Syst., no. 100, pp. 104-116, 2018.

[24] R. K. Senobari, J. Sadeh, and H. Borsi, “Frequency response analysis (FRA) of transformers as a tool for fault detection and location: A review”, Electr Pow Syst Res., vol. 155, pp. 172-183, 2018.

[25] S. D. Mitchell and J. S. Welsh, "Modeling Power Transformers to Support the Interpretation of Frequency-Response Analysis," in IEEE Transactions on Power Delivery, vol. 26, no. 4, pp. 2705-2717, Oct. 2011.

[26] B. Mohseni, N. Hashemnia, S. Islam and Z. Zhao, "Application of online impulse technique to diagnose inter-turn short circuit in transformer windings," *2016 Australasian Universities Power Engineering Conference (AUPEC)*, Brisbane, QLD, 2016, pp. 1-4.

[27] F. Haghjoo, M. Mostafaei and H. Mohammadi, "A New Leakage Flux-Based Technique for Turn-to-Turn Fault Protection and Faulty Region Identification in Transformers," in IEEE Transactions on Power Delivery, vol. 33, no. 2, pp. 671-679, April 2018.

[28] O. Aljohani and A. Abu-Siada, "Application of Digital Image Processing to Detect Short-Circuit Turns in Power Transformers Using Frequency Response Analysis," in IEEE Transactions on Industrial Informatics, vol. 12, no. 6, pp. 2062-2073, Dec. 2016.

[29] S. Mortazavian, M. M. Shabestary, Y. A. I. Mohamed and G. B. Gharehpetian, "Experimental Studies on Monitoring and Metering of Radial Deformations on Transformer HV Winding Using Image Processing and UWB Transceivers," in IEEE Transactions on Industrial Informatics, vol. 11, no. 6, pp. 1334-1345, Dec. 2015.

[30] N. Hashemnia, A. Abu-Siada and S. Islam, "Improved power transformer winding fault detection using FRA diagnostics – part 1: axial displacement simulation," in IEEE Transactions on Dielectrics and Electrical Insulation, vol. 22, no. 1, pp. 556-563, Feb. 2015.

[31] N. Hashemnia, A. Abu-Siada and S. Islam, "Improved power transformer winding fault detection using FRA diagnostics – part 2: radial deformation simulation," in IEEE Transactions on Dielectrics and Electrical Insulation, vol. 22, no. 1, pp. 564-570, Feb. 2015.

[32] A. A. Reykherdt and V. G. Davydov, "Effects of test cable ground extensions on repeatability of frequency response analysis measurements on power transformers," in IEEE Electrical Insulation Magazine, vol. 28, no. 3, pp. 26-31, May-June 2012.

[33] E. Al Murawwi, R. Mardiana and C. Q. Su, "Effects of terminal connections on sweep frequency response analysis of transformers," in IEEE Electrical Insulation Magazine, vol. 28, no. 3, pp. 8-13, May-June 2012. doi: 10.1109/MEI.2012.6192362

[34] M. Wang, A. J. Vandermaar and K. D. Srivastava, "Improved detection of power transformer winding movement by extending the FRA high frequency range," in IEEE Transactions on Power Delivery, vol. 20, no. 3, pp. 1930-1938, July 2005.

[35] M. F. M. Yousof, C. Ekanayake and T. K. Saha, "Locating inter-disc faults in transformer winding using frequency response analysis," *2013 Australasian Universities Power Engineering Conference (AUPEC)*, Hobart, TAS, 2013, pp. 1-6.

[36] M. F. M. Yousof, C. Ekanayake and T. K. Saha, "Frequency response analysis to investigate deformation of transformer winding," in *IEEE Transactions on Dielectrics and Electrical Insulation*, vol. 22, no. 4, pp. 2359-2367, August 2015.

[37] V. Behjat, A. Vahedi, A. Setayeshmehr, H. Borsi and E. Gockenbach, "Diagnosing Shorted Turns on the Windings of Power Transformers Based Upon Online FRA Using Capacitive and Inductive Couplings," in *IEEE Transactions on Power Delivery*, vol. 26, no. 4, pp. 2123-2133, Oct. 2011.

[38] X. Zhao, C. Yao, C. Zhang and A. Abu-Siada, "Toward reliable interpretation of power transformer sweep frequency impedance signatures: experimental analysis," in *IEEE Electrical Insulation Magazine*, vol. 34, no. 2, pp. 40-51, March-April 2018.

[39] R. Rajamani, M Rajappa, and B Madanmohan.,. Sweep frequency response analysis based diagnosis of shorts within transformer windings. IET Generation, Transmission & Distribution, 11(17), pp.4274-4281.2017.

[40] M. Bagheri, M. S. Naderi, T. Blackburn and B. T. Phung, "Bushing characteristic impacts on on-line Frequency Response Analysis of transformer winding," *2012 IEEE International Conference on Power and Energy (PECon)*, Kota Kinabalu, 2012, pp. 956-961.

[41] N. Abeywickrama, T. Bengtsson and R. Saers, "Transformer explorer: Monitoring transformer status by fundamental frequency signals," *2016 International Conference on Condition Monitoring and Diagnosis (CMD)*, Xi'an, 2016, pp. 396-399.

[42] A. Srikanta Murthy, N. Azis, S. Al-Ameri, M. Mohd Yousof, J. Jasni, and M. Talib, "Investigation of the Effect of Winding Clamping Structure on Frequency Response Signature of 11 kV Distribution Transformer," Energies, vol. 11, no. 9, p. 2307, September 2018.

[43] S. Sardar, A. Kumar, B. Chatterjee and S. Dalai, "Application of statistical interpretation technique for frequency response analysis and detection of axial displacement in transformer winding," 2017 IEEE Calcutta Conference (CALCON), Kolkata, 2017, pp. 461-464.

[44] M. F. M. Yousof, S. Riang and M. K. A. Uyup, "The influence of data size in statistical analysis of power transformer frequency response," 2016 IEEE International Conference on Power and Energy (PECon), Melaka, 2016, pp. 595-599.

[45] V. Behjat, M. Mahvi and E. Rahimpour, "A new statistical approach to interpret power transformer frequency response analysis: Nonparametric statistical methods," 2015 30th International Power System Conference (PSC), Tehran, 2015, pp. 142-148.

[46] A. R. Abbasi, M. R. Mahmoudi and Z. Avazzadeh, "Diagnosis and clustering of power transformer winding fault types by cross-correlation and clustering analysis of FRA results," in IET Generation, Transmission & Distribution, vol. 12, no. 19, pp. 4301-4309, 30 10 2018.

[47] S. Ab Ghani, Y. H. Md Thayoob, Y. Z. Y. Ghazali, M. S. A. Khiar and I. S. Chairul, "Evaluation of transformer core and winding conditions from SFRA measurement results using statistical techniques for distribution transformers," 2012 IEEE International Power Engineering and Optimization Conference Melaka, Malaysia, Melaka, 2012, pp. 448-453.

[48] V. Behjat and M. Mahvi, "Statistical approach for interpretation of power transformers frequency response analysis results," in IET Science, Measurement & Technology, vol. 9, no. 3, pp. 367-375, 5 2015.

[49] H. Tarimoradi and G. B. Gharehpetian, "Novel Calculation Method of Indices to Improve Classification of Transformer Winding Fault Type, Location, and Extent," in IEEE Transactions on Industrial Informatics, vol. 13, no. 4, pp. 1531-1540, Aug. 2017.

[50] Y. Luo, J. Gao, P. Chen, L. Hu, Y. Shen and L. Ruan, "A test method of winding deformation excited by pseudorandom M-Sequences — Part I: Theory and simulation," in IEEE Transactions on Dielectrics and Electrical Insulation, vol. 23, no. 3, pp. 1605-1612, June 2016.

[51] Y. Luo, J. Gao, P. Chen, L. Hu, Y. Shen and L. Ruan, "A test method of winding deformation excited by pseudorandom M-Sequences — Part II: Experiments and outlook," in IEEE Transactions on Dielectrics and Electrical Insulation, vol. 23, no. 3, pp. 1613-1619, June 2016.

[52] M. Rezaei, M. Neshat and H. S. yazdi, "A New Frequency Dependent Resistor for modeling skin effect of wire and echo cancellation by PSO," 2010 The 2nd International Conference on Computer and Automation Engineering (ICCAE), Singapore, 2010, pp. 573-577.

[53] J. Acero and C. R. Sullivan, "A dynamic equivalent network model of the skin effect," 2013 Twenty-Eighth Annual IEEE Applied Power Electronics Conference and Exposition (APEC), Long Beach, CA, 2013, pp. 2392-2397.

[54] IEEE Guide for the Application and Interpretation of Frequency Response Analysis for Oil-Immersed Transformers," in IEEE Std C57.149-2012, vol., no., pp. 1-72, 8 March 2013.

[55] M. H. Samimi, S. Tenbohlen, A. A. S. Akmal and H. Mohseni, "Effect of Different Connection Schemes, Terminating Resistors and Measurement Impedances

on the Sensitivity of the FRA Method," in IEEE Transactions on Power Delivery, vol. 32, no. 4, pp. 1713-1720, August 2017.

[56] M. H. Samimi and S. Tenbohlen, "FRA interpretation using numerical indices: State-of-the-art," in International Journal of Electrical Power & Energy Systems, vol. 89, no C, pp. 115-125, 2017.

[57] S. Banaszak and W. Szoka, "Cross Test Comparison in Transformer Windings Frequency Response Analysis," in Energies, vol. 11, no. 6, p. 1349, May 2018.

[58] P. M. Nirgude, D. Ashokraju, A. D. Rajkumar and B. P. Singh, "Application of numerical evaluation techniques for interpreting frequency response measurements in power transformers," in IET Science, Measurement & Technology, vol. 2, no. 5, pp. 275-285, September 2008

[59] J. C. Gonzales Arispe and E. E. Mombello, "Detection of Failures Within Transformers by FRA Using Multiresolution Decomposition," in IEEE Transactions on Power Delivery, vol. 29, no. 3, pp. 127-1137, June 2014.

[60] M. Bagheri, M. Lu, M. S. Naderi and B. T. Phung, "Transformer frequency response: a new technique to analyze and distinguish the low-frequency band in the frequency response analysis spectrum," in IEEE Electrical Insulation Magazine, vol. 34, no. 5, pp. 39-49, September-October 2018.

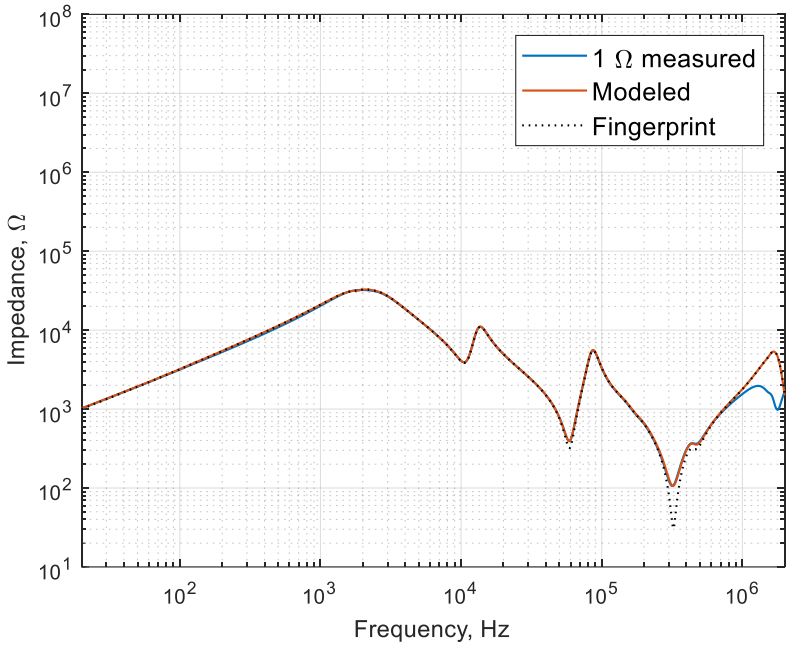

Figure 5.1 Comparison of measured and modeled 1 Ω series resistances impedance response for a 350 VA transformer

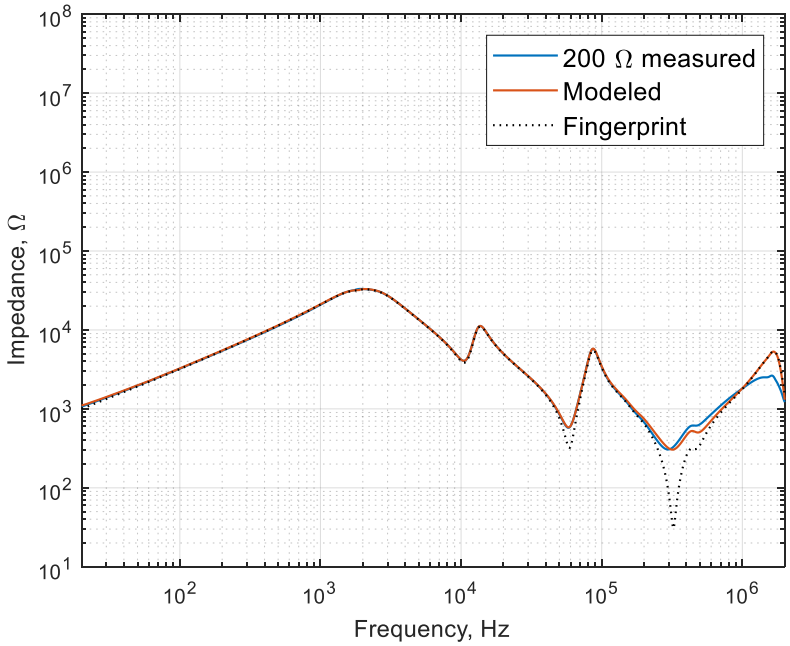

Figure 5.2 Comparison of measured and modeled 200 Ω series resistances impedance response for a 350 VA transformer

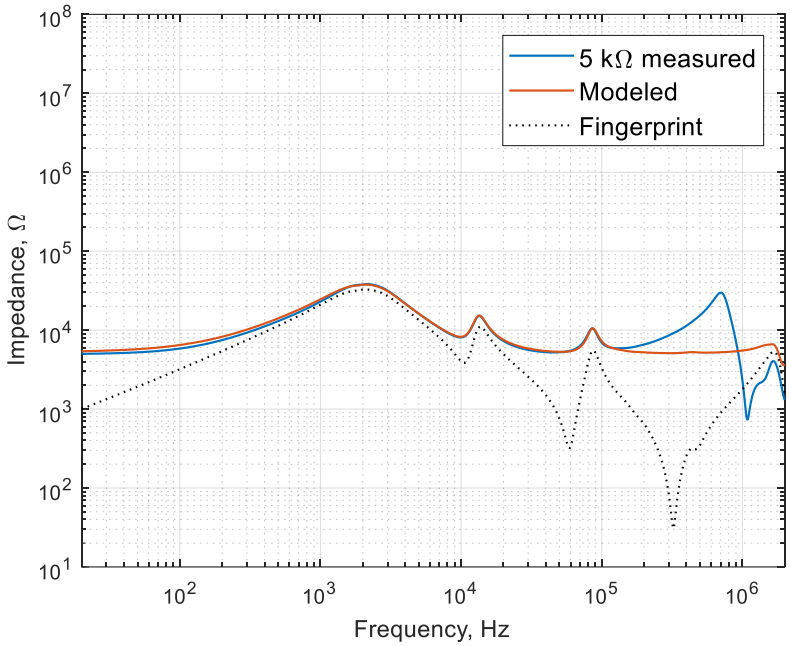

Figure 5.3 Comparison of measured and modeled 5 kΩ series resistances impedance response for a 350 VA transformer

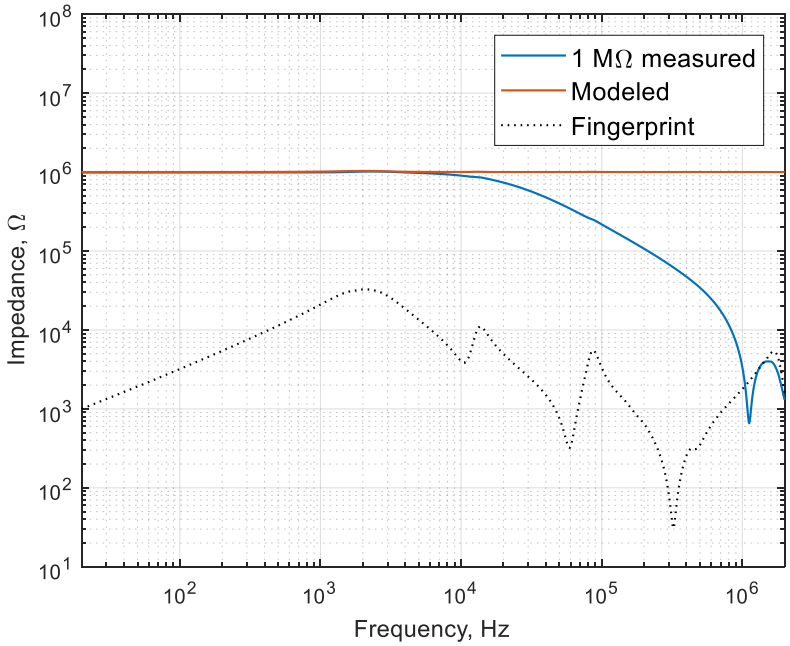

Figure 5.4 Comparison of measured and modeled 1 MΩ series resistances impedance response for a 350 VA transformer

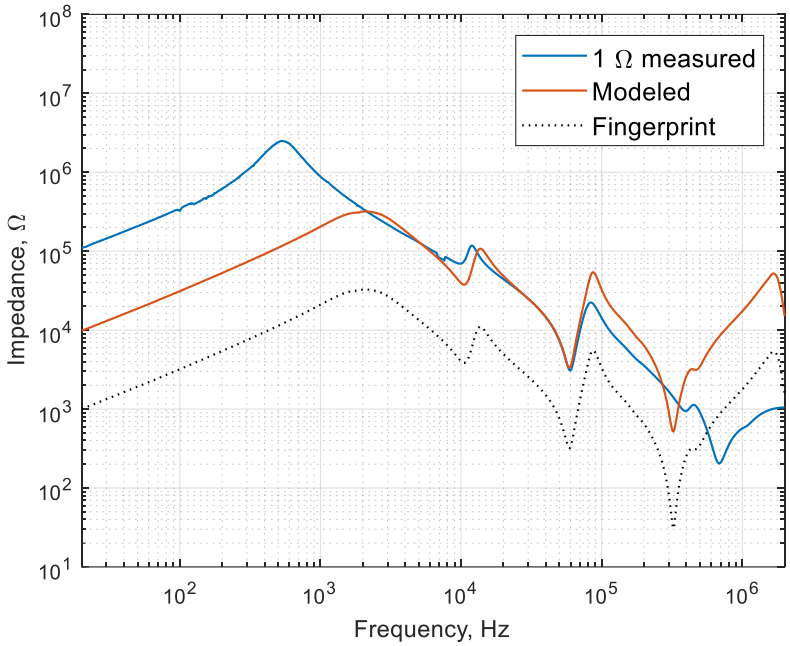

Figure 5.5 Comparison of measured and modeled 1 Ω shunt resistances impedance response for a 350 VA transformer

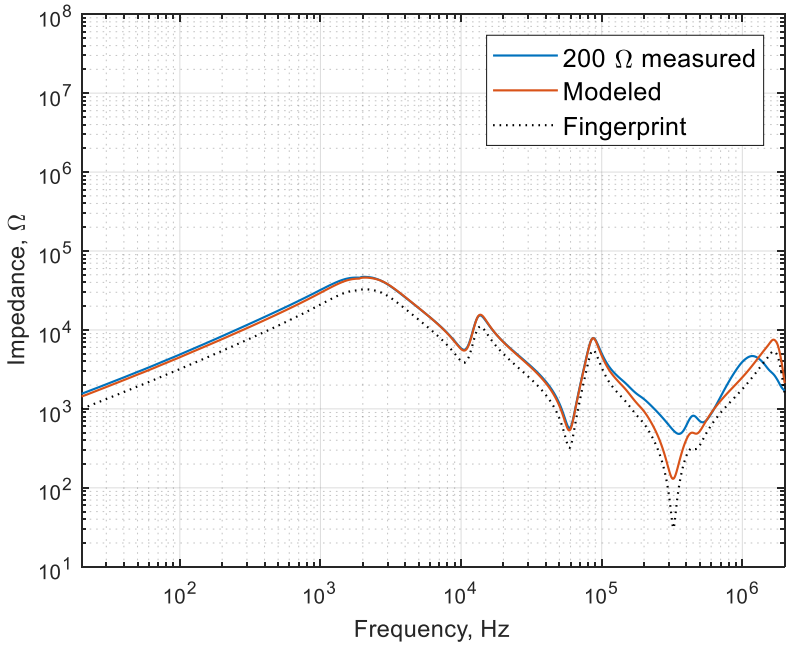

Figure 5.6 Comparison of measured and modeled 200 Ω shunt resistances impedance response for a 350 VA transformer

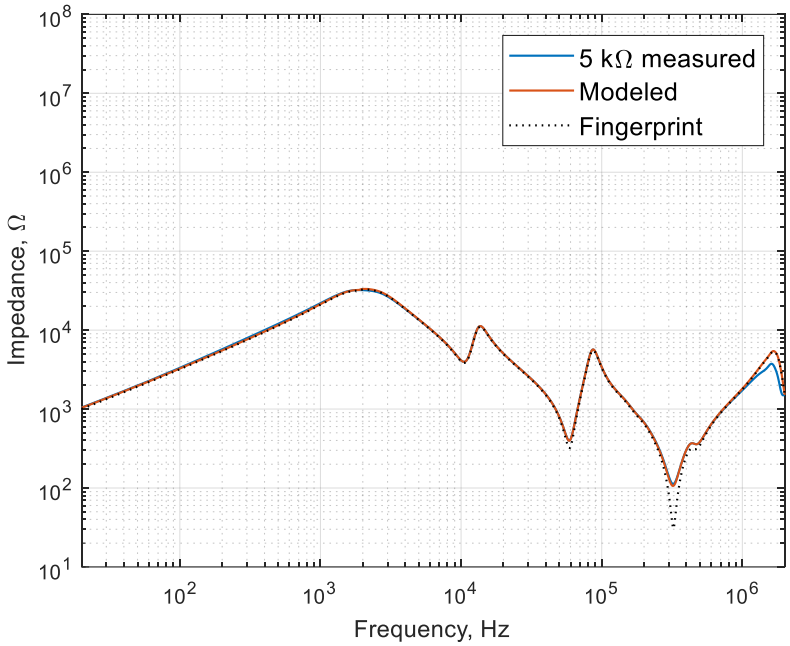

Figure 5.7 Comparison of measured and modeled 5 kΩ shunt resistances impedance response for a 350 VA transformer

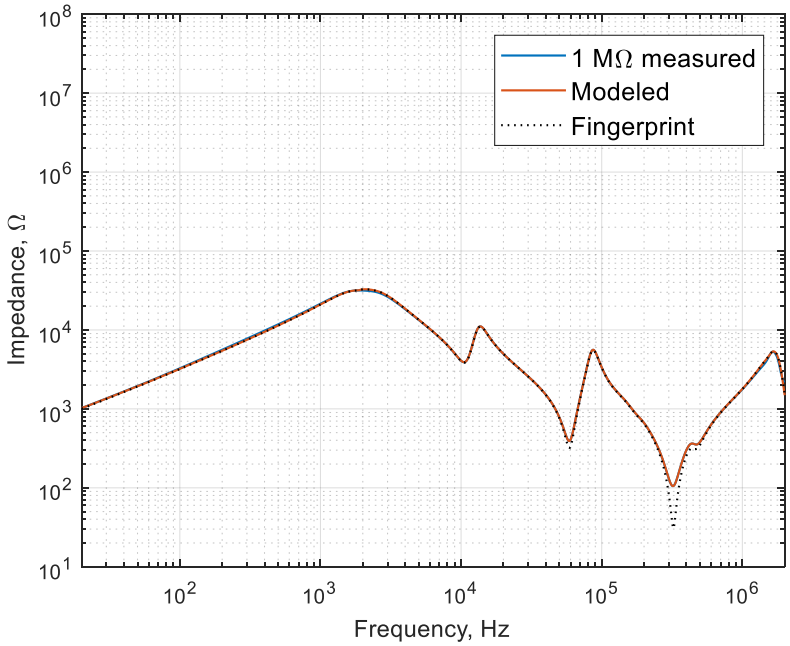

Figure 5.8 Comparison of measured and modeled 1 MΩ shunt resistances impedance response for a 350 VA transformer

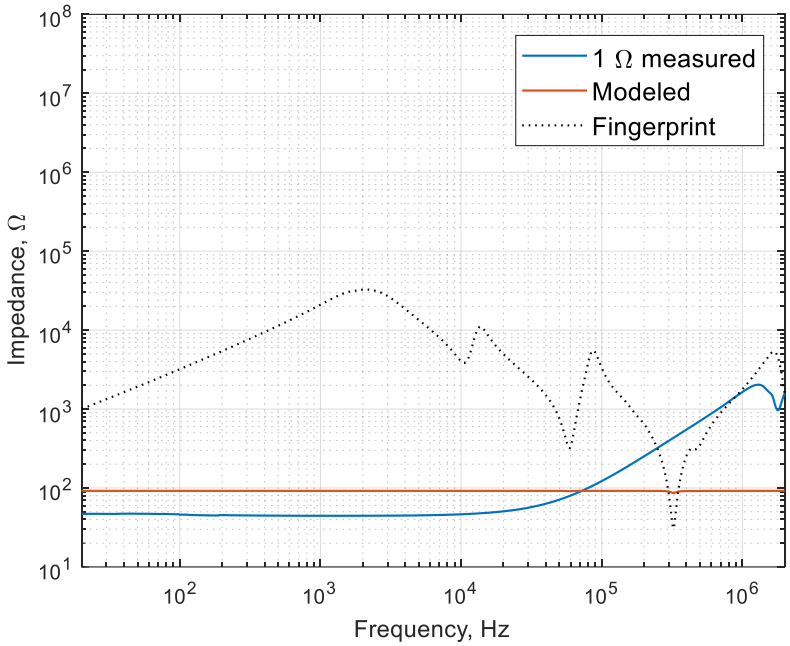

Figure 5.9 Comparison of measured and modeled 1 Ω parallel resistances impedance response for a 350 VA transformer

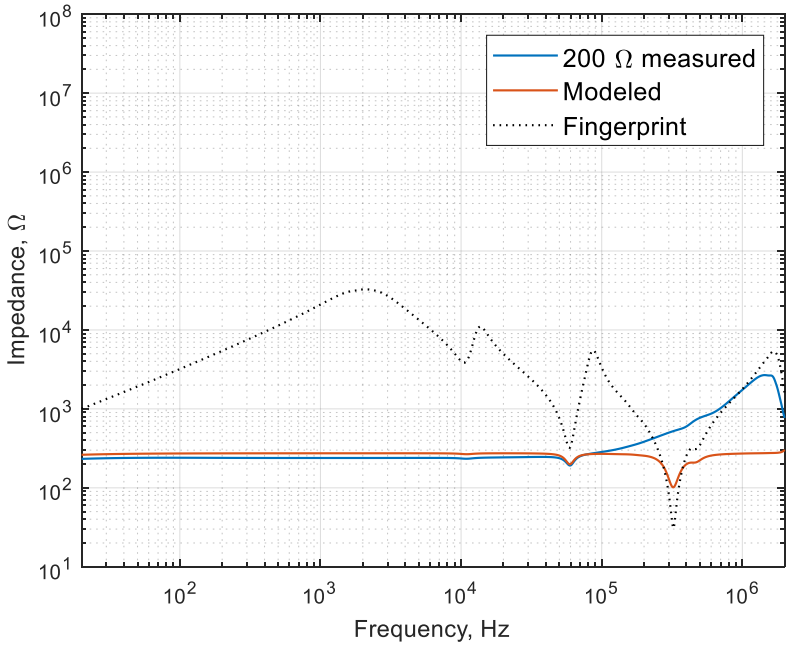

Figure 5.10 Comparison of measured and modeled 200 Ω parallel resistances impedance response for a 350 VA transformer

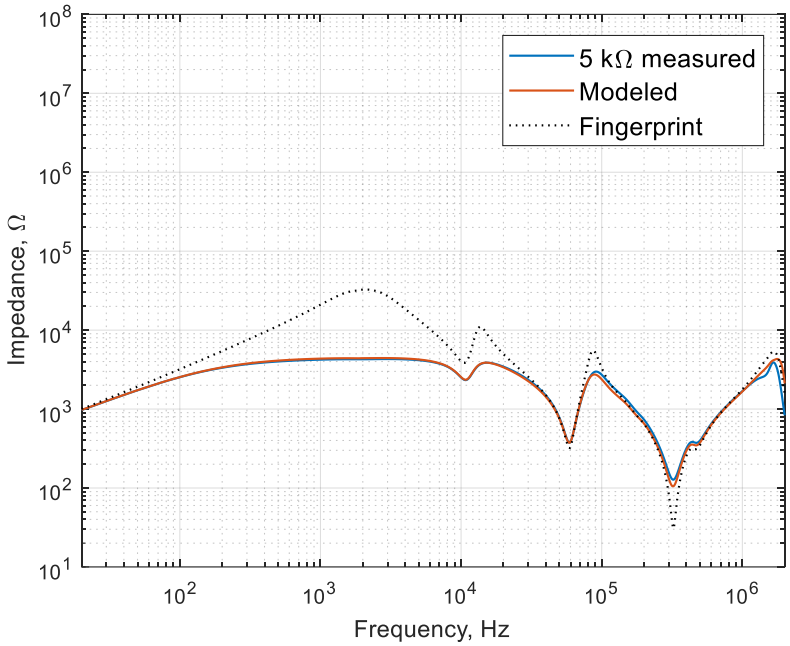

Figure 5.11 Comparison of measured and modeled 5 kΩ parallel resistances impedance response for a 350 VA transformer

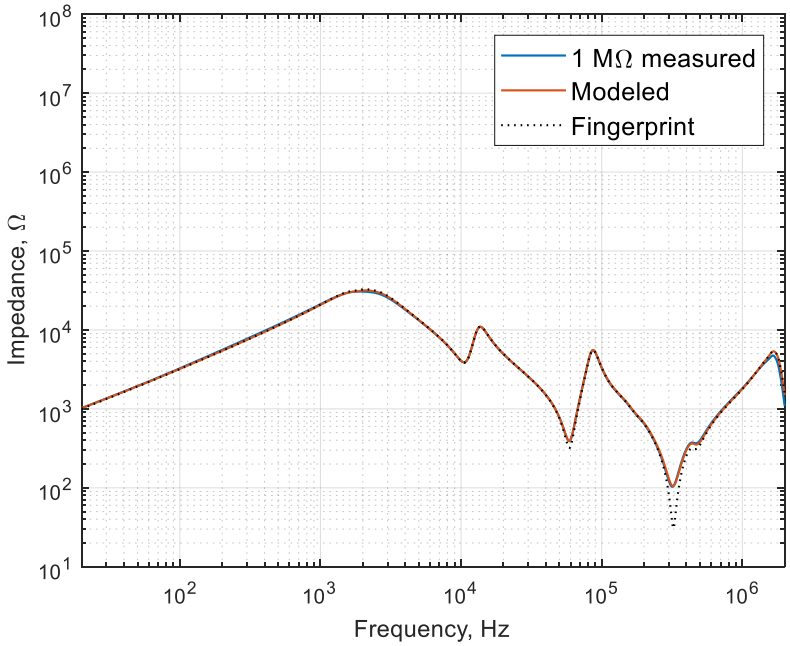

Figure 5.12 Comparison of measured and modeled 1 MΩ parallel resistances impedance response for a 350 VA transformer

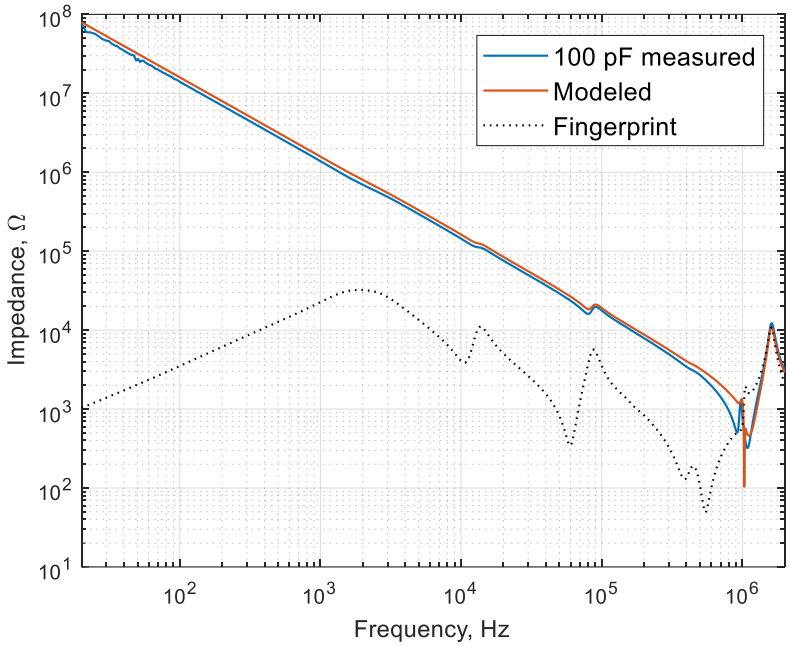

Figure 6.1 Comparison of measured and modeled 100 pF series capacitances impedance response for a 350 VA transformer

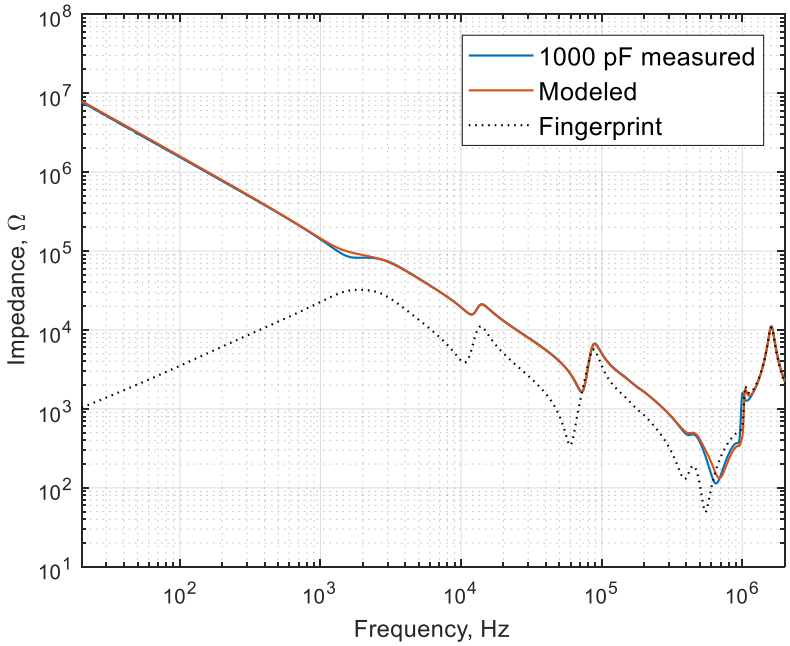

Figure 6.2 Comparison of measured and modeled 1000 pF series capacitances impedance response for a 350 VA transformer

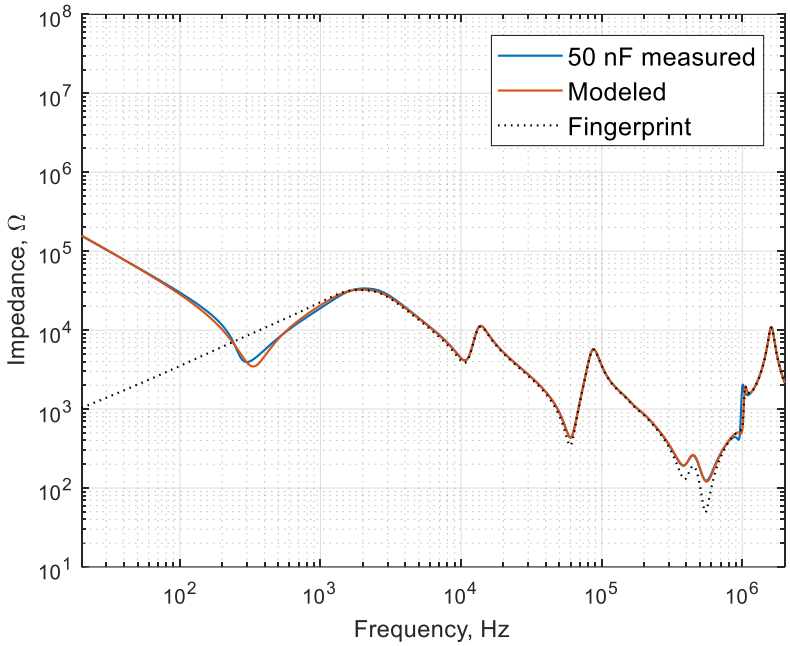

Figure 6.3 Comparison of measured and modeled 50 nF series capacitances impedance response for a 350 VA transformer

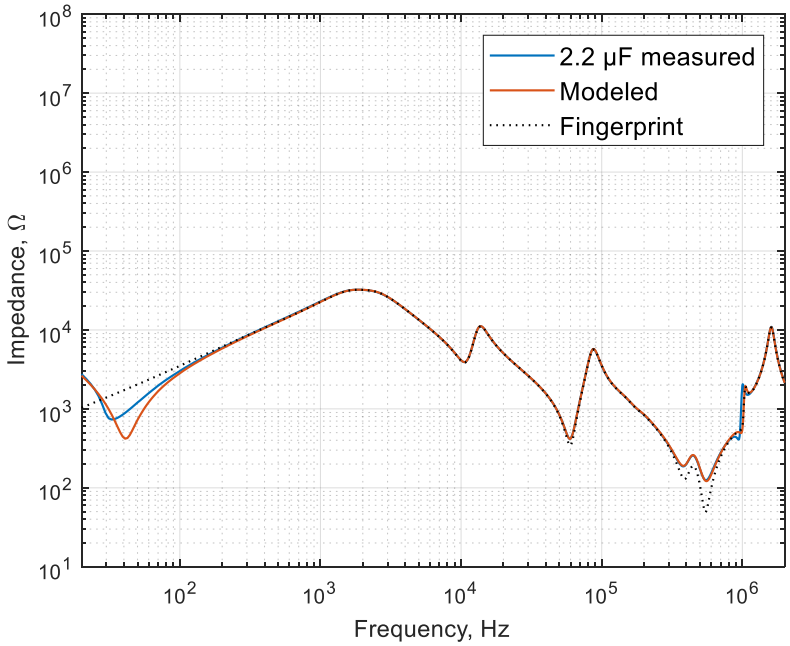

Figure 6.4 Comparison of measured and modeled 2.2 µF series capacitances impedance response for a 350 VA transformer

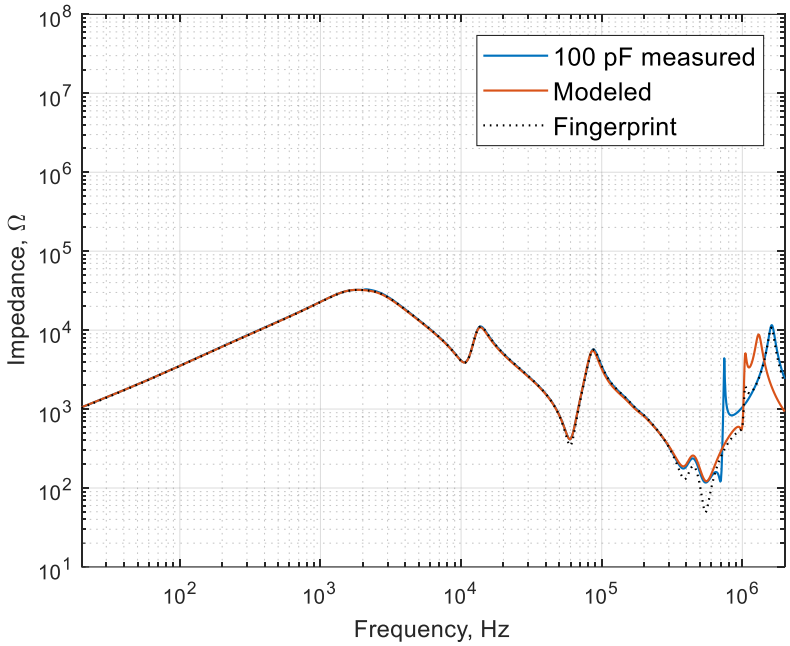

Figure 6.5 Comparison of measured and modeled 100 pF shunt capacitances impedance response for a 350 VA transformer

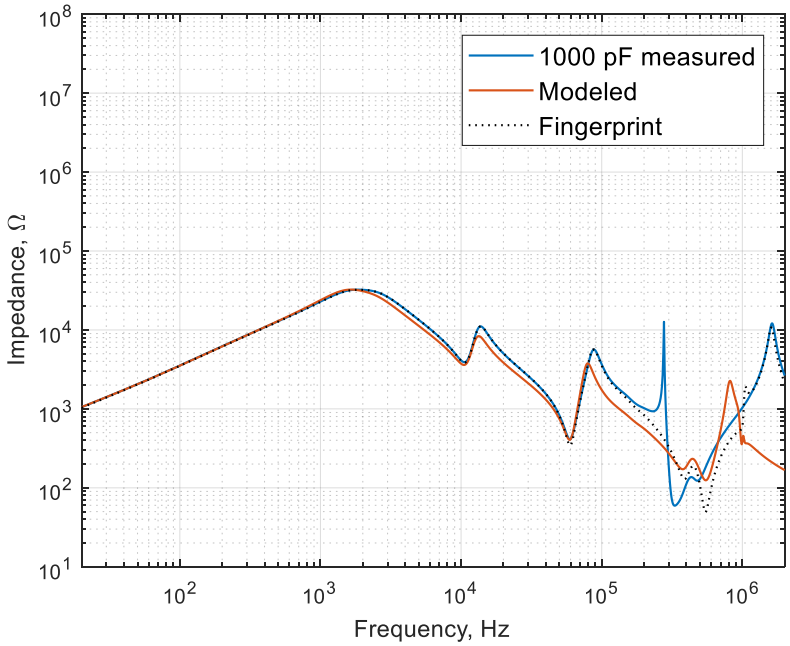

Figure 6.6 Comparison of measured and modeled 1000 pF shunt capacitances impedance response for a 350 VA transformer

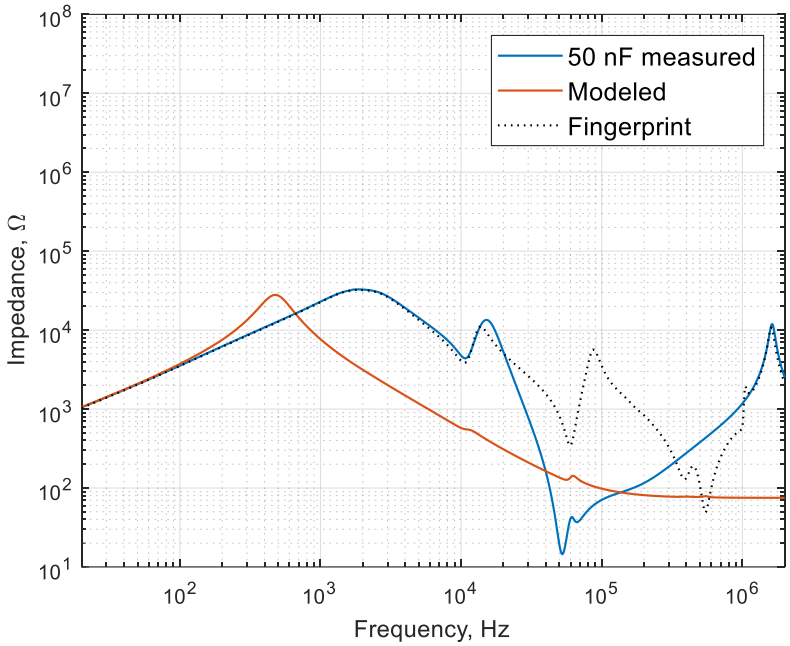

Figure 6.7 Comparison of measured and modeled 50 nF shunt capacitances impedance response for a 350 VA transformer

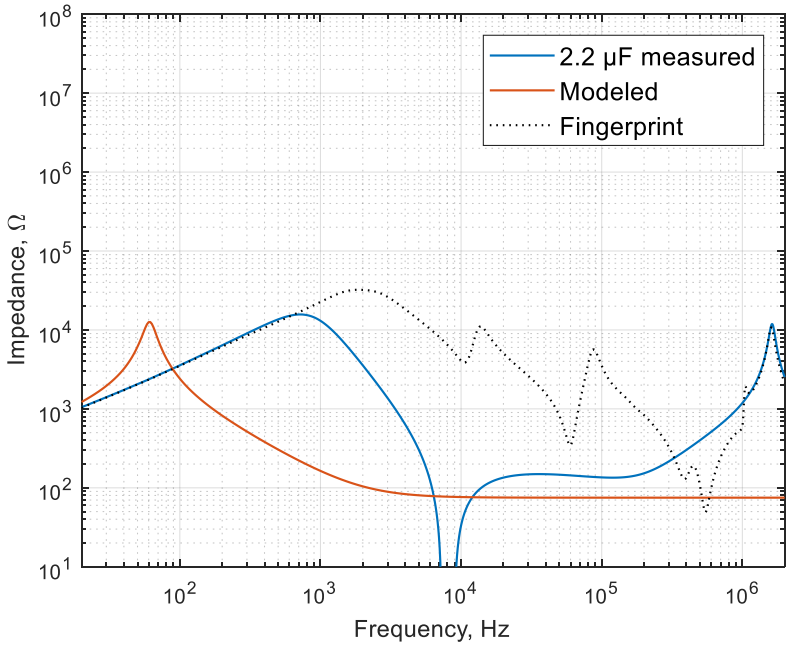

Figure 6.5 Comparison of measured and modeled 2.2 µF shunt capacitances impedance response for a 350 VA transformer

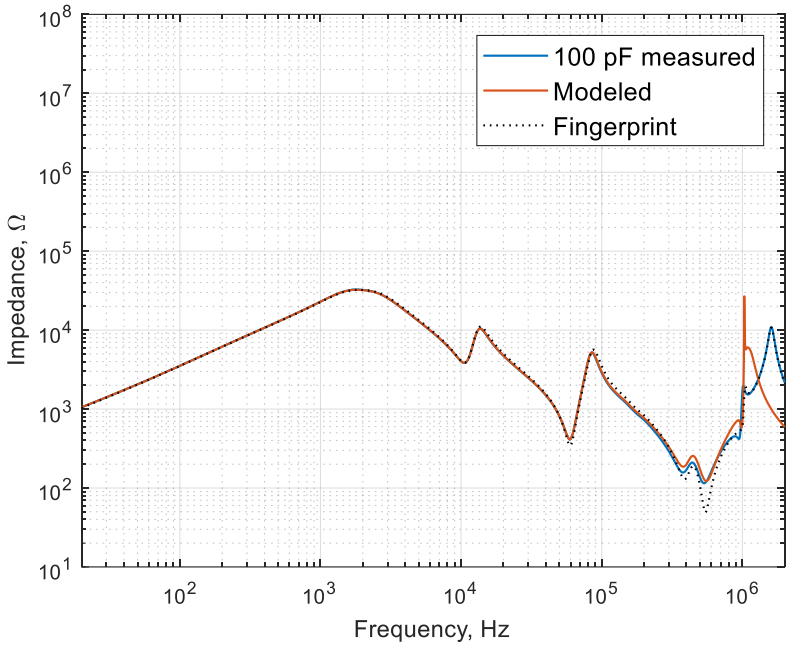

Figure 6.9 Comparison of measured and modeled 100 pF parallel capacitances impedance response for a 350 VA transformer

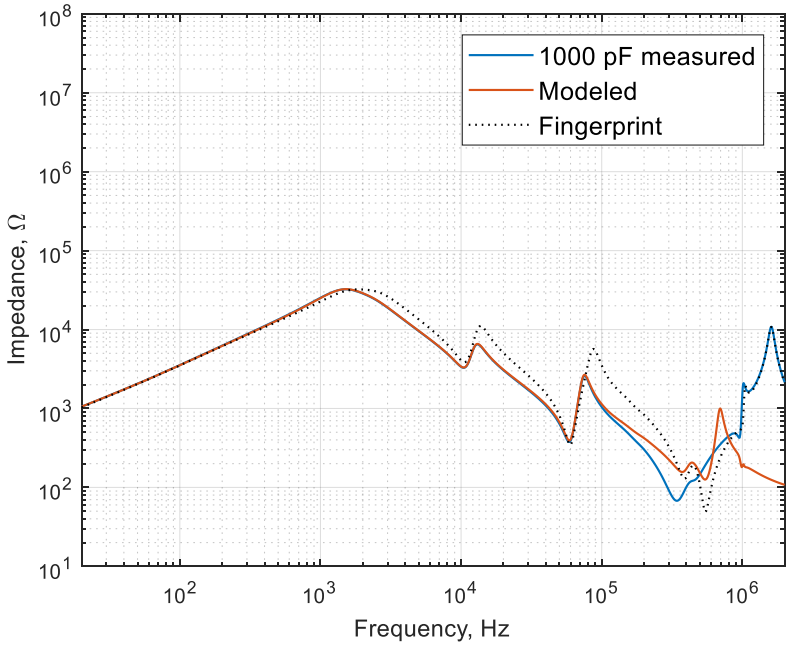

Figure 6.10 Comparison of measured and modeled 1000 pF parallel capacitances impedance response for a 350 VA transformer

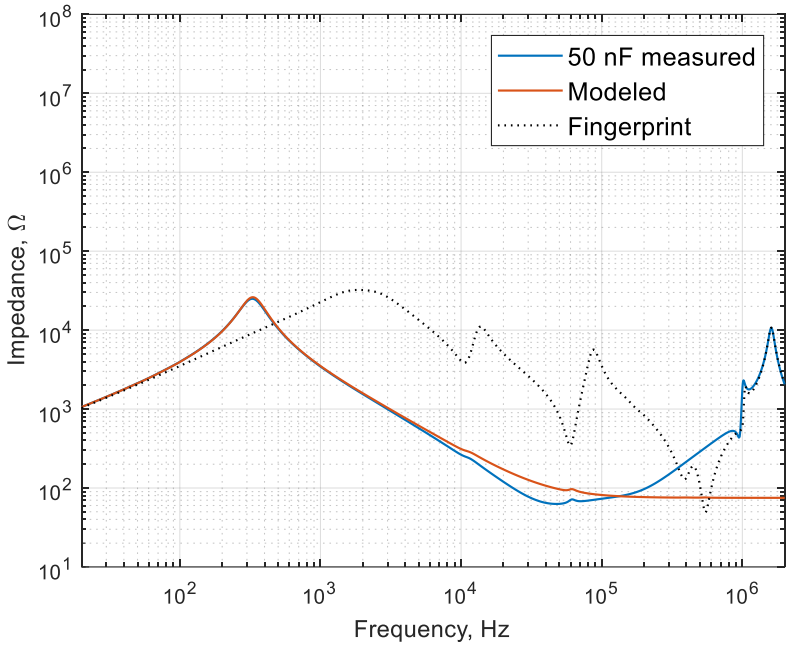

Figure 6.11 Comparison of measured and modeled 50 nF parallel capacitances impedance response for a 350 VA transformer

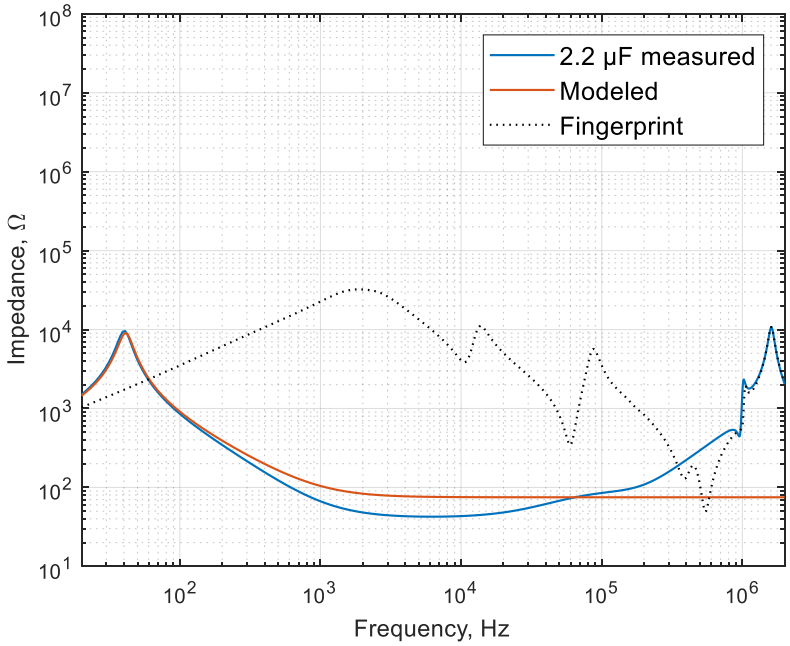

Figure 6.12 Comparison of measured and modeled 2.2 µF parallel capacitances impedance response for a 350 VA transformer

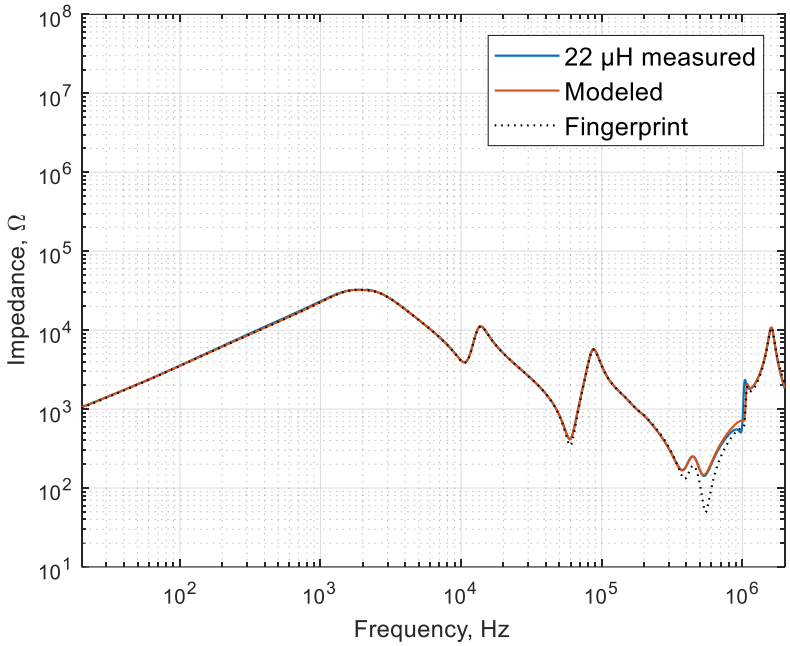

Figure 7.1 Comparison of measured and modeled 22 µH series inductances impedance response for a 350 VA transformer

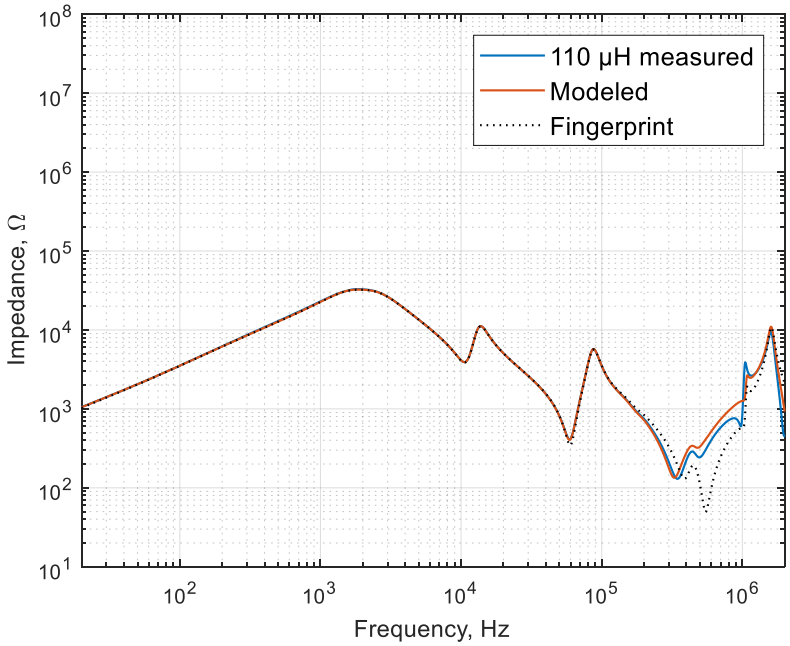

Figure 7.2 Comparison of measured and modeled 110 µH series inductances impedance response for a 350 VA transformer

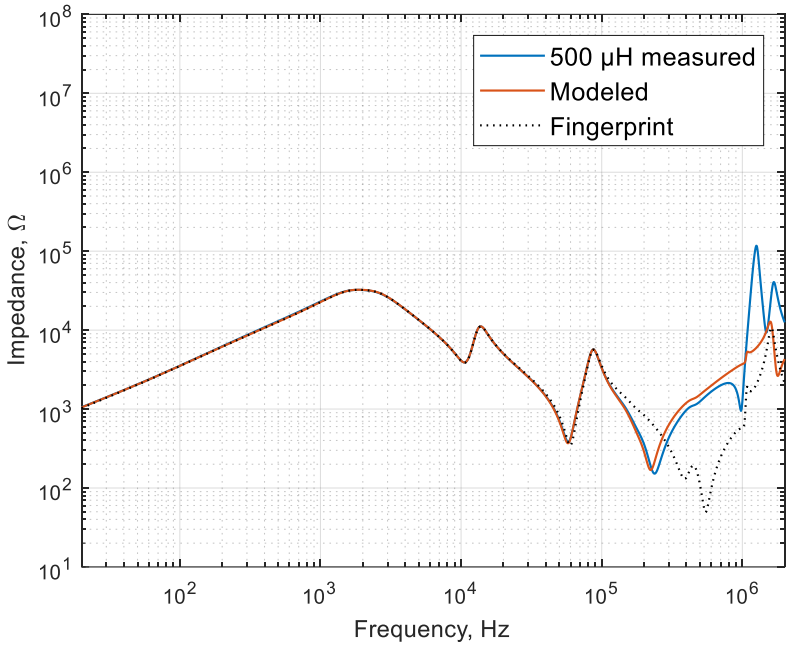

Figure 7.3 Comparison of measured and modeled 500 μH series inductances impedance response for a 350 VA transformer

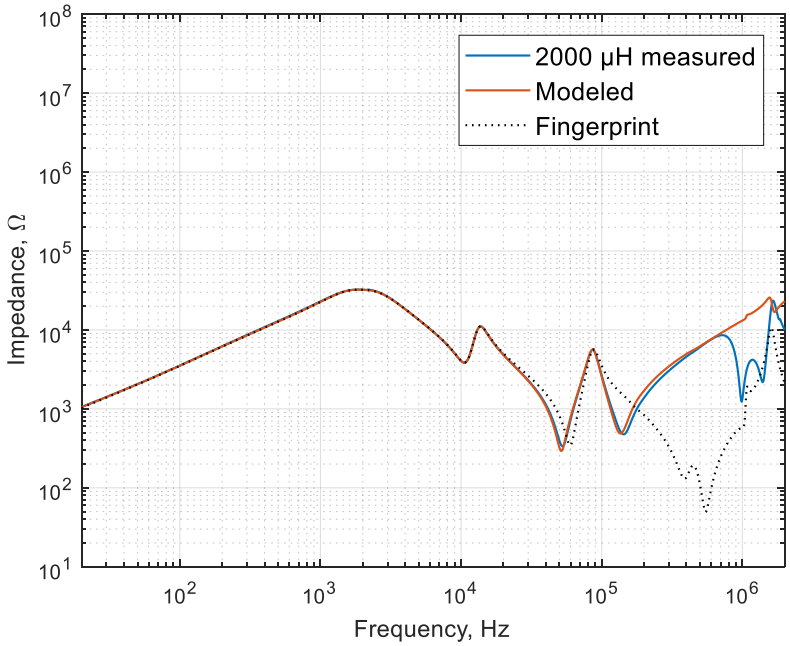

Figure 7.4 Comparison of measured and modeled 2000 μH series inductances impedance response for a 350 VA transformer

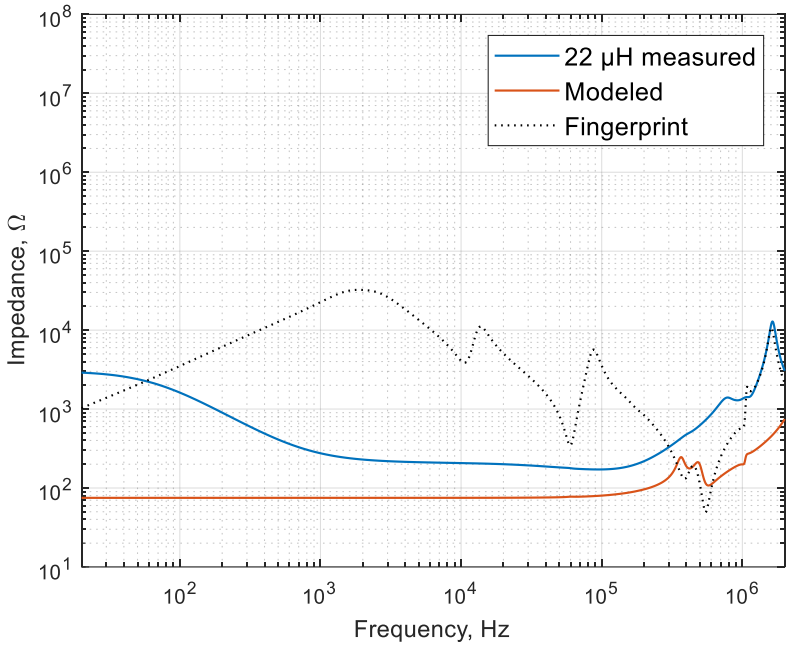

Figure 7.5 Comparison of measured and modeled 22 µH shunt inductances impedance response for a 350 VA transformer

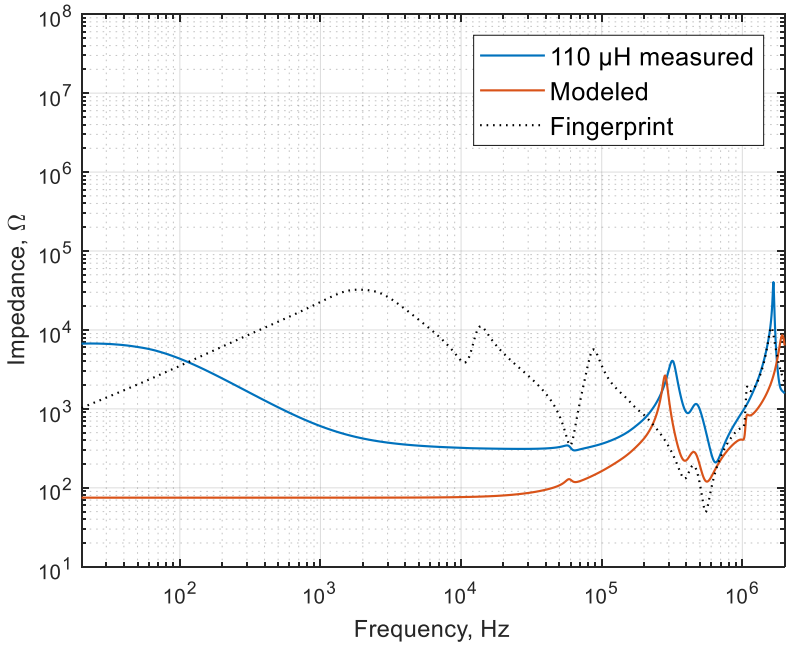

Figure 7.6 Comparison of measured and modeled 110 µH shunt inductances impedance response for a 350 VA transformer

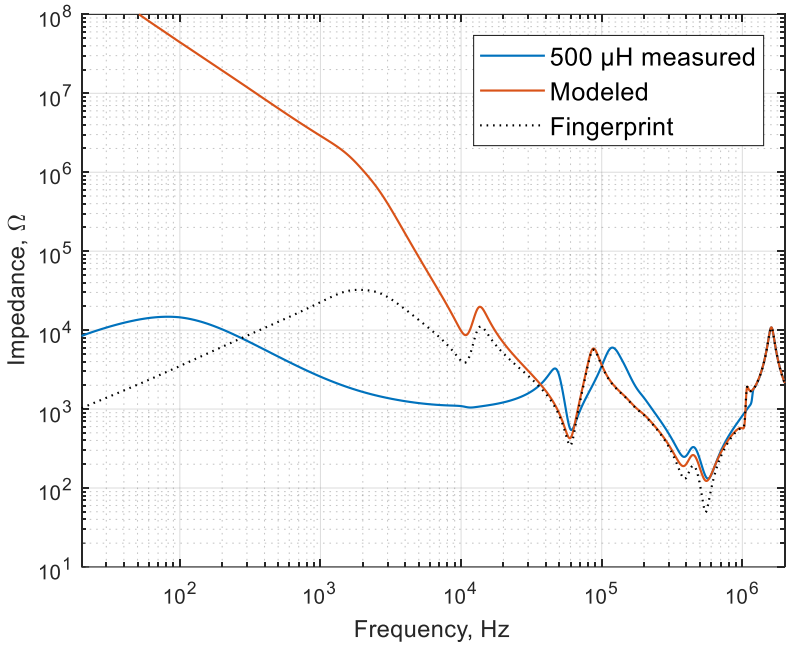

Figure 7.7 Comparison of measured and modeled 500 µH shunt inductances impedance response for a 350 VA transformer

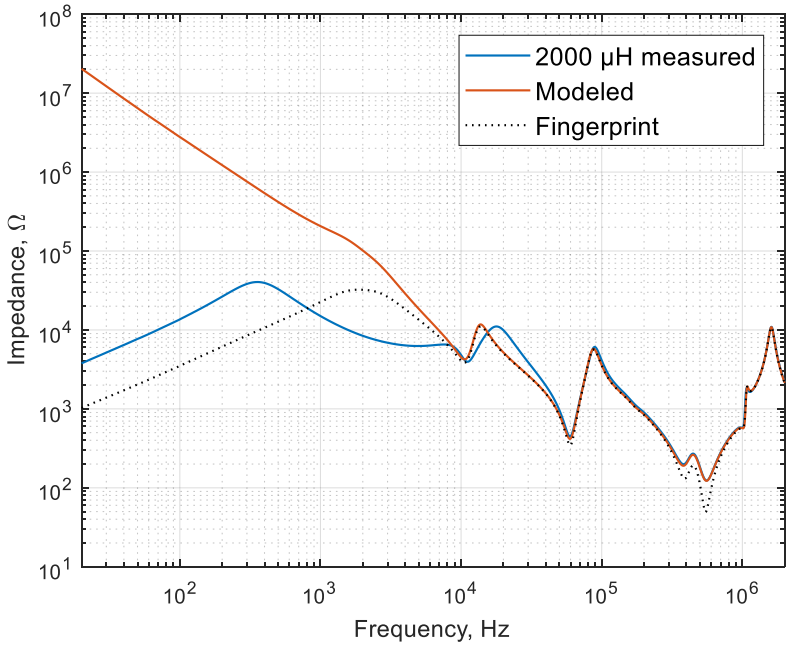

Figure 7.8 Comparison of measured and modeled 2000 µH shunt inductances impedance response for a 350 VA transformer

\

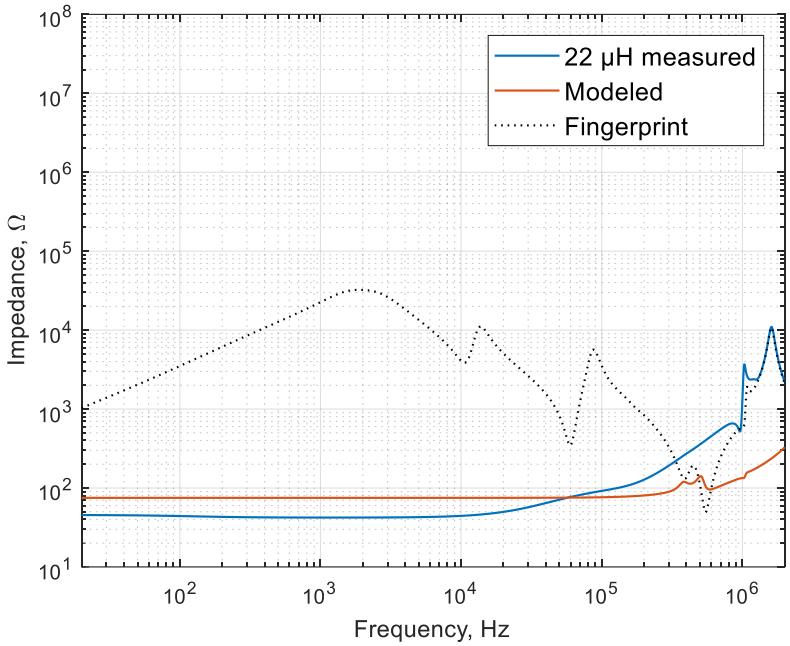

Figure 7.9 Comparison of measured and modeled 22 µH parallel inductances impedance response for a 350 VA transformer

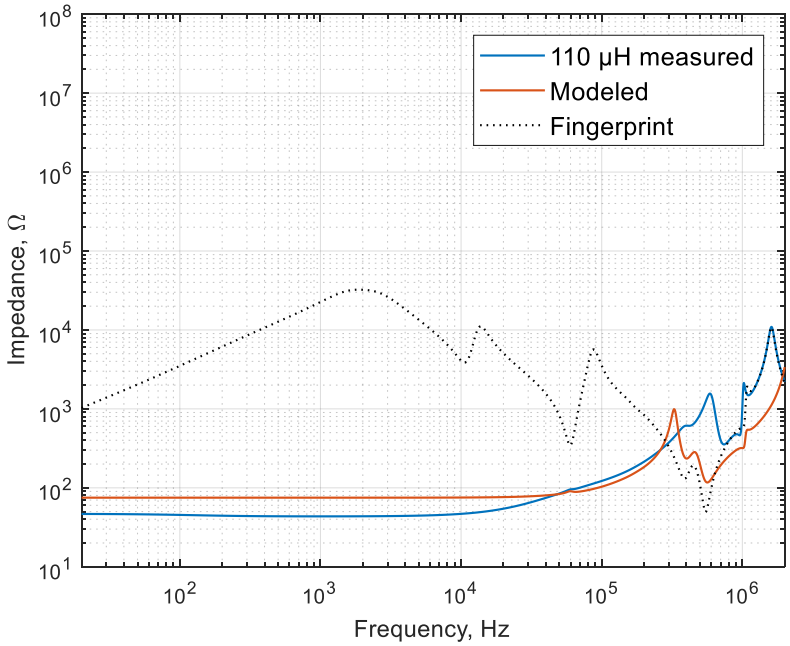

Figure 7.10 Comparison of measured and modeled 110 µH parallel inductances impedance response for a 350 VA transformer

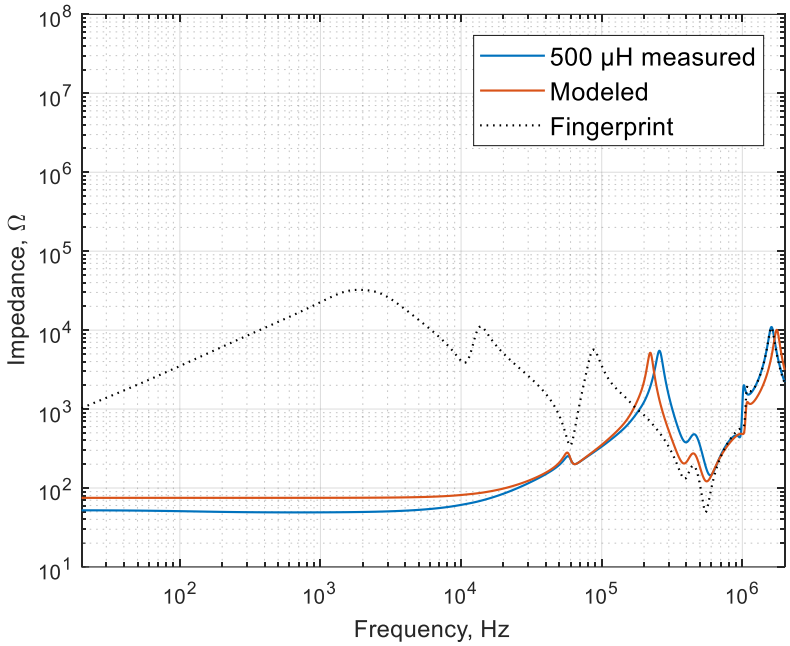

Figure 7.11 Comparison of measured and modeled 500 µH parallel inductances impedance response for a 350 VA transformer

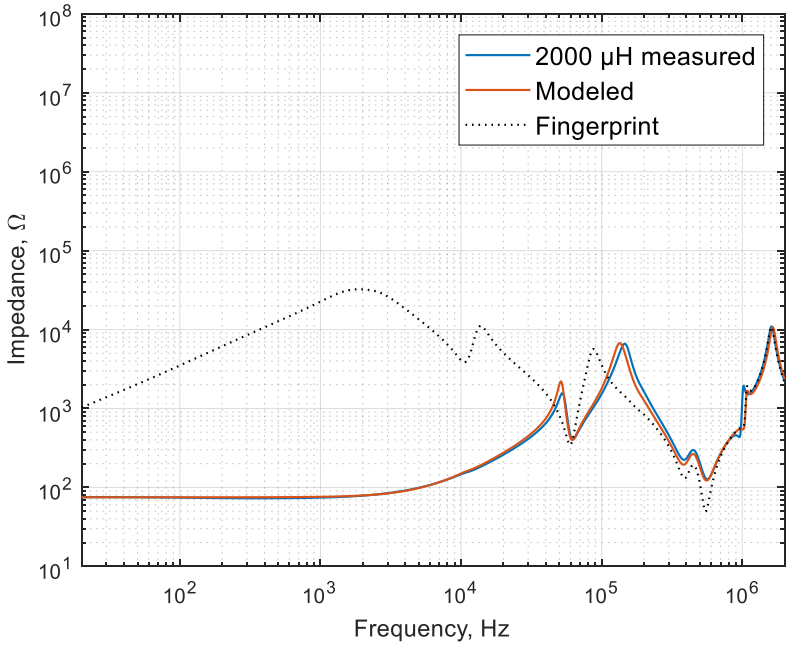

Figure 7.10 Comparison of measured and modeled 2000 µH parallel inductances impedance response for a 350 VA transformer

Table 13. Numerical indices and corresponding formulas

Name	Formula
Standard Deviation	$SD = \sqrt{\frac{\sum_{i=1}^{N}\left(Y(i) - X(i)\right)^2}{N}}$
Comparative Standard Deviation	$CSD = \sqrt{\frac{\sum_{i=1}^{N}[(Y(i) - \bar{Y}) - (X(i) - \bar{X})]^2}{N-1}}$
Minimum-Maximum ratio	$MM = \frac{\sum_{i=1}^{N} min\left(Y(i), X(i)\right)}{\sum_{i=1}^{N} max\left(Y(i), X(i)\right)}$
Normalized correlation coefficient	$\rho = \frac{\sum_{i=1}^{N}[\lvert X(i)\rvert - \frac{1}{N}\sum_{i=1}^{N} X(i)]\,[\lvert Y(i)\rvert - \frac{1}{N}\sum_{i=1}^{N} Y(i)]}{\sum_{i=1}^{N}\left[\lvert X(i)\rvert - \frac{1}{N}\sum_{i=1}^{N} X(i)\right]^2 \sum_{i=1}^{N}\left[\lvert Y(i)\rvert - \frac{1}{N}\sum_{i=1}^{N} Y(i)\right]^2}$
Sum Squared Error	$SSE = \frac{\sum_{i=1}^{N}\left(Y(i) - X(i)\right)^2}{N}$
Sum Squared Ratio Error	$SSRE = \frac{\sum_{i=1}^{N}\left(\frac{X(i)}{Y(i)} - 1\right)^2}{N}$
Sum Squared Max-Min Ratio Error	$SSMMRE = \frac{\sum_{i=1}^{N}\left(\frac{\max(Y(i), X(i))}{\min(Y(i), X(i))} - 1\right)^2}{N}$
Spectrum Deviation	$\sigma = \frac{1}{N}\sum_{i=1}^{N}\sqrt{\left[\frac{Y(i) - \left(\frac{Y(i)+X(i)}{2}\right)}{\left(\frac{Y(i)+X(i)}{2}\right)}\right]^2 + \left[\frac{X(i) - \left(\frac{Y(i)+X(i)}{2}\right)}{\left(\frac{Y(i)+X(i)}{2}\right)}\right]^2}$
Stochastic spectrum deviation	$\sigma_s = \frac{100}{N}\sum_{i=1}^{N}\left\lvert\frac{Y(i) - X(i)}{X(i)}\right\rvert$

Y(i) – fingerprint measurement, X(i) – compared measurement data set

Table 23.1 40 kVA transformer

Test Config.	Statistical Method	1 Ω	2 Ω	3 Ω	5 Ω	10 Ω	200 Ω
Series resistance	*SD*	0.3098	0.3624	0.4136	0.5801	1.0479	1.6422
	CSD	0.2893	0.3503	0.4058	0.5779	1.0438	1.5357
	MM	1.0045	1.0053	1.0057	1.0077	1.0120	1.0158
	ρ	1.0000	1.0000	1.0000	1.0000	1.0000	0.9999
Shunt resistance	*SD*	16.9740	16.9191	16.4748	15.8035	15.0727	6.0412
	CSD	13.3483	13.1427	12.5246	11.5002	10.1327	4.4482
	MM	1.2144	1.2170	1.2170	1.2185	1.2244	1.0876
	ρ	0.9946	0.9948	0.9952	0.9958	0.9963	0.9991
Parallel resistance	*SD*	50.5301	50.4565	50.3569	50.2076	49.7569	42.7161
	CSD	28.5783	28.5638	28.5451	28.5388	28.5249	24.9852
	MM	5.0578	5.0216	4.9746	4.8992	4.6859	3.0399
	ρ	0.8735	0.8749	0.8767	0.8793	0.8863	0.9588
		1 kΩ	**2 kΩ**	**3 kΩ**	**4 kΩ**	**5 kΩ**	**1 MΩ**
Series resistance	*SD*	6.1351	7.9396	9.0027	9.6986	10.2029	24.9444
	CSD	5.6335	7.2363	8.1415	8.7073	9.0680	11.7078
	MM	1.0531	1.0717	1.0833	1.0924	1.0993	1.4254
	ρ	0.9984	0.9974	0.9968	0.9963	0.9960	0.9938
Shunt resistance	*SD*	3.4781	3.0283	2.8445	2.7189	2.7509	2.6431
	CSD	3.0009	2.7309	2.6058	2.5025	2.5337	2.4900
	MM	1.0432	1.0349	1.0324	1.0312	1.0317	1.0318
	ρ	0.9996	0.9997	0.9997	0.9997	0.9997	0.9997
Parallel resistance	*SD*	33.9073	29.2968	27.0454	25.2171	23.9003	2.6092
	CSD	21.4708	19.3924	18.3155	17.3952	16.7147	2.6082
	MM	2.0568	1.7561	1.6398	1.5581	1.5051	1.0297
	ρ	0.9812	0.9866	0.9885	0.9899	0.9908	0.9997

Table 13.2 40 kVA transformer

Test Config.	Statistical Method	1 Ω	2 Ω	3 Ω	5 Ω	10 Ω	200 Ω
Series resistance	*SSE*	0.0960	0.1313	0.1711	0.3365	1.0982	2.6970
	SSRE	0.0002	0.0003	0.0004	0.0009	0.0033	0.0102
	SSMMRE	0.0002	0.0003	0.0004	0.0008	0.0024	0.0055
	σ	0.0053	0.0064	0.0073	0.0102	0.0177	0.0250
	σs	0.7493	0.9026	1.0380	1.4645	2.6163	3.9670
Shunt resistance	*SSE*	288.1150	286.2544	271.4187	249.7512	227.1857	36.4965
	SSRE	0.1073	0.1086	0.1090	0.1171	0.1568	0.0338
	SSMMRE	0.0424	0.0435	0.0444	0.0473	0.0542	0.0156
	σ	0.1334	0.1360	0.1385	0.1451	0.1573	0.0713
	σs	22.8770	23.3239	23.7229	24.9438	27.7970	11.3874
Parallel resistance	*SSE*	2553.2896	2545.8603	2535.8186	2520.8018	2475.7449	1824.6654
	SSRE	0.5799	0.5778	0.5750	0.5706	0.5576	0.4031
	SSMMRE	0.5783	0.5762	0.5734	0.5688	0.5553	0.4004
	σ	0.8482	0.8454	0.8419	0.8360	0.8187	0.6256
	σs	68.3525	68.2196	68.0581	67.7716	66.9349	57.0132
		1 kΩ	**2 kΩ**	**3 kΩ**	**4 kΩ**	**5 kΩ**	**1 MΩ**
Series resistance	*SSE*	37.6390	63.0380	81.0480	94.0629	104.0990	622.2253
	SSRE	0.1307	0.2153	0.2648	0.2864	0.2966	0.6056
	SSMMRE	0.0325	0.0414	0.0452	0.0483	0.0503	0.1286
	σ	0.0724	0.0893	0.0974	0.1043	0.1087	0.2812
	σs	14.4445	18.7784	20.9307	22.3680	23.3322	57.7761
Shunt resistance	*SSE*	12.0970	9.1703	8.0914	7.3926	7.5674	6.9862
	SSRE	0.0042	0.0029	0.0027	0.0026	0.0026	0.0026
	SSMMRE	0.0034	0.0024	0.0022	0.0021	0.0022	0.0022
	σ	0.0315	0.0242	0.0228	0.0224	0.0227	0.0236
	σs	4.6472	3.5513	3.3384	3.2720	3.3200	3.4281
Parallel resistance	*SSE*	1149.7077	858.3029	731.4537	635.8998	571.2224	6.8078
	SSRE	0.2355	0.1657	0.1373	0.1170	0.1036	0.0024
	SSMMRE	0.2329	0.1650	0.1369	0.1166	0.1033	0.0021
	σ	0.4154	0.3224	0.2814	0.2511	0.2308	0.0229
	σs	42.5690	34.6110	30.8679	28.0471	26.1336	3.2651

Table 13.3 20 kVA transformer

Test Config.	Statistical Method	1 Ω	2 Ω	3 Ω	5 Ω	10 Ω	200 Ω
Series resistance	*SD*	0.1139	0.1823	0.2876	0.4560	0.9886	1.7124
	CSD	0.1114	0.1821	0.2848	0.4457	0.9697	1.5359
	MM	1.0020	1.0027	1.0051	1.0078	1.0155	1.0242
	ρ	1.0000	1.0000	1.0000	1.0000	0.9999	0.9997
Shunt resistance	*SD*	25.5188	22.9878	21.4576	19.7478	16.5484	4.1418
	CSD	14.7238	12.4465	10.9006	8.8562	6.9108	2.2681
	MM	1.6283	1.5800	1.5517	1.5223	1.4432	1.1027
	ρ	0.9894	0.9918	0.9932	0.9946	0.9962	0.9993
Parallel resistance	*SD*	28.5728	28.4823	28.3892	28.2080	27.7402	20.7854
	CSD	15.1004	15.0852	15.0694	15.0645	15.1377	12.0586
	MM	3.5973	3.5633	3.5297	3.4697	3.3228	2.0628
	ρ	0.9106	0.9121	0.9135	0.9160	0.9215	0.9785
		1 kΩ	**2 kΩ**	**3 kΩ**	**4 kΩ**	**5 kΩ**	**1 MΩ**
Series resistance	*SD*	6.3043	8.5534	10.2826	11.6407	12.7200	43.4850
	CSD	5.3554	6.9106	7.9380	8.7571	9.2381	16.2503
	MM	1.1005	1.1548	1.1965	1.2350	1.2686	2.2010
	ρ	0.9967	0.9947	0.9934	0.9924	0.9917	0.9925
Shunt resistance	*SD*	1.0610	0.6867	0.5443	0.4974	0.4322	0.3421
	CSD	0.5860	0.3721	0.3070	0.2997	0.2752	0.2667
	MM	1.0266	1.0175	1.0135	1.0122	1.0107	1.0075
	ρ	1.0000	1.0000	1.0000	1.0000	1.0000	1.0000
Parallel resistance	*SD*	12.4938	9.0349	7.2971	6.1670	5.3335	0.3391
	CSD	8.5154	6.6006	5.5252	4.7904	4.2210	0.3326
	MM	1.4064	1.2458	1.1803	1.1431	1.1179	1.0074
	ρ	0.9932	0.9962	0.9974	0.9981	0.9985	1.0000

Table 13.4 20 kVA transformer

Test Config.	Statistical Method	1 Ω	2 Ω	3 Ω	5 Ω	10 Ω	200 Ω
Series resistance	*SSE*	0.0130	0.0332	0.0827	0.2079	0.9773	2.9325
	SSRE	0.0001	0.0002	0.0004	0.0010	0.0045	0.0176
	SSMMRE	0.0001	0.0001	0.0003	0.0008	0.0029	0.0070
	σ	0.0022	0.0033	0.0057	0.0088	0.0180	0.0278
	σs	0.3149	0.4763	0.8138	1.2768	2.6751	4.5956
Shunt resistance	*SSE*	651.2075	528.4388	460.4266	389.9775	273.8483	17.1548
	SSRE	0.7303	0.6056	0.5504	0.5335	0.3977	0.0527
	SSMMRE	0.1576	0.1464	0.1401	0.1355	0.1116	0.0186
	σ	0.3229	0.3095	0.3025	0.2975	0.2634	0.0805
	σs	68.1306	63.1460	60.6523	59.1770	50.2952	13.2468
Parallel resistance	*SSE*	816.4066	811.2391	805.9484	795.6936	769.5201	432.0336
	SSRE	0.5329	0.5295	0.5261	0.5198	0.5068	0.2754
	SSMMRE	0.5263	0.5227	0.5190	0.5120	0.4948	0.2627
	σ	0.7811	0.7764	0.7718	0.7638	0.7445	0.4608
	σs	66.1216	65.8873	65.6679	65.3749	64.9466	47.5378
		1 kΩ	**2 kΩ**	**3 kΩ**	**4 kΩ**	**5 kΩ**	**1 MΩ**
Series resistance	*SSE*	39.7437	73.1615	105.7313	135.5070	161.7983	1890.9461
	SSRE	0.1852	0.3107	0.4177	0.5075	0.5807	2.2586
	SSMMRE	0.0369	0.0503	0.0585	0.0676	0.0761	0.2958
	σ	0.0910	0.1248	0.1459	0.1667	0.1849	0.5174
	σs	18.2961	25.8171	30.8968	35.5063	39.5078	129.9745
Shunt resistance	*SSE*	1.1257	0.4716	0.2963	0.2474	0.1868	0.1170
	SSRE	0.0027	0.0008	0.0004	0.0003	0.0002	0.0001
	SSMMRE	0.0019	0.0007	0.0004	0.0003	0.0002	0.0001
	σ	0.0217	0.0140	0.0105	0.0094	0.0083	0.0057
	σs	3.1871	2.0228	1.5002	1.3495	1.1806	0.8173
Parallel resistance	*SSE*	156.0938	81.6299	53.2473	38.0318	28.4467	0.1150
	SSRE	0.0920	0.0428	0.0264	0.0182	0.0133	0.0003
	SSMMRE	0.0855	0.0416	0.0260	0.0181	0.0132	0.0003
	σ	0.2161	0.1367	0.1013	0.0810	0.0669	0.0065
	σs	25.9968	17.1535	12.9658	10.5218	8.7841	0.9143

Table 13.5 0.76 kVA transformer

Test Config.	Statistical Method	1 Ω	2 Ω	3 Ω	5 Ω	10 Ω	200 Ω
Series resistance	*SD*	5.5732	5.6858	5.6267	5.7869	5.9649	4.0324
	CSD	5.0387	5.1409	5.1156	5.2618	5.4693	4.0007
	MM	1.0129	1.0138	1.0129	1.0153	1.0189	1.0395
	ρ	0.9973	0.9972	0.9972	0.9970	0.9968	0.9984
Shunt resistance	*SD*	26.9693	24.2887	22.9208	20.5230	17.2287	4.5051
	CSD	17.2196	15.0633	13.7856	11.2986	7.1092	3.0570
	MM	1.8896	1.8133	1.7709	1.6839	1.5609	1.1363
	ρ	0.9823	0.9851	0.9868	0.9899	0.9944	0.9986
Parallel resistance	*SD*	21.6645	21.5904	21.5079	21.3524	20.9321	14.7843
	CSD	12.3855	12.3836	12.3976	12.3931	12.6469	9.8431
	MM	2.6301	2.6118	2.5900	2.5554	2.4410	1.6652
	ρ	0.9286	0.9294	0.9301	0.9321	0.9333	0.9808
		1 kΩ	**2 kΩ**	**3 kΩ**	**4 kΩ**	**5 kΩ**	**1 MΩ**
Series resistance	*SD*	7.5572	11.0470	13.5258	15.2658	16.4461	47.8221
	CSD	6.8231	9.3802	11.3453	12.5404	12.9160	28.5966
	MM	1.1667	1.2759	1.3608	1.4247	1.4744	2.5382
	ρ	0.9948	0.9907	0.9873	0.9851	0.9846	0.9686
Shunt resistance	*SD*	1.2039	0.2611	1.0316	1.7554	1.6020	0.6884
	CSD	0.9582	0.2611	1.0320	1.7416	1.5716	0.6769
	MM	1.0333	1.0064	1.0189	1.0234	1.0195	1.0110
	ρ	0.9999	1.0000	0.9999	0.9996	0.9997	0.9999
Parallel resistance	*SD*	8.4312	5.9510	4.8621	3.9937	3.2823	0.8911
	CSD	6.3877	4.6922	3.8919	3.2584	2.6795	0.8454
	MM	1.2579	1.1566	1.1190	1.0913	1.0734	1.0098
	ρ	0.9948	0.9975	0.9983	0.9988	0.9992	0.9999

Table 13.6 0.76 kVA transformer

Test Config.	Statistical Method	1 Ω	2 Ω	3 Ω	5 Ω	10 Ω	200 Ω
Series resistance	*SSE*	31.0604	32.3288	31.6597	33.4887	35.5804	16.2599
	SSRE	0.0175	0.0183	0.0180	0.0195	0.0223	0.0267
	SSMMRE	0.0008	0.0009	0.0008	0.0012	0.0022	0.0098
	σ	0.0547	0.0567	0.0557	0.0599	0.0658	0.0691
	σs	6.6909	6.9423	6.8161	7.3567	8.1683	10.1537
Shunt resistance	*SSE*	727.3450	589.9407	525.3652	421.1924	296.8264	20.2955
	SSRE	1.1883	0.9726	0.8747	0.7304	0.5612	0.0510
	SSMMRE	0.2280	0.2110	0.2008	0.1797	0.1492	0.0221
	σ	0.4348	0.4136	0.4005	0.3701	0.3265	0.0993
	σs	93.5172	86.1314	82.3359	75.0353	64.4051	15.8212
Parallel resistance	*SSE*	469.3505	466.1436	462.5902	455.9231	438.1529	218.5760
	SSRE	0.4428	0.4394	0.4357	0.4286	0.4127	0.1882
	SSMMRE	0.4309	0.4272	0.4232	0.4151	0.3954	0.1708
	σ	0.6732	0.6686	0.6635	0.6538	0.6286	0.3407
	σs	61.2806	61.0164	60.7143	60.1956	58.7332	37.8987
		1 kΩ	**2 kΩ**	**3 kΩ**	**4 kΩ**	**5 kΩ**	**1 MΩ**
Series resistance	*SSE*	57.1118	122.0359	182.9460	233.0461	270.4755	2286.9577
	SSRE	0.2027	0.4207	0.6079	0.7645	0.8976	5.1347
	SSMMRE	0.0523	0.0866	0.1106	0.1282	0.1415	0.3657
	σ	0.1607	0.2274	0.2715	0.3015	0.3167	0.6183
	σs	28.8173	44.0897	54.7884	62.5856	67.9211	186.5188
Shunt resistance	*SSE*	1.4495	0.0681	1.0643	3.0813	2.5663	0.4739
	SSRE	0.0025	0.0001	0.0008	0.0020	0.0017	0.0003
	SSMMRE	0.0020	0.0001	0.0008	0.0020	0.0017	0.0003
	σ	0.0253	0.0047	0.0127	0.0149	0.0121	0.0073
	σs	3.6559	0.6627	1.7711	2.0052	1.6243	1.0205
Parallel resistance	*SSE*	71.0852	35.4147	23.6399	15.9494	10.7738	0.7941
	SSRE	0.0545	0.0232	0.0145	0.0094	0.0062	0.0005
	SSMMRE	0.0479	0.0222	0.0142	0.0093	0.0062	0.0005
	σ	0.1432	0.0873	0.0660	0.0503	0.0404	0.0060
	σs	18.0420	11.2767	8.6113	6.6372	5.4011	0.8184

Table 13.7 0.35 kVA transformer

Test Config.	Statistical Method	1 Ω	2 Ω	3 Ω	5 Ω	10 Ω	200 Ω
Series resistance	*SD*	2.5605	2.5049	2.3218	2.7065	2.2784	2.0836
	CSD	2.4489	2.4064	2.2537	2.6168	2.2360	2.0751
	MM	1.0210	1.0213	1.0210	1.0256	1.0241	1.0271
	ρ	0.9995	0.9995	0.9995	0.9994	0.9996	0.9996
Shunt resistance	*SD*	25.9451	23.3072	21.7520	19.9649	16.9463	4.2259
	CSD	16.9756	14.6155	12.9974	10.6839	6.4218	2.3684
	MM	1.6368	1.5848	1.5500	1.5002	1.4295	1.1041
	ρ	0.9907	0.9927	0.9939	0.9952	0.9974	0.9994
Parallel resistance	*SD*	31.6324	31.5937	31.5105	31.3638	30.9252	24.1006
	CSD	17.6287	17.6519	17.6564	17.6694	17.6405	14.3676
	MM	3.4270	3.4122	3.3866	3.3455	3.2395	2.1339
	ρ	0.8952	0.8956	0.8969	0.8992	0.9063	0.9691
		1 kΩ	**2 kΩ**	**3 kΩ**	**4 kΩ**	**5 kΩ**	**1 MΩ**
Series resistance	*SD*	5.3249	8.0853	10.0594	11.4509	12.4293	39.2955
	CSD	4.7790	6.9239	8.5033	9.5112	10.0374	15.8074
	MM	1.0785	1.1288	1.1695	1.1999	1.2216	1.9786
	ρ	0.9979	0.9956	0.9937	0.9923	0.9915	0.9903
Shunt resistance	*SD*	1.0132	0.5429	0.4721	0.9876	0.8935	0.2458
	CSD	0.4551	0.3484	0.4262	0.9877	0.8919	0.2456
	MM	1.0247	1.0124	1.0099	1.0128	1.0113	1.0037
	ρ	1.0000	1.0000	1.0000	0.9999	0.9999	1.0000
Parallel resistance	*SD*	15.5063	11.8207	9.8353	8.5740	7.4934	0.6061
	CSD	10.1997	8.1271	6.8930	6.0883	5.4620	0.5674
	MM	1.4777	1.3095	1.2380	1.1974	1.1626	1.0060
	ρ	0.9913	0.9952	0.9968	0.9976	0.9981	1.0000

Table 13.8 0.35 kVA transformer

Test Config.	Statistical Method	1 Ω	2 Ω	3 Ω	5 Ω	10 Ω	200 Ω
Series resistance	*SSE*	6.5560	6.2746	5.3908	7.3253	5.1911	4.3416
	SSRE	0.0042	0.0041	0.0037	0.0051	0.0050	0.0135
	SSMMRE	0.0042	0.0041	0.0037	0.0050	0.0046	0.0069
	σ	0.0169	0.0174	0.0172	0.0218	0.0228	0.0289
	σs	2.1427	2.2297	2.2219	2.8186	3.0897	4.4811
Shunt resistance	*SSE*	673.1504	543.2235	473.1510	398.5977	287.1786	17.8580
	SSRE	0.5143	0.4440	0.4178	0.4263	0.3575	0.0415
	SSMMRE	0.1536	0.1412	0.1328	0.1231	0.1074	0.0183
	σ	0.3365	0.3196	0.3069	0.2870	0.2645	0.0839
	σs	63.4016	59.2928	56.9355	54.3522	49.3623	13.4021
Parallel resistance	*SSE*	1000.6082	998.1632	992.9130	983.6883	956.3668	580.8397
	SSRE	0.5314	0.5301	0.5274	0.5231	0.5117	0.3070
	SSMMRE	0.5202	0.5185	0.5154	0.5098	0.4941	0.2904
	σ	0.7792	0.7772	0.7733	0.7667	0.7484	0.4947
	σs	66.3361	66.2529	66.0990	65.8949	65.4238	50.0426
		1 kΩ	**2 kΩ**	**3 kΩ**	**4 kΩ**	**5 kΩ**	**1 MΩ**
Series resistance	*SSE*	28.3546	65.3729	101.1920	131.1232	154.4868	1544.1364
	SSRE	0.1177	0.2429	0.3501	0.4405	0.5090	2.0281
	SSMMRE	0.0286	0.0463	0.0589	0.0678	0.0738	0.2585
	σ	0.0762	0.1120	0.1373	0.1551	0.1672	0.4659
	σs	14.3573	22.6554	28.7322	33.2253	36.4703	115.1245
Shunt resistance	*SSE*	1.0266	0.2947	0.2229	0.9754	0.7983	0.0604
	SSRE	0.0020	0.0005	0.0003	0.0007	0.0006	0.0000
	SSMMRE	0.0016	0.0004	0.0002	0.0007	0.0006	0.0000
	σ	0.0209	0.0104	0.0080	0.0098	0.0085	0.0025
	σs	3.0533	1.4894	1.1398	1.3598	1.1841	0.3487
Parallel resistance	*SSE*	240.4450	139.7286	96.7325	73.5130	56.1517	0.3674
	SSRE	0.1151	0.0611	0.0408	0.0304	0.0224	0.0003
	SSMMRE	0.1096	0.0600	0.0404	0.0303	0.0224	0.0003
	σ	0.2505	0.1689	0.1317	0.1100	0.0909	0.0044
	σs	29.1190	20.4963	16.3665	13.8728	11.6187	0.6094

Table 14.1 40 kVA transformer

Test Config.	Statistical Method	100 pF	470 pF	1000 pF	50 nF	100 nF
Series capacitance	*SD*	21.3067	12.8273	9.4666	0.7830	0.4083
	CSD	12.0428	9.2912	7.7065	0.7661	0.3881
	MM	1.3395	1.1775	1.1177	1.0057	1.0040
	ρ	0.9966	0.9974	0.9980	1.0000	1.0000
Shunt capacitance	*SD*	1.3502	3.2280	4.6934	15.6722	18.0294
	CSD	1.3429	3.2215	4.6612	14.1995	15.8199
	MM	1.0057	1.0188	1.0323	1.2059	1.2661
	ρ	0.9999	0.9996	0.9991	0.9883	0.9840
Parallel capacitance	*SD*	2.4688	7.1140	10.8784	32.8927	36.5277
	CSD	2.0462	5.5334	8.1632	19.4233	20.9085
	MM	1.0363	1.1173	1.1947	2.0471	2.3277
	ρ	0.9998	0.9985	0.9964	0.9654	0.9567
		200 nF	**470 nF**	**940 nF**	**2.2 µF**	
Series capacitance	*SD*	0.3708	0.3652	0.3778	0.3932	
	CSD	0.3561	0.3550	0.3692	0.3847	
	MM	1.0039	1.0041	1.0044	1.0045	
	ρ	1.0000	1.0000	1.0000	1.0000	
Shunt capacitance	*SD*	20.3968	23.1906	26.1605	29.3929	
	CSD	17.3457	16.8599	18.0922	19.6732	
	MM	1.3389	1.4481	1.5722	1.7181	
	ρ	0.9791	0.9760	0.9709	0.9647	
Parallel capacitance	*SD*	39.8321	43.5541	45.8699	48.0207	
	CSD	22.3296	24.1778	25.4041	26.5546	
	MM	2.6559	3.1476	3.5483	4.0222	
	ρ	0.9469	0.9304	0.9159	0.8972	

Table 14.2 40 kVA transformer

Test Config.	Statistical Method	100 pF	470 pF	1000 pF	50 nF	100 nF
Series capacitance	*SSE*	453.9755	164.5403	89.6167	0.6131	0.1667
	SSRE	0.2369	0.0647	0.0295	0.0003	0.0002
	SSMMRE	0.0827	0.0325	0.0169	0.0002	0.0002
	σ	0.2186	0.1201	0.0796	0.0043	0.0034
	σs	39.0873	19.4762	12.4169	0.6064	0.4721
Shunt capacitance	*SSE*	1.8232	10.4202	22.0284	245.6189	325.0581
	SSRE	0.0029	0.0138	0.0274	0.1584	0.1839
	SSMMRE	0.0029	0.0129	0.0259	0.1480	0.1729
	σ	0.0095	0.0311	0.0540	0.2491	0.2895
	σs	1.1833	3.6990	6.0849	24.5110	28.2517
Parallel capacitance	*SSE*	6.0950	50.6094	118.3402	1081.9309	1334.2708
	SSRE	0.0025	0.0210	0.0540	0.3591	0.4109
	SSMMRE	0.0024	0.0207	0.0522	0.3336	0.3849
	σ	0.0277	0.0888	0.1496	0.5410	0.6071
	σs	3.8185	11.5073	18.2928	52.2827	56.8135
		200 nF	**470 nF**	**940 nF**	**2.2 µF**	
Series capacitance	*SSE*	0.1375	0.1333	0.1427	0.1546	
	SSRE	0.0002	0.0002	0.0002	0.0002	
	SSMMRE	0.0002	0.0002	0.0002	0.0002	
	σ	0.0034	0.0035	0.0037	0.0039	
	σs	0.4713	0.4948	0.5190	0.5448	
Shunt capacitance	*SSE*	416.0309	537.8058	684.3711	863.9451	
	SSRE	0.2077	0.2362	0.2644	0.2950	
	SSMMRE	0.1964	0.2261	0.2542	0.2847	
	σ	0.3285	0.3754	0.4189	0.4632	
	σs	31.9470	35.9927	39.9224	43.6730	
Parallel capacitance	*SSE*	1586.5983	1896.9639	2104.0456	2305.9885	
	SSRE	0.4587	0.5139	0.5494	0.5847	
	SSMMRE	0.4325	0.4875	0.5229	0.5581	
	σ	0.6681	0.7384	0.7830	0.8269	
	σs	60.7917	65.1790	67.8318	70.3121	

Table 14.3 20 kVA transformer

Test Config.	Statistical Method	100 pF	470 pF	1000 pF	50 nF	100 nF
Series capacitance	*SD*	42.8134	33.6330	29.3215	11.0761	8.2547
	CSD	27.0417	24.2920	22.4035	10.3101	7.9009
	MM	1.9523	1.6653	1.5390	1.1573	1.1098
	ρ	0.9757	0.9747	0.9754	0.9912	0.9945
Shunt capacitance	*SD*	1.9938	3.8776	5.1235	16.0250	17.9343
	CSD	1.9948	3.8743	5.0953	13.7828	15.1742
	MM	1.0128	1.0365	1.0573	1.3296	1.4028
	ρ	0.9996	0.9986	0.9974	0.9742	0.9673
Parallel capacitance	*SD*	1.5930	5.0264	7.5802	21.2370	22.9635
	CSD	1.4622	4.5400	6.7513	17.1211	17.8791
	MM	1.0269	1.0937	1.1529	1.6826	1.8230
	ρ	0.9998	0.9978	0.9950	0.9521	0.9420
		200 nF	**470 nF**	**940 nF**	**2.2 µF**	
Series capacitance	*SD*	6.1060	3.7530	2.4260	1.3585	
	CSD	5.9756	3.7443	2.4251	1.3422	
	MM	1.0764	1.0431	1.0265	1.0146	
	ρ	0.9967	0.9987	0.9994	0.9998	
Shunt capacitance	*SD*	19.2809	20.4643	21.2439	21.8835	
	CSD	16.0528	16.6740	17.0038	17.2995	
	MM	1.4664	1.5435	1.6097	1.6811	
	ρ	0.9620	0.9574	0.9540	0.9517	
Parallel capacitance	*SD*	24.2217	25.6716	26.4990	27.3069	
	CSD	18.1924	18.1295	17.7052	17.0286	
	MM	1.9645	2.2042	2.4013	2.6518	
	ρ	0.9337	0.9227	0.9164	0.9102	

Table 14.4 20 kVA transformer

Test Config.	Statistical Method	100 pF	470 pF	1000 pF	50 nF	100 nF
Series capacitance	*SSE*	1832.9856	1131.1803	859.7510	122.6798	68.1395
	SSRE	2.0362	1.2968	1.0051	0.1647	0.0956
	SSMMRE	0.2282	0.1632	0.1357	0.0412	0.0274
	σ	0.4180	0.3126	0.2613	0.0981	0.0732
	σs	106.7732	76.2664	62.7122	18.9404	13.3741
Shunt capacitance	*SSE*	3.9753	15.0356	26.2499	256.8003	321.6373
	SSRE	0.0070	0.0229	0.0355	0.1550	0.1759
	SSMMRE	0.0058	0.0201	0.0329	0.1488	0.1695
	σ	0.0152	0.0423	0.0650	0.2459	0.2774
	σs	1.9148	4.9097	7.2010	23.4167	26.1465
Parallel capacitance	*SSE*	2.5376	25.2650	57.4600	451.0096	527.3220
	SSRE	0.0028	0.0278	0.0598	0.2615	0.2983
	SSMMRE	0.0028	0.0258	0.0523	0.2396	0.2765
	σ	0.0211	0.0763	0.1219	0.3932	0.4452
	σs	2.8513	9.4868	14.4655	38.1949	42.1616
		200 nF	**470 nF**	**940 nF**	**2.2 µF**	
Series capacitance	*SSE*	37.2829	14.0852	5.8854	1.8455	
	SSRE	0.0547	0.0222	0.0097	0.0032	
	SSMMRE	0.0176	0.0083	0.0042	0.0018	
	σ	0.0539	0.0328	0.0213	0.0126	
	σs	9.3805	5.3451	3.3046	1.8574	
Shunt capacitance	*SSE*	371.7513	418.7895	451.3022	478.8874	
	SSRE	0.1930	0.2126	0.2301	0.2483	
	SSMMRE	0.1864	0.2059	0.2234	0.2415	
	σ	0.3032	0.3334	0.3604	0.3908	
	σs	28.3749	31.0855	33.4529	36.1668	
Parallel capacitance	*SSE*	586.6919	659.0292	702.1961	745.6647	
	SSRE	0.3320	0.3826	0.4188	0.4599	
	SSMMRE	0.3102	0.3607	0.3970	0.4379	
	σ	0.4929	0.5644	0.6149	0.6711	
	σs	45.8578	51.5143	55.4655	59.7888	

Table 14.5 0.76 kVA transformer

Test Config.	Statistical Method	100 pF	470 pF	1000 pF	50 nF	100 nF
Series capacitance	*SD*	47.9098	38.0907	33.4220	14.5768	11.9116
	CSD	28.1920	25.6336	23.9324	13.2852	11.1430
	MM	2.3908	2.0071	1.8372	1.2517	1.1943
	ρ	0.9676	0.9662	0.9661	0.9793	0.9842
Shunt capacitance	*SD*	1.2651	2.1217	3.8144	8.9640	8.9936
	CSD	1.2574	2.1173	3.7378	8.6098	8.7095
	MM	1.0136	1.0291	1.0549	1.1950	1.2164
	ρ	0.9998	0.9993	0.9978	0.9874	0.9871
Parallel capacitance	*SD*	1.3055	3.2885	4.8713	12.6746	14.7543
	CSD	1.2935	3.2073	4.7057	10.3022	11.7135
	MM	1.0194	1.0534	1.0840	1.4687	1.6059
	ρ	0.9997	0.9984	0.9965	0.9759	0.9661
		200 nF	**470 nF**	**940 nF**	**2.2 µF**	
Series capacitance	*SD*	9.4860	6.8154	5.1063	3.6203	
	CSD	9.0719	6.6223	5.0389	3.6203	
	MM	1.1456	1.0943	1.0661	1.0454	
	ρ	0.9889	0.9938	0.9963	0.9981	
Shunt capacitance	*SD*	9.3314	10.2292	11.8190	13.5369	
	CSD	8.8480	8.8698	9.9005	11.3200	
	MM	1.2424	1.2813	1.3653	1.4476	
	ρ	0.9858	0.9841	0.9797	0.9740	
Parallel capacitance	*SD*	16.5596	18.7268	19.8535	20.8027	
	CSD	12.9461	14.3027	14.7968	15.0101	
	MM	1.7413	1.9475	2.1007	2.2750	
	ρ	0.9554	0.9393	0.9294	0.9197	

Table 14.6 0.76 kVA transformer

Test Config.	Statistical Method	100 pF	470 pF	1000 pF	50 nF	100 nF
Series capacitance	*SSE*	2295.3508	1450.9008	1117.0280	212.4836	141.8871
	SSRE	5.9008	3.9783	3.1988	0.8351	0.6018
	SSMMRE	0.3216	0.2429	0.2044	0.0717	0.0582
	σ	0.5399	0.4267	0.3695	0.1414	0.1177
	σs	172.4636	127.8306	107.6786	36.8193	29.2202
Shunt capacitance	*SSE*	1.6004	4.5017	14.5498	80.3537	80.8851
	SSRE	0.0054	0.0137	0.0301	0.1311	0.1357
	SSMMRE	0.0026	0.0113	0.0257	0.1034	0.1051
	σ	0.0124	0.0312	0.0563	0.1835	0.1944
	σs	1.9137	4.1356	6.7520	20.6031	22.5432
Parallel capacitance	*SSE*	1.7044	10.8139	23.7299	160.6454	217.6898
	SSRE	0.0039	0.0204	0.0371	0.1830	0.2297
	SSMMRE	0.0032	0.0179	0.0318	0.1684	0.2141
	σ	0.0176	0.0491	0.0740	0.3084	0.3710
	σs	2.4338	6.1986	8.9781	33.0066	38.2809
		200 nF	**470 nF**	**940 nF**	**2.2 µF**	
Series capacitance	*SSE*	89.9834	46.4502	26.0747	13.1069	
	SSRE	0.4152	0.2414	0.1483	0.0789	
	SSMMRE	0.0460	0.0315	0.0228	0.0168	
	σ	0.0963	0.0702	0.0544	0.0433	
	σs	22.5965	15.4400	11.1298	7.7328	
Shunt capacitance	*SSE*	87.0751	104.6357	139.6880	183.2476	
	SSRE	0.1453	0.1571	0.1759	0.1949	
	SSMMRE	0.1182	0.1319	0.1509	0.1698	
	σ	0.2166	0.2379	0.2710	0.3025	
	σs	24.0326	25.2975	28.4434	31.1379	
Parallel capacitance	*SSE*	274.2209	350.6935	394.1614	432.7504	
	SSRE	0.2690	0.3194	0.3530	0.3913	
	SSMMRE	0.2521	0.3003	0.3320	0.3664	
	σ	0.4231	0.4901	0.5343	0.5813	
	σs	42.4345	47.7140	51.2574	55.0426	

Table 14.7 0.35 kVA transformer

Test Config.	Statistical Method	100 pF	470 pF	1000 pF	50 nF	100 nF
Series capacitance	*SD*	36.5758	27.0378	22.7693	7.4339	5.4705
	CSD	21.3048	18.7189	17.0699	7.2019	5.4150
	MM	1.8197	1.5360	1.4123	1.0807	1.0555
	ρ	0.9878	0.9875	0.9877	0.9958	0.9975
Shunt capacitance	*SD*	1.4852	1.1111	2.3119	9.7077	11.4408
	CSD	1.4791	1.1063	2.3016	9.0574	10.4454
	MM	1.0115	1.0120	1.0240	1.1529	1.2146
	ρ	0.9998	0.9999	0.9995	0.9912	0.9875
Parallel capacitance	*SD*	0.8862	2.3410	3.8812	18.0741	20.8828
	CSD	0.8413	2.0585	3.3300	13.3672	15.0551
	MM	1.0125	1.0412	1.0728	1.5722	1.7397
	ρ	0.9999	0.9996	0.9988	0.9720	0.9610
		200 nF	**470 nF**	**940 nF**	**2.2 µF**	
Series capacitance	*SD*	3.9687	2.4890	1.5912	0.9164	
	CSD	3.9687	2.4890	1.5842	0.9027	
	MM	1.0379	1.0217	1.0133	1.0072	
	ρ	0.9987	0.9995	0.9998	0.9999	
Shunt capacitance	*SD*	12.9390	14.8471	16.4858	18.2941	
	CSD	11.6832	12.4510	13.2265	14.2943	
	MM	1.2516	1.3240	1.4102	1.5017	
	ρ	0.9838	0.9798	0.9757	0.9711	
Parallel capacitance	*SD*	23.4484	26.3047	27.9431	29.5342	
	CSD	16.4285	17.5664	17.9070	18.1420	
	MM	1.9335	2.2206	2.4565	2.7611	
	ρ	0.9486	0.9324	0.9224	0.9102	

Table 14.8 0.35 kVA transformer

Test Config.	Statistical Method	100 pF	470 pF	1000 pF	50 nF	100 nF
Series capacitance	*SSE*	1337.7914	731.0443	518.4422	55.2624	29.9267
	SSRE	1.1370	0.5696	0.3984	0.0513	0.0293
	SSMMRE	0.2038	0.1236	0.0893	0.0158	0.0103
	σ	0.3951	0.2743	0.2144	0.0468	0.0342
	σs	87.6538	55.5774	42.2335	8.2757	5.7479
Shunt capacitance	*SSE*	2.2057	1.2346	5.3451	94.2396	130.8922
	SSRE	0.0062	0.0039	0.0169	0.1168	0.1409
	SSMMRE	0.0030	0.0032	0.0116	0.1066	0.1300
	σ	0.0134	0.0159	0.0343	0.1842	0.2264
	σs	2.0506	2.2609	4.7382	18.8341	23.1039
Parallel capacitance	*SSE*	0.7854	5.4801	15.0641	326.6740	436.0901
	SSRE	0.0016	0.0104	0.0241	0.2204	0.2683
	SSMMRE	0.0013	0.0099	0.0232	0.2153	0.2629
	σ	0.0132	0.0435	0.0738	0.3718	0.4362
	σs	1.8532	5.7006	9.2339	37.2009	42.1818
		200 nF	**470 nF**	**940 nF**	**2.2 µF**	
Series capacitance	*SSE*	15.7503	6.1951	2.5318	0.8398	
	SSRE	0.0160	0.0065	0.0027	0.0009	
	SSMMRE	0.0067	0.0034	0.0018	0.0008	
	σ	0.0251	0.0156	0.0103	0.0063	
	σs	3.9788	2.3513	1.4893	0.8681	
Shunt capacitance	*SSE*	167.4172	220.4376	271.7825	334.6746	
	SSRE	0.1565	0.1752	0.1986	0.2220	
	SSMMRE	0.1453	0.1642	0.1875	0.2108	
	σ	0.2492	0.2829	0.3210	0.3575	
	σs	25.0065	28.1981	31.7370	34.8801	
Parallel capacitance	*SSE*	549.8292	691.9389	780.8175	872.2676	
	SSRE	0.3142	0.3693	0.4050	0.4461	
	SSMMRE	0.3084	0.3634	0.3993	0.4404	
	σ	0.4975	0.5703	0.6183	0.6724	
	σs	46.7396	51.8186	55.1566	58.8834	

Table 15.1 40 kVA transformer

Test Config.	Statistical Method	22 µH	44 µH	66 µH	110 µH
Series inductance	*SD*	0.4500	0.8714	1.2667	2.0597
	CSD	0.4495	0.8718	1.2673	2.0603
	MM	1.0047	1.0087	1.0124	1.0194
	ρ	1.0000	1.0000	0.9999	0.9998
Shunt inductance	*SD*	41.3247	39.0896	37.1429	36.8481
	CSD	23.9664	23.3822	22.7822	23.0987
	MM	2.7819	2.5132	2.3124	2.2536
	ρ	0.9555	0.9619	0.9665	0.9671
Parallel inductance	*SD*	51.6602	51.5782	51.5203	51.4029
	CSD	28.8546	29.2432	29.5345	29.3501
	MM	5.1699	5.0959	5.0308	4.9223
	ρ	0.8406	0.8405	0.8404	0.8453
		220 µH	**0.5 mH**	**1 mH**	**2 mH**
Series inductance	*SD*	3.3116	7.8598	10.2015	12.4371
	CSD	3.2558	7.4335	9.6896	11.7798
	MM	1.0320	1.0716	1.0902	1.1092
	ρ	0.9996	0.9976	0.9960	0.9942
Shunt inductance	*SD*	32.6187	28.0052	23.5401	18.0655
	CSD	21.3795	19.7652	17.8704	14.8259
	MM	1.9260	1.6465	1.4495	1.2844
	ρ	0.9761	0.9822	0.9865	0.9912
Parallel inductance	*SD*	50.8535	50.0395	48.8963	47.3472
	CSD	28.6258	28.9315	29.5883	30.3081
	MM	4.5882	4.0715	3.5869	3.1679
	ρ	0.8618	0.8730	0.8828	0.8928

Table 15.2 40 kVA transformer

Test Config.	Statistical Method	22 µH	44 µH	66 µH	110 µH
Series inductance	*SSE*	0.2025	0.7594	1.6046	4.2425
	SSRE	0.0004	0.0017	0.0035	0.0091
	SSMMRE	0.0004	0.0014	0.0026	0.0059
	σ	0.0066	0.0124	0.0176	0.0273
	σs	0.9487	1.8060	2.5823	4.0949
Shunt inductance	*SSE*	1707.7323	1527.9950	1379.5960	1357.7835
	SSRE	0.4286	0.4240	0.4328	0.4210
	SSMMRE	0.4018	0.3622	0.3273	0.3103
	σ	0.6351	0.5844	0.5384	0.5146
	σs	60.4543	58.3448	55.9536	53.9616
Parallel inductance	*SSE*	2668.7720	2660.3132	2654.3374	2642.2559
	SSRE	0.6695	0.6897	0.7221	0.6952
	SSMMRE	0.6268	0.6228	0.6192	0.6096
	σ	0.9147	0.9103	0.9052	0.8916
	σs	75.6221	76.3386	76.9446	75.2586
		220 µH	**0.5 mH**	**1 mH**	**2 mH**
Series inductance	*SSE*	10.9667	61.7762	104.0699	154.6826
	SSRE	0.0300	0.1396	0.3063	0.6082
	SSMMRE	0.0134	0.0372	0.0492	0.0571
	σ	0.0444	0.0846	0.1010	0.1136
	σs	7.2678	16.2395	22.2145	28.6749
Shunt inductance	*SSE*	1063.9787	784.2906	554.1353	326.3630
	SSRE	0.2694	0.1866	0.1296	0.0620
	SSMMRE	0.2357	0.1602	0.1058	0.0578
	σ	0.4178	0.3112	0.2272	0.1489
	σs	44.5747	34.8220	26.5644	18.0331
Parallel inductance	*SSE*	2586.0813	2503.9559	2390.8444	2241.7596
	SSRE	0.5915	0.5359	0.4932	0.4503
	SSMMRE	0.5787	0.5349	0.4929	0.4482
	σ	0.8500	0.7885	0.7297	0.6720
	σs	69.6233	64.0297	59.7842	56.5344

Table 15.3 20 kVA transformer

Test Config.	Statistical Method	22 µH	44 µH	66 µH	110 µH
Series inductance	*SD*	0.5563	1.0038	1.6162	2.3623
	CSD	0.5564	1.0029	1.6153	2.3612
	MM	1.0072	1.0135	1.0214	1.0307
	ρ	1.0000	0.9999	0.9998	0.9995
Shunt inductance	*SD*	21.4654	20.5149	19.6821	18.5274
	CSD	15.2781	16.0070	16.4375	15.2103
	MM	1.8968	1.7817	1.7030	1.6303
	ρ	0.9593	0.9604	0.9619	0.9685
Parallel inductance	*SD*	29.0632	28.9811	28.8471	28.5684
	CSD	15.5869	16.0384	16.0344	15.3087
	MM	3.4257	3.3857	3.3271	3.2413
	ρ	0.8868	0.8860	0.8888	0.8976
		220 µH	**0.5 mH**	**1 mH**	**2 mH**
Series inductance	*SD*	3.9309	8.6247	10.8921	8.9891
	CSD	3.8257	8.1945	10.3549	8.5144
	MM	1.0535	1.1110	1.1366	1.1262
	ρ	0.9986	0.9940	0.9906	0.9934
Shunt inductance	*SD*	16.1449	12.8450	9.3621	6.2909
	CSD	14.7104	12.5481	9.3518	5.9621
	MM	1.4888	1.3443	1.2282	1.1408
	ρ	0.9747	0.9839	0.9917	0.9966
Parallel inductance	*SD*	27.8025	26.5298	25.2349	23.0367
	CSD	14.7072	15.2343	15.8864	14.8572
	MM	2.9870	2.6366	2.4006	2.1127
	ρ	0.9110	0.9196	0.9261	0.9440

Table 15.4 20 kVA transformer

Test Config.	Statistical Method	22 µH	44 µH	66 µH	110 µH
Series inductance	*SSE*	0.3095	1.0075	2.6120	5.5806
	SSRE	0.0007	0.0023	0.0059	0.0125
	SSMMRE	0.0006	0.0019	0.0042	0.0079
	σ	0.0074	0.0138	0.0217	0.0306
	σs	1.0547	2.0042	3.1713	4.5500
Shunt inductance	*SSE*	460.7646	420.8603	387.3854	343.2649
	SSRE	0.2777	0.2848	0.2806	0.2138
	SSMMRE	0.2558	0.2261	0.2020	0.1778
	σ	0.4435	0.4019	0.3708	0.3377
	σs	45.9910	44.3599	42.8871	38.5185
Parallel inductance	*SSE*	844.6715	839.9069	832.1527	816.1526
	SSRE	0.5824	0.5948	0.5946	0.5547
	SSMMRE	0.5518	0.5464	0.5389	0.5282
	σ	0.8200	0.8141	0.8036	0.7884
	σs	70.8930	71.4743	70.9828	68.5393
		220 µH	**0.5 mH**	**1 mH**	**2 mH**
Series inductance	*SSE*	15.4521	74.3855	118.6389	80.8042
	SSRE	0.0382	0.1732	0.3758	0.2352
	SSMMRE	0.0164	0.0384	0.0460	0.0419
	σ	0.0490	0.0841	0.0964	0.0938
	σs	8.0035	16.5907	21.9197	19.2766
Shunt inductance	*SSE*	260.6585	164.9939	87.6485	39.5749
	SSRE	0.1551	0.1083	0.0720	0.0411
	SSMMRE	0.1278	0.0792	0.0453	0.0243
	σ	0.2712	0.1990	0.1402	0.0937
	σs	33.2896	26.9442	20.8636	14.5248
Parallel inductance	*SSE*	772.9808	703.8323	636.7990	530.6873
	SSRE	0.5014	0.4559	0.4245	0.3560
	SSMMRE	0.4962	0.4524	0.4120	0.3509
	σ	0.7436	0.6834	0.6325	0.5536
	σs	63.8938	59.4688	57.2336	51.4616

Table 15.5 0.76 kVA transformer

Test Config.	Statistical Method	22 µH	44 µH	66 µH	110 µH
Series inductance	*SD*	0.9881	1.3289	1.6706	2.5439
	CSD	0.9861	1.3273	1.6674	2.5422
	MM	1.0098	1.0168	1.0228	1.0374
	ρ	0.9999	0.9997	0.9996	0.9991
Shunt inductance	*SD*	16.0931	15.8664	15.6364	14.5208
	CSD	13.9526	14.8458	15.2213	14.1192
	MM	1.7290	1.6630	1.6140	1.5492
	ρ	0.9600	0.9596	0.9610	0.9670
Parallel inductance	*SD*	22.0337	21.9030	21.8153	21.7612
	CSD	13.3873	13.4764	13.6954	14.0027
	MM	2.7448	2.6971	2.6672	2.6139
	ρ	0.9039	0.9065	0.9077	0.9075
		220 µH	**0.5 mH**	**1 mH**	**2 mH**
Series inductance	*SD*	3.5187	6.5532	6.8672	8.6317
	CSD	3.4601	6.0872	6.3335	7.8254
	MM	1.0566	1.1130	1.1203	1.1554
	ρ	0.9983	0.9951	0.9945	0.9918
Shunt inductance	*SD*	13.2515	11.3317	8.7587	6.4215
	CSD	13.2581	11.0163	7.4950	4.8662
	MM	1.4342	1.3122	1.2119	1.1483
	ρ	0.9741	0.9833	0.9926	0.9970
Parallel inductance	*SD*	21.2856	20.2481	19.2312	17.8833
	CSD	14.1340	13.9380	13.6924	13.2671
	MM	2.4635	2.1996	2.0063	1.8116
	ρ	0.9132	0.9249	0.9359	0.9481

Table 15.6 0.76 kVA transformer

Test Config.	Statistical Method	22 µH	44 µH	66 µH	110 µH
Series inductance	*SSE*	0.9762	1.7659	2.7909	6.4715
	SSRE	0.0026	0.0056	0.0096	0.0211
	SSMMRE	0.0016	0.0034	0.0053	0.0104
	σ	0.0098	0.0165	0.0221	0.0341
	σs	1.4620	2.4778	3.3608	5.2500
Shunt inductance	*SSE*	258.9874	251.7427	244.4982	210.8531
	SSRE	0.3685	0.4957	0.5491	0.4103
	SSMMRE	0.2037	0.1836	0.1667	0.1457
	σ	0.3799	0.3515	0.3289	0.3000
	σs	47.9275	50.1194	50.6844	45.4892
Parallel inductance	*SSE*	485.4827	479.7411	475.9072	473.5516
	SSRE	0.4810	0.4822	0.4904	0.5312
	SSMMRE	0.4614	0.4546	0.4492	0.4418
	σ	0.7077	0.6985	0.6921	0.6805
	σs	63.7281	63.5084	63.8144	64.0272
		220 µH	**0.5 mH**	**1 mH**	**2 mH**
Series inductance	*SSE*	12.3814	42.9445	47.1583	74.5067
	SSRE	0.0519	0.1541	0.2457	0.3977
	SSMMRE	0.0167	0.0321	0.0366	0.0488
	σ	0.0484	0.0804	0.0898	0.1123
	σs	8.2454	15.5970	18.7654	24.9455
Shunt inductance	*SSE*	175.6024	128.4067	76.7148	41.2362
	SSRE	0.3492	0.2589	0.1485	0.0744
	SSMMRE	0.1097	0.0771	0.0511	0.0327
	σ	0.2460	0.1853	0.1344	0.0986
	σs	40.8021	32.9109	24.1654	16.8848
Parallel inductance	*SSE*	453.0758	409.9866	369.8404	319.8134
	SSRE	0.5001	0.3724	0.3201	0.2676
	SSMMRE	0.4135	0.3616	0.3165	0.2645
	σ	0.6436	0.5726	0.5105	0.4370
	σs	61.1527	52.9187	47.5635	41.7316

Table 15.7 0.35 kVA transformer

Test Config.	Statistical Method	22 µH	44 µH	66 µH	110 µH
Series inductance	*SD*	0.8431	1.1837	1.5107	2.4332
	CSD	0.8389	1.1782	1.5061	2.4311
	MM	1.0075	1.0123	1.0165	1.0276
	ρ	0.9999	0.9999	0.9998	0.9995
Shunt inductance	*SD*	23.3481	21.7483	20.3304	19.8402
	CSD	15.8460	15.9322	15.8131	15.2889
	MM	2.0043	1.8417	1.7276	1.6894
	ρ	0.9619	0.9652	0.9682	0.9715
Parallel inductance	*SD*	32.1882	32.0961	32.0022	31.9593
	CSD	18.4600	18.6925	18.8282	19.1287
	MM	3.5752	3.5301	3.4873	3.4344
	ρ	0.8745	0.8768	0.8789	0.8791
		220 µH	**0.5 mH**	**1 mH**	**2 mH**
Series inductance	*SD*	3.4249	7.8786	7.2789	9.2465
	CSD	3.3702	7.3816	6.8353	8.6308
	MM	1.0437	1.1009	1.0981	1.1225
	ρ	0.9990	0.9955	0.9960	0.9936
Shunt inductance	*SD*	16.5658	12.5594	10.0854	6.7391
	CSD	14.0297	11.5675	10.0009	6.6097
	MM	1.4915	1.3150	1.2241	1.1307
	ρ	0.9790	0.9874	0.9912	0.9964
Parallel inductance	*SD*	31.5568	30.8132	29.7151	28.1167
	CSD	19.4223	19.6835	19.5856	19.1921
	MM	3.2572	2.9599	2.6631	2.3593
	ρ	0.8849	0.8934	0.9063	0.9224

Table 15.8 0.35 kVA transformer

Test Config.	Statistical Method	22 µH	44 µH	66 µH	110 µH
Series inductance	*SSE*	0.7108	1.4012	2.2822	5.9205
	SSRE	0.0017	0.0039	0.0065	0.0149
	SSMMRE	0.0011	0.0025	0.0041	0.0089
	σ	0.0090	0.0149	0.0199	0.0321
	σs	1.3272	2.2187	2.9875	4.8187
Shunt inductance	*SSE*	545.1328	472.9882	413.3238	393.6340
	SSRE	0.3054	0.3122	0.2825	0.2420
	SSMMRE	0.2730	0.2359	0.2058	0.1899
	σ	0.4709	0.4211	0.3806	0.3584
	σs	49.2604	46.8996	44.0655	41.3244
Parallel inductance	*SSE*	1036.0799	1030.1618	1024.1424	1021.3993
	SSRE	0.5486	0.5517	0.5560	0.5722
	SSMMRE	0.5393	0.5349	0.5306	0.5259
	σ	0.8002	0.7954	0.7899	0.7827
	σs	67.4635	67.8293	67.9705	68.1311
		220 µH	**0.5 mH**	**1 mH**	**2 mH**
Series inductance	*SSE*	11.7302	62.0725	52.9823	85.4977
	SSRE	0.0384	0.1435	0.2173	0.3783
	SSMMRE	0.0167	0.0399	0.0428	0.0530
	σ	0.0496	0.0906	0.0945	0.1101
	σs	8.0303	17.0218	19.2067	24.9159
Shunt inductance	*SSE*	274.4268	157.7392	101.7143	45.4157
	SSRE	0.1469	0.0772	0.0524	0.0247
	SSMMRE	0.1260	0.0668	0.0391	0.0170
	σ	0.2705	0.1787	0.1262	0.0739
	σs	32.5675	22.8956	17.5869	11.0145
Parallel inductance	*SSE*	995.8295	949.4544	882.9863	790.5476
	SSRE	0.5423	0.4795	0.4253	0.3681
	SSMMRE	0.5043	0.4634	0.4182	0.3646
	σ	0.7547	0.7002	0.6381	0.5651
	σs	66.2249	61.0970	55.9210	50.4225